Universiteit
Leiden
The Netherlands

Programmed cell death in plants and caspase-like activities

Gaussand, G.M.D.J.

Citation
Gaussand, G. M. D. J. (2007, April 25). *Programmed cell death in plants and caspase-like activities*. Retrieved from https://hdl.handle.net/1887/11864

Version:	Corrected Publisher's Version
License:	Licence agreement concerning inclusion of doctoral thesis in the Institutional Repository of the University of Leiden
Downloaded from:	https://hdl.handle.net/1887/11864

Note: To cite this publication please use the final published version (if applicable).

Programmed cell death in plants and caspase-like activities

Gwénaël Gaussand

Cover: Rice suspension cells stained with Sytox orange
Designed by Peter Hock & Ridderprint
Publisher: Sociotext Press, Veghel, 2007
Printed by: Ridderprint, Ridderkerk, The Netherlands

ISBN: 978-90-809584-2-5

Programmed cell death in plants and caspase-like activities

Proefschrift

Ter verkrijging van
de graad van Doctor aan de Universiteit Leiden,
op gezag van Rector Magnificus Prof. Mr. P.F. van der Heijden,
volgens besluit van het College voor Promoties
te verdedigen op woensdag 25 april 2007
klokke 13:45 uur

door

Gwénaël Martial Daniel Jean-Marie Gaussand

geboren te Blois (France) in 1975

Promotiecomissie

Promotor:	Prof. Dr. P.J.J. Hooykaas
Co-promotor:	Dr. M. Wang
Referent:	Dr. E.J. Woltering (Wageningen University & Research Centre)
Overige leden:	Prof. Dr. P.M. Brakefield Prof. Dr. J. Memelink Prof. Dr. R. Verpoorte

“Programmed cell death in plants and caspase-like activities” by Gwénaël Gaussand

Reproduction of color prints was financially supported by the Leiden University Foundation.

A ma famille,
papa, maman, mes frères
et mes grands-parents.

Contents **Page**

Abbreviations		8
Chapter 1	Involvement of caspases and caspase-like proteases in programmed cell death	11
	Outline of the thesis	41
Chapter 2	Programmed cell death in the leaves of the *Arabidopsis* spontaneous necrotic spot (sns) mutant	55
Chapter 3	Programmed cell death during the transition from multicellular structures to globular embryos in barley androgenesis	81
Chapter 4	Heat-shock induced cell death is associated with an increase of caspase-3 and caspase-6 like activities in rice suspension cells	103
Chapter 5	Purification of caspase-3 like proteases in *Oryza sativa* with the fluorogenic Biotin-DEVD-CHO	123
Chapter 6	Summary and general discussion	149
Samenvatting		159
Curriculum vitae		167
Color supplement		169

List of abbreviations

acd2, accelerated cell death 2
Ac-DEVD-AMC N-acetyl-Asp-Glu-Val-Asp-7-amino-4-methylcoumarin
Ac-DEVD-CHO N-acetyl-Asp-Glu-Val-Asp-aldehyde
Ac-VEID-AMC, N-acetyl-Val-Glu-Ile-Asp-7-amino-4-methylcoumarin
Ac-VEID-CHO, N-acetyl-Val-Glu-Ile-Asp-aldehyde
AIF, apoptosis inducing factor
AMC, 7-amino-4-methylcoumarin
APAF-1, apoptotic protease activating factor-1
APMSF, (4-Amidino-Phenyl)-Methane-Sulfonyl Fluoride
AtMCP1b and 2b, Arabidopsis metacaspase type I class gene b and Arabidopsis metacaspase type II class gene b
ATP/dATP, adenosine triphosphate / deoxyadenosine triphosphate
Bcl-2, B-cell lymphoma 2
BH domain, Bcl-2 homology domain
Biotin-DEVD-CHO, biotin-Asp-Glu-Val-Asp-aldehyde
BSA, bovine serum albumin
CA-074, (L-3-*trans*-(Propylcarbamyl) oxirane-2-carbonyl)-L-isoleucyl-L-proline
CARD, caspase activation and recruitment domain
CCH, copper chaperone homolog
CED, cell death-defective
CHAPS, 3-[(3-Cholamidopropyl) dimethylammonio]-1-propanesulfonate
CLSM, confocal laser scanning microscopy
cmk, chloromethylketone
DAPI, 4', 6-diamino-2-phenylindole
DCI, 3, 4 dichloroisocoumarin
DED, death effector domain
DFP, Di-isopropylfluorophosphate
DIABLO, direct IAP-binding protein with low pI
DISC, death-inducing signaling complex
dmk, diazomethylketone
DNA, deoxyribonucleic acid
DNase, deoxyribonuclease
DTT, Dithiothreitol
E-64, (L-transepoxy succinyl-leucylamide-(4-guanido)-butane or N-[N-(L-trans carboxyoxiran-2-carbonyl)-L-leucyl]-agmatine)
EDTA-Na_2, Ethylenediaminetetraacetic acid disodium salt
EDTA, ethylenediaminetetraacetic acid
EGL-1, egg-laying abnormal 1
EGTA, Ethylene-bis (oxyethylenenitrilo) tetraacetic acid Glycol ether diamine tetraacetic acid
ELS, embryo-like structure released out of the exine wall
ER, endoplasmic reticulum
FADD, Fas-associated via death domain
FAK, focal adhesion kinase
FasL, Fas ligand
fmk, fluoromethylketone
FDA, fluorescein-diacetate
FISH, fluorescence in situ hybridization
fmk, fluoromethylketone
FPLC fast protein liquid chromatography
GFP, green fluorescent protein
HEPES, 4-(2-hydroxyethyl)-1-piperazineethanesulfonic acid
HIC, hydrophobic interaction chromatography

HR, hypersensitive response
IAP, inhibitor of apoptosis protein
ICAD/CAD, inhibitor of caspase-activated DNase / caspase-activated DNase
ICE, interleukin-1β-converting enzyme or caspase-1
kDa, kilodalton
LeMCA1, *Lycopersicon esculentum* metacaspase 1
lsd, lesion simulating disease
mcII-Pa, metacaspase type II in *Picea abies* (Norway spruce)
MCS, multicellular structure inside the exine wall
MEKK, mitogen activated protein kinase kinase
MOPS, 3-(N-morpholino) propanesulfonic acid
MPT, mitochondrial permeability transition
MPTP, mitochondrial permeability transition pore
MS, Mass spectrometry
OMM, outer mitochondrial membrane
p53, or TP53 tumor protein 53
PARP, poly (ADP-ribose) polymerase
PCD, programmed cell death
PEMs, proliferating proembryogenic masses
PMSF, phenylmethylsulphonylfluoride
PPVs, precursor protease vesicles
pRb, retinoblastoma protein
RAIDD, Rip-associated protein with a death domain
RNase, ribonuclease
ROS, reactive oxygen species
SI, self-incompatibility
SIC, selected ion chromatogram
Smac, second mitochondrial activator of caspases
sns, spontaneous necrotic spots
STAT-1, signal transducer and activator of transcription 1
TE, tracheary element
TLCK, Tosyl Lysyl ChloromethylKetone: 1-Chloro-3-tosylamido-7-amino-2-heptanone
TMV, tobacco mosaic virus
TNF, tumour necrosis factor
TPCK, Tosyl Phenylalanyl Chloromethyl Ketone: 1-Chloro-3-tosylamido-4-phenyl-2-butanone
TRADD, TNFRSF1A-associated via death domain
TRAIL, TNF-related apoptosis-inducing ligand
TUNEL, terminal deoxynucleotidyl transferase-mediated dUTP nick end labeling
VPE, vacuolar processing enzyme
YCA1, yeast caspase-1

Chapter 1

Involvement of caspases and caspase-like proteases in programmed cell death

Gwénaël M.D.J-M Gaussand

Abstract

Programmed cell death (PCD) plays an important role in development and maintenance of tissue homeostasis, and in defense against pathogens and environmental stresses. The molecular details of the signaling pathways underlying PCD, apoptosis in particular, have been well studied in animals. Cells undergo apoptosis through two major pathways controlled by complex regulatory networks: the extrinsic pathway (death receptor pathway) or the intrinsic pathway (mitochondrial pathway). Caspases are the key executioners of apoptosis in animals. In the past few years, the understanding of PCD mechanisms in plants has deepened. In plants, PCD plays an important role in development, response to pathogens and abiotic stress. The main question, still unanswered, is which proteases are the key executioners of PCD in plants.

Introduction

Cell death is divided in animal species into programmed cell death (PCD) and necrosis. PCD is an important process for multicellular organisms. As it removes superfluous, damaged or infected cells in an organized manner, PCD plays an important role in development, in tissue homeostasis, in defense against pathogens and to cope with adverse environmental stresses (Steller et al. 1995; Meier et al. 2000; Lawen 2003; Jin & El-Deiry 2005). In the past decades, PCD was held synonymous with apoptosis. The term apoptosis is derived from the Greek word for the process of leaves falling from trees or petals falling from flowers. It was introduced in the 1970s to differentiate a morphologically distinctive form of cell death associated with normal physiology (Kerr et al. 1972). Apoptosis is associated with activation of caspases, executioners of cell destruction. There are four mechanistic classes of proteases that have been recognized by the International Union of Biochemistry and Molecular Biology in 1984, including serine, cysteine, aspartic and metallo proteases (Table 1). Caspases belong to an evolutionary conserved family of cysteine proteases (Kroemer & Martin 2005). Necrosis is associated with acute injury to cells, leading to loss of membrane integrity, swelling and disruption of the cells. During necrosis, cellular contents are released uncontrolled into the cell's environment which results in damage of surrounding cells and a strong inflammatory response in the corresponding tissue (Leist & Jaatela 2001). Since, other types of PCD have been proposed for which cell death was found to occur in a programmed fashion but in complete absence and independent of caspase activation. PCD has been

classified into three main types according to Clarke's classification based on lysosomal involvement (Clarke 1990; Chipuk & Green 2004; Kim 2005):

- apoptosis (or type I cell death),
- autophagic cell death (also known as cytoplasmic, or type II cell death),
- necrosis-like cell death (also known as type III or non-lysosomal cell death).

Type I cell death, apoptosis, is a form of PCD morphologically defined by condensation of the nucleus and cytoplasm, association of chromatin with the nuclear periphery, DNA fragmentation, membrane blebbing, and engulfment and lysosomal degradation of the dying cell by a phagocyte (Kerr et al. 1972). Biochemical evidence has indicated the caspase family of cysteine protease as well as certain proteins of the mitochondria to be mediators of type I PCD. Type II, autophagic cell death, is characterized by sequestration of bulk cytoplasm and organelles in double or multi-membrane autophagic vesicles and their delivery to and subsequent degradation by the cell's own lysosomal system before the nucleus is destroyed (Bursch et al. 2000; Levine & Klionsky 2004). The sequestered cytoplasmic components may be degraded prior to heterophagocytosis of cellular remains. Type III, non-lysosomal or necrosis-like cell death, is characterized by breakdown of the plasma membrane, swelling of organelles, lysosome-independent formation of 'empty spaces' in the cytoplasm and disintegration of the cytoplasm (Gozuacik & Kimchi 2004).

Types I and II cell death have been observed in many animal species during development, whereas type III cell death is common in pathological conditions. Types II and III cell death are genetically regulated and often have morphological features resembling necrosis, yet their underlying molecular mechanisms are unclear. The various types of PCD have in common that they are executed by active cellular processes that can be intercepted by interfering with intracellular signaling. Those types can not be categorized because they might overlap since they share the same activation intermediaries or they can be activating each other (Lockshin & Zakeri 2004). The cellular components are safely isolated by membranes, and then consumed by adjacent cells and/or resident phagocytes without inflammation. The elimination of PCD debris may remain virtually unnoticed by the body (Fietta 2006). This distinguishes them from "accidental" necrosis. The caspase-independent cell death pathways - type II and type III cell death - are important safeguard mechanisms to protect the organism against unwanted and potential harmful cells when caspase-mediated routes fail but can also be triggered in response to cytotoxic agents or other death stimuli. In the case of accidental necrosis, cytosolic constituents chaotically spill into extracellular space through damaged plasma membrane and provoke an inflammatory response. The necrotic cell removal induces and amplifies pathological processes.

Mitochondria play not only a key role in cellular metabolism and in signal transduction cascades but also an important role in the regulation of PCD (Ferri & Kroemer 2001). Mitochondrial alterations – following release of sequestered apoptogenic proteins, loss of transmembrane potential, production of reactive oxygen species (ROS), disruption of electron transport chain, and decreases in ATP synthesis - have been shown to be responsible for the different types of cell death (Bras et al. 2005). Thus, the mitochondria can be viewed as a central regulator of the decision between cellular survival and cell death.

During cell death, the ATP levels are determinant in directing toward PCD or necrosis (Leist al. 1997; Nicotera et al. 1998; Formigli et al. 2000). The disruption of the mitochondrial electron transport chain would result in diminished ATP production and consequently in a striking perturbation of the bioenergetic state of the cell. The inhibition of ATP production has been observed in both type I and type III cell death. However, this phenomenon occurs relatively late in type I cell death, as the complete apoptotic program involves the energy-dependent formation of the apoptosome (cytochrome c/ Apaf-1 / dATP complex) and hydrolysis of macromolecules. By contrast, type III cell death is characterized by an early loss of ATP synthesis and seems to proceed in conditions of low cytosolic ATP levels (Kim et al 2003). ATP dependency has been observed for the autophagic type II pathway, apparently at the lysosomal level (Plomp et al. 1989). Moreover, intracellular nucleotides can regulate apoptosis. They can directly block the cytochrome c initiated apoptosome formation and the caspase activation by interfering with Apaf-1 (Chandra et al. 2006).

Calcium is a key regulator of mitochondrial function and acts at several levels within the organelle to stimulate ATP synthesis. Mitochondrial matrix Ca^{2+} overload can lead to enhanced generation of reactive oxygen species (ROS). ROS will trigger the opening of the mitochondrial permeability transition pore (MPTP). If the pore remains open, cells cannot maintain their ATP levels and this will lead to cell death by necrosis. When cells experience a less severe insult, the MPTP may open transiently. The resulting mitochondrial swelling may be sufficient to cause release of cytochrome c and activation of the apoptotic pathway rather than necrosis (Forte & Bernardi 2005; Green & Kroemer 2004).

The efflux of cytochrome c from mitochondria is also a pivotal event in apoptosis, as it drives the assembly of the apoptosome in the cytoplasm (Adrain & Martin 2001). Afterwards the activation of a proteolytic cascade involving caspase proteases is an irreversible step (Abraham et al. 2004). Caspases cleave a variety of proteins after specific aspartate residues, ultimately leading to cell death. The contents of dead cells are packaged into apoptotic bodies, which are recognized by neighboring cells or macrophages and cleared by phagocytes.

Table 1: Protease classification according to their catalytic mechanisms (IUBMB, 1984). The inhibitors described here are just some examples which are commercially available from several companies. Those inhibitors may be used separately or in inhibitory cocktails to identify the class of a protease.

Protease classes	Examples of proteases	Protease inhibitors
serine proteases	chymotrypsin	Trypsin inhibitor
	trypsin	TPCK (does not inhibit trypsin)
	elastase	TLCK (does not inhibit chymotrypsin)
	kallikrein	PMSF
	thrombin	Leupeptin-hemisulfate
	plasmin	Hirudin (inhibits thombin)
	urokinase	Elastatinal (inhibits elastase)
	subtilisin	DFP
		DCI
		Chymostatin
		Benzamidine-HCl (inhibits thrombin and trypsin)
		AEBSF-HCl
		Antipain-HCL
		Antithrombin III
		(alpha)1-Antitrypsin
		APMSF-HCl (does not inhibit chymotrypsin and acetylcholine esterase)
		Aprotinin (does not inhibit subtilisin and thrombin)
cysteine proteases	Papain	TPCK
	Actinidin	TLCK
	bromelain,	E-64
	cathepsins B, L, S,	PMSF (inhibits papain)
	calpains	Leupeptin-hemisulfate
		Chymostatin
		Cathepsin Inhibitor (inhibits papain and Cathepsins B, L and S)
		Calpain Inhibitor I (inhibits calpain I, cathepsins B and L)
		Calpain Inhibitor II (inhibits calpain II, cathepsins B and L)
		CA-074 (inhibits cathepsin B)
		Antipain-HCL

Table 1: continued

aspartic proteases	pepsin chymosin cathepsin D renin	Pepstatin
metallo proteases	Aminopeptidases Leucine aminopeptidase	1,10-Phenanthroline Phosphoramidon EGTA EDTA-Na_2 Bestatin-HCl Leuhistin (inhibits aminopeptidase M) Phebestin (inhibits aminopeptidase N) Amastatin-HCl (does not inhibit aminopeptidase B) Arphamenine A or B (inhibits aminopeptidase B)

De-regulation of apoptosis may lead to pathological disorders such as developmental defects, autoimmune diseases, neurodegeneration or cancer (Thompson 1995).

In plants, PCD plays normal physiological roles in a variety of processes in plants, including deletion of cells with temporary functions such as the aleurone cells in seeds and the suspensor cells in embryos; removal of unwanted cells, such as the root cap cells found in the tips of elongating plant roots and the stamen primordia cells in unisexual flowers; deletion of cells during sculpting of the plant body and formation of leaf lobes and perforations; death of cells during plant specialization, such as the death of TE cells which creates channels for water transport in vascular plants; leaf senescence; and responses to plant pathogens and abiotic stresses (Pennell & Lamb 1997; Danon et al. 2004; Kuriyama & Fukuda 2002). PCD in plants is an active suicidal process that removes unwanted or severely damaged cells (Dangl & Jones 2001; Kuriyama & Fukuda 2002). PCD in plant cells mostly resembles that of type II or autophagic cell death in animals (van Doorn & Woltering 2005; Liu et al. 2005). Some common features of type I cell death or apoptosis are conserved in both plants and metazoa (Danon & Gallois 1998; Yao et al. 2004). These include cytoplasm shrinkage, cytochrome c leakage out of mitochondria, chromatin condensation, altered nuclear morphology, DNA fragmentation in large fragments and DNA laddering. While the signalling events and cell death cascades have been well studied in animals, little is known about the regulation and execution of PCD in plants (Hoeberichts & Woltering 2003a). After

the elucidation of the complete Arabidopsis genome, it has become clear that no genes for the caspases and for the apoptotic regulators of the IAP and Bcl-2 families are present in plants. However, animal Bcl-2 members have been found to modify cell death processes in plants (Lam et al. 1999; Baek et al. 2004), indicating a possible identical apoptotic machinery in plants. Caspase-like activities have been measured in plant extracts and they seem to be involved in PCD processes, even though no sequence homologues have been found at the molecular level. Caspase-like activities cannot be inhibited by protease inhibitors other than animal caspase-specific ones (Korthout et al 2000; Lockshin & Zakeri 2002; Bozhkov et al 2004). Identification of such proteases is essential to reveal the molecular mechanism that operates in plant PCD and to provide some insights into differences between plant and animal PCD. The identification in plants of a class of putative proteases related to animal caspases and termed metacaspases (Uren et al. 2000) has stimulated research in this protein family. Two recent studies identified new types of substilisin-like proteases (named saspases-A and -B) from oats and a vacuolar processing enzyme (VPE) from tobacco that may play important roles as caspase-like proteases in the execution of PCD in plants (Coffeen & Wolpert 2004; Hatsugai et al. 2004; Hatsugai et al. 2006).

The aim of this review is to provide an overview of the molecular and cellular events that characterize PCD in animals and in plants. In addition, the recent developments concerning the possible involvement of proteases with caspase-like specificity in plant PCD will be described.

Caspases and programmed cell death in animals

The apoptotic cascade: discovery

The development of multicellular organisms involves an important balance between cell growth, cell division and cell death. The coordination of these cellular programs ensures appropriate organ and body size. Apoptosis has an important role in all animals, by forming and deleting structures, controlling cell numbers and eliminating abnormal damaged cells (Baehrecke 2002). Programmed cell death is a genetically encoded form of cell suicide that is central to the development and homeostasis of multicellular organisms.

The molecular mechanisms of apoptosis were discovered after intensive efforts (Jin & El-Deiry 2005). An early discovery was made in genetic studies of the nematode *Caenorhabditis elegans* which contains the basic components of the cell death machinery (as shown in figure 1). In *C. elegans*, cell death relies on the presence of CED-3 (ced, cell death

abnormal), CED-4, CED-9 and EGL-1 (egg-laying abnormal 1) (Liu & Hengartner 1999). The regulator of cell death in *C. elegans*, CED-3, was found to be related to the mammalian cysteine protease, interleukin-lβ converting enzyme, also named ICE or caspase-1 (Yuan et al. 1993). This finding suggested that the mechanism of cell death is conserved across species and that proteases are integral to the death program.

Gene interaction studies have defined a genetic pathway in *C. elegans* and have ordered the functions of *egl-1*, *ced-9*, *ced-3* and *ced-4* (Liu & Hengartner 1999). Homologues of the nematode core apoptotic pathway genes have been identified and have been shown to be conserved throughout evolution, along with additional activators, effectors and inhibitors of cell death (Putcha & Johnson 2004; Chinnaiyan 1999; Riedl & Shi 2004). In *C. elegans*, CED-4 (Apaf-1 homologue) binds to and activates CED-3 (caspase homologue). In healthy cells, CED-4 remains inactive by its association with CED-9 (antiapoptotic Bcl-2 homologue). The protein EGL-1 is a trigger of cell death and is expressed in response to certain developmental cues. EGL-1 binds to CED-9, displacing CED-4, which in turn activates CED-3 to induce apoptosis (Liu & Hengartner 1999). Activation and regulation of apoptosis in higher organisms depends on components such as those found in *C.elegans*, but more complex. The first caspase, caspase-1, was identified due to its ability to convert the precursor of interleukin-1β (IL-1β) to its mature form, a potent mediator of inflammation (Cerretti et al. 1992; Thornberry et al. 1992). Subsequent cloning of *ced-3*, a pro-apoptotic gene in *C. elegans*, revealed that it encodes a protein highly homologous to caspase-1 (Yuan et al. 1993).

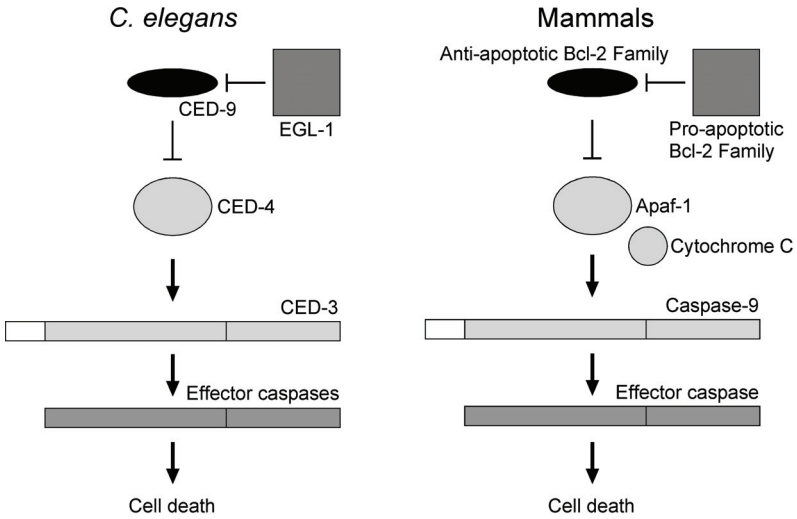

Figure 1: Evolutionary conserved cell death pathways in *C. elegans* and mammals. Functional homologues of caspases and their regulators across species are indicated by the same shape and shading.

A human sequence was identified, cloned and was shown to encode a 32 KDa cysteine protease, called CPP32 (Fernandes Alnemri et al. 1994). This identification was done with the DNA sequence encoding the active site of caspase-1 and CED-3 which was used to search an expressed sequence tag (est) database. Independently, two other groups identified a related caspase that was called caspase-3, one group naming it Yama (the Hindu god of death) and the other group Apopain (Tewari et al. 1995; Nicholson et al. 1995). Caspases (cysteine-dependent aspartate-specific proteases) are the key executioners of apoptosis and they belong to an evolutionary conserved family of cysteine proteases (Kroemer & Martin 2005). After discovery of caspase-1 and caspase-3 other caspases were found.

The apoptotic cascade: description

The apoptotic cascade can be initiated via two major pathways (figure 2). These pathways involve either the activation of death receptors in response to ligand binding (death receptor pathway), or the release of cytochrome c from the mitochondria (mitochondria pathway) (Ashkenazi & Dixit 1998; Hengartner 2000; Broker et al. 2005).

PCD can be triggered by the two pathways mentioned before. Both pathways involve a specific family of cysteine proteases, the caspases, that are activated to execute PCD. The execution of PCD results in the typical morphologic changes (Degterev et al. 2003).

In mammals, the cell surface death receptor-mediated pathway (figure 2, left) involves cell surface death receptors such as Fas, Tumor Necrosis Factor (TNF), or TRAIL receptors (Ashkenazi & Dixit 1998). Death ligand stimulation, via a series of protein-protein interactions, results in oligomerization of the receptors and recruitment of an adaptor protein and caspase-8 or -10, forming a death-inducing signalling complex (DISC). Autoactivation of caspase-8 at the DISC is followed by activation of other caspases, including caspase-3, -6 and -7. These activated caspases function as downstream effectors of the cell death program.

The other caspase activation pathway in mammals is the mitochondria pathway (figure 2, right). This pathway is characterized by a depolarization of the mitochondrial membrane and a release of mitochondrial proteins (Danial & Korsmeyer 2004) including pro-apoptotic proteins, such as cytochrome c, into the cytosol. A cytosolic complex, the apoptosome, is then formed. This complex consists of oligomerised Apaf-1 (apoptotic protease-activating factor 1), ATP/dATP, cytochrome c and the initiator caspase, pro-caspase-9 (Chinnaiyan 1999; Riedl & Shi 2004). Oligomerisation of Apaf-1 allows the

recruitment and autocatalytic activation of caspase-9, and consequently the propagation of a death signal by proteolytic processing and activation of effector caspases (Li et al. 1997).

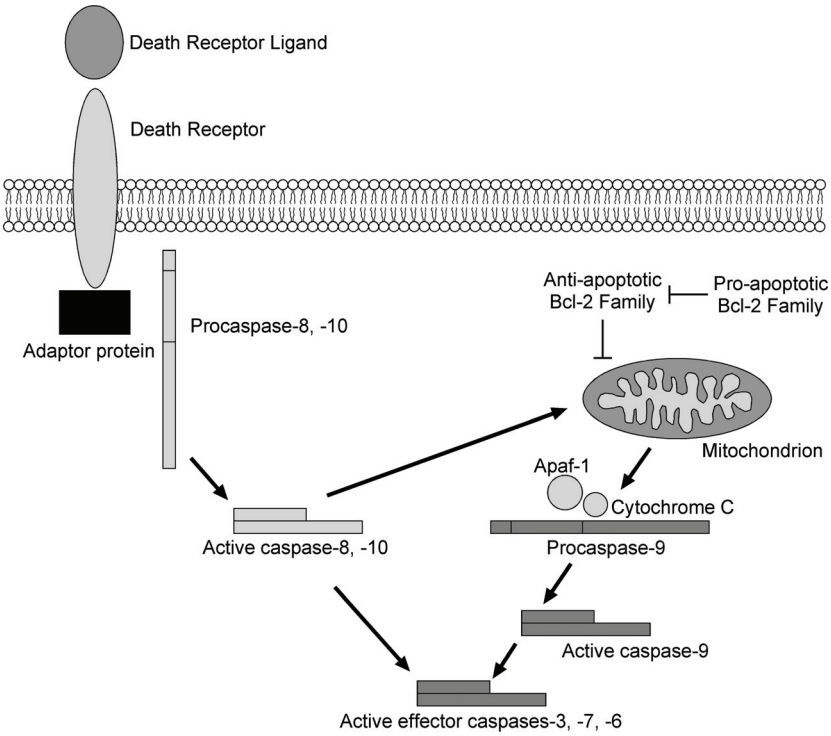

Figure 2: Apoptotic pathways leading to mammalian cell death. The extrinsic apoptotic pathway (left) is induced by a death receptor ligand (TNF, TRAIL, FasL etc) which results in the recruitment and formation of a multiprotein complex DISC that includes the death receptor, intracellular adaptor proteins (TRADD, FADD, RAIDD) and initiator caspases (procaspase-8 or -10). The complex leads to autocatalytic processing and activation of the initiator caspase. The intrinsic pathway (right) is initiated by the majority of apoptotic stimuli, including irradiation, cytotoxic drugs, DNA damage etc. Loss of mitochondrial membrane potential and release of pro-apoptotic cell death proteins results in the formation of another multiprotein complex, the apoptosome, that includes Apaf-1, cytochrome c, ATP/dATP and the initiator caspase, procaspase 9. That complex leads to autocatalytic activation of caspase-9 and subsequent effector caspases. Pro- and anti-apoptotic bcl-2 homologues regulate the release of pro-cell death mitochondrial proteins.

Apart from the pathways now described, there is another cell death pathway. That pathway involves the endoplasmic reticulum (ER), and it is known as the apoptotic pathway of ER stress-mediated cell death (Momoi 2004). The endoplasmic reticulum (ER) is the site of assembly of polypeptide chains that are destined for secretion or routing into various subcellular compartments. The ER-initiated PCD pathway comprises the activation of caspase-12 and/or the cytochrome c-dependent apoptotic pathway.

The caspases

Caspases are present in the cytosol of most cells. Caspases are expressed as inactive single-chain zymogens of 30-50 kDa (figure 3) with three domains: a pro-domain, a large subunit domain (*ca.* 20 kDa), and small subunit domain (*ca.* 10 kDa). The domains are separated by aspartate cleavage sites in interdomain linkers (Chang & Yang 2000). The pro-domain is important for the regulation of activation, which results in proteolytic cleavage of the linkers, usually accompanied by loss of the pro-domain. Activation can be by autoactivation, transactivation, or proteolysis by other peptidases (Wolf & Green 1999).

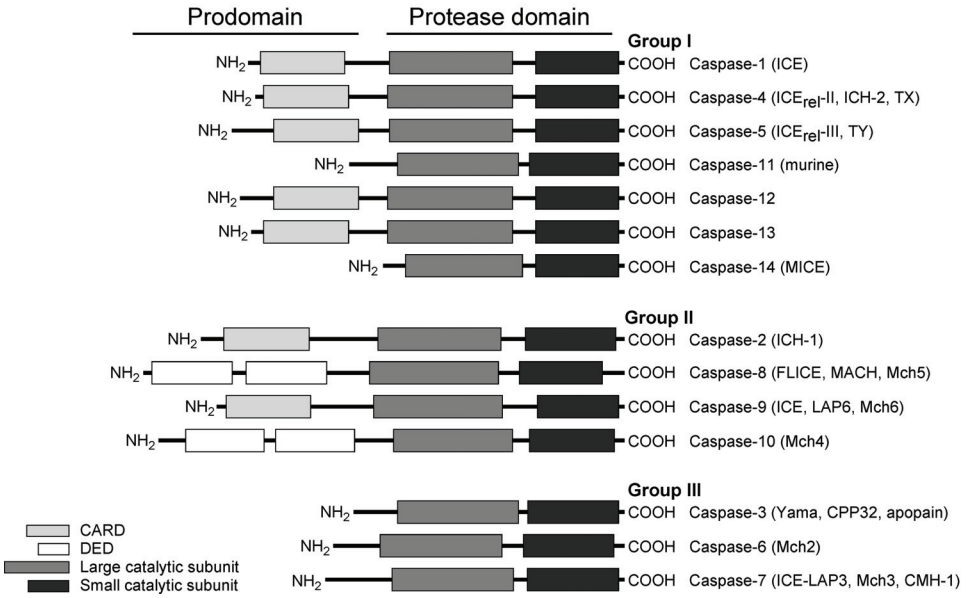

Figure 3: Mammalian caspase family. All mammalian caspases shown are of human origin except for murine caspase-11 and -12. Three major groups of caspases are presented. Group I: inflammatory caspases; group II: apoptosis initiator caspases; group III: apoptosis effector caspases. The CARD, the DED, the large (p20) and small (p10) catalytic subunits are indicated.

Based on their function, caspases can be classified into three groups (figure 3, Thornberry & Lazebnik 1998). The first group consists of inflammatory caspases. This group includes caspase-1, -4, -5, -11, -12, -13 and -14, which are involved in inflammation. The second group consists of apoptotic initiator caspases. Initiator caspases possess long pro-domains that contain either a death effector domain (DED) (caspase-8 and -10) or a caspase activation and recruitment domain (CARD) (caspase-2 and -9). Both domains interact with upstream adaptor molecules. The third group consists of effector caspases. This executioner

class (caspase-3, -6 and -7) is characterized by the presence of a short pro-domain. These caspases are processed and activated by upstream caspases. The caspases of the executioner class perform the downstream execution steps of apoptosis by cleaving multiple cellular substrates such as regulators of apoptosis, housekeeping and structural proteins (reviewed in Cohen 1997; Nunez et al. 1998; Thornberry & Lazebnik 1998; Wolf & Green 1999).

Initiator but not effector caspases have long pro-domains that contain modules which mediate protein-protein interactions between the caspases themselves and with regulatory adaptor molecules. Two types of modules have been defined: death effector domains (DEDs) and caspase recruitment domains (CARDs). These modules allow for the assembly of proteins into oligomeric structures, and this assembly induces autoprocessing and activation of the initiator caspases (reviewed in Nunez et al. 1998; Wolf & Green 1999; Stennicke & Salvesen 2000).

The other members of the apoptotic cascade

The caspase-cascade signalling pathway is regulated by various molecules, receptors, enzymes and gene regulating proteins such as the Bcl-2 family proteins and the inhibitor of apoptosis protein (IAP) (Launay et al. 2005; Fan et al. 2005). A few of them are here described.

Bcl-2 derives its name from B-cell lymphoma 2, a tumor which was the consequence of a reciprocal gene translocation in chromosomes 14 and 18 in follicular lymphomas including the Bcl-2 gene (Vaux et al. 1988). The members of the Bcl-2 family are a group of regulatory factors crucial in apoptosis. According to functional and structural criteria, the members can be divided into two groups:

- Group I proteins are all anti-apoptotic proteins, including A1/Bfl1, Bcl-2, Bcl-w, Bcl-xL, Boo/Diva, Mcl-1, NR-13 and Nrf3 in mammals, BHRF-1, E1B19K, Ks-Bcl-2, LMW5-HL, and Ced-9 in *C. elegans* (Fu & Fan 2002; Milosevic et al. 2003; Gross et al. 1999). They all have four short Bcl-2 homology (BH) domains: BH1, BH2, BH3 and BH4. Their function is to inhibit pro-apoptotic proteins of the Bcl-2 family by binding to them.
- Group II proteins are all pro-apoptotic proteins, including Bad, Bak, Bax, Bcl-rambo, Bcl-xS, Bid, Bik, Bim, Blk, BNIP3, Bok/Mtd, Hrk and Nip3 in mammals, and Egl-1 in *C. elegans* (Milosevic et al. 2003). Bax and Bak, originally localized in the cytoplasm, can translocate to the mitochondrial outer membrane after an apoptotic program starts. Following the translocation, they will undergo conformation changes, oligomerization and insertion into

the mitochondrial outer membrane to elevate the permeability of mitochondrial permeability transition pores (MPTPs).

Group I proteins bind to the active conformation of Bax to prevent it from inserting into the mitochondrial outer membrane. The binding maintains the normal permeability of MPTPs, and it prevents the release of mitochondrial pro-apoptotic factors such as cytochrome c, AIF and Smac/DIABLO (Lü et al. 2003; Fan et al. 2001). Through cytochrome c, AIF, and others, the Bcl-2 family proteins indirectly regulate the activity of caspases in related apoptotic pathways (Fan et al. 2001). There are a number of theories concerning how the Bcl-2 family proteins exert their pro- or anti-apoptopic effect. According to one such theory, the effect depends on activation or inactivation of an inner MPTP, which is involved in the regulation of matrix Ca^{2+}, pH, and voltage. It is also thought that some Bcl-2 family proteins induce (pro-apoptopic members) or inhibit (anti-apoptopic members) the release of cytochrome c in to the cytosol which, once there, activates caspase-9 and caspase-3, leading to apoptosis. Zamzami et al. (1998) suggest that the release of cytochrome c is in fact mediated by effects of the permeability transition pore on the inner mitochondrial membrane, linking the theories. The site of action for the Bcl-2 family is mostly on the outer mitochondrial membrane (OMM). There are apoptogenic factors (cytochrome c, Smac/DIABLO, Omi) within the mitochondria. If these factors are released, they activate the executioners of apoptosis: the caspases. Depending on their function, once activated, Bcl-2 proteins either promote the release of these factors, or keep them sequestered in the mitochondria.

The Inhibitor of Apoptosis Protein (IAP) was first identified in insect cells infected by *baculovirus*. Encoded by a viral gene, IAP can inhibit infected host cells from executing the apoptotic program. So far, in humans, the identified members of the IAP family include cIAP1, cIAP2, XIAP (X-linked mammalian inhibitor of apoptosis protein), NAIP (neuronal apoptosis inhibitory protein), survivin and livin (Fan et al. 2005). The activity of mammalian IAP can be inhibited by Smac/DIABLO released from mitochondria (Costantini et al. 2002). IAP family proteins may also have other functions besides caspase inhibition. As reported by Uren et al. (1998), IAP family members in yeast could neither unite caspases nor induce apoptosis. Caspases are suppressed by IAP (Fesik & Shi 2001). When a cell receives an apoptotic stimulus, IAP activity is relieved after SMAC (Second Mitochondria-derived Activator of Caspases), a mitochondrial protein, is released into the cytosol. SMAC binds to IAPs, effectively preventing them from arresting the apoptotic process.

The death substrates

The list of putative proteins that are cleaved by caspases either *in vivo* or *in vitro* is growing (Earnshaw et al. 1999; Nicholson 1999; Fischer et al. 2003). However, only a few of these proteins have been established as biologically relevant death substrates, and many others may just represent 'innocent bystanders' (Hengartner 2000).

Caspases are synthesized as proenzymes that are activated through cleavage at internal aspartate residues by other caspases or by autoactivation. The proteolytic cleavage of a caspase can induce a dramatic conformational change that exposes the catalytic pocket of the enzyme, and therefore results in the enzyme's activation. The proteolytic activation of caspases can be achieved either by autocatalysis or by an upstream protease. A caspase that cleaves and activates itself is called an initiator caspase. Once an initiator caspase is activated, it triggers a cascade to activate downstream executioner caspases. Subsequently, the activated executioner caspases cleave numerous cellular targets to destroy normal cellular functions, activate other apoptotic factors, inactivate anti-apoptotic proteins, and eventually lead to apoptotic cell death. The executioner caspases recognize specific tertiary motifs in their substrates and cleave their substrates after specific aspartate residues, ultimately leading to cell death. The cleaved substrates are cytoskeletal proteins including lamins, α-fodrin and actin, proteins involved in DNA repair and cell-cycle regulation such as poly(ADP-ribose) polymerase (PARP) and retinoblastoma protein (Launay et al. 2005; Ruchaud et al. 2002; Zhivotovsky 2003).

Table 2: the substrate specificity of caspases

	Caspase	Substrate specificity
Group I	Caspase-1	WEHD YVAD
	Caspase-4	(W/L)EHD
	Caspase-5	(W/L)EHD
	Caspase-13	WEHD
	Caspase-14	WEHD
Group II	Caspase-2	DEHD
	Caspase-8	I/LETD
	Caspase-9	LEHD
	Caspase-10	LEXD
Group III	Caspase-3	DEVD
	Caspase-6	VE(H/I)D
	Caspase-7	DEVD

The specificity requirements of the caspases were derived from studies with short synthetic peptides. The abundant nuclear enzyme PARP catalyses the attachment of poly (ADP-ribose) to several acceptor proteins, including itself, in response to DNA strand breaks. PARP cleavage by caspases-3 and -7 bisects a bipartite nuclear localization signal (Schreiber et al. 1992), and results in a form that cannot attach ADP-ribose polymers in response to damaged DNA (Lazebnik et al. 1994). PARP was one of the first identified examples of a substrate processed by an effector caspase much more efficiently than by either the inflammatory caspase-1 (Gu et al. 1995) or the initiator caspase-8 (Nicholson et al. 1995). Based on the cleavage site of PARP (DEVD↓G), a synthetic model substrate was developed: Ac-DEVD-AMC. Ac-DEVD-CHO and its biotinylated derivative (biotin-DEVD-CHO) were synthesized as specific inhibitors of PARP cleavage and as affinity ligands for purification of the protease.

Caspase-3 turned out to be one of the key executioners of apoptosis; this caspase bears either full of partial responsibility for the proteolytic cleavage of many key proteins, each of which contains an Asp-Xaa-Xaa-Asp (DXXD) motif that is similar to the one in PARP. Because all substrates of caspase-3 contain DEVD sequences, artificially synthesized tetra peptides Ac-DEVD-AMC and Ac-DEVD-CHO are used as the specific substrate and inhibitor of caspase-3, respectively. The inhibitors described in table 1 are used individually or in inhibitory cocktails to inhibit specific protease or protease classes. Caspases can only be inhibited with specific caspase inhibitors. Most of the synthetic peptide caspase inhibitors were developed based on the tetrapeptide caspase recognition motif. Therefore, the selectivity of inhibitors matches the caspase substrate specificities described above (Table 2). The introduction of an aldehyde group at the C terminus of the tetrapeptide results in the generation of reversible inhibitors (Graybill et al. 1994), whereas a fluoromethyl ketone (fmk), a chloromethyl ketone (cmk) (Estrov et al. 1995), or a diazomethyl ketone (dmk) (Thornberry et al. 1992) at this position irreversibly inactivates the enzyme.

Developmental defects, autoimmune diseases, neurodegeneration or cancer

Balance between cell division and cell death is of utmost importance for the development and maintenance of multicellular organisms. Deregulation of apoptosis may lead to pathological disorders such as developmental defects, autoimmune diseases, neurodegeneration or cancer (Broker et al. 2005). Understanding of cell death signaling pathways is relevant to understanding cancer and to developing more effective therapies.

Numerous diseases have been attributed to apoptotic machinery malfunction. Altered expression and / or activity of pathway components - including receptors, ligands, adaptors, caspases and substrates - contribute to several neurodegenerative diseases, some

types of autoimmune disorder and cancer. Alzheimer's disease, Parkinson's disease and Huntington's disease are associated with excessive cell death that involves defective regulation of caspase activity (Ho & Hawkins 2005). Increased activities of caspases-8 and -9 have been observed in brain tissues (Rohn et al. 2001; Yew et al. 2004; Rohn et al. 2002) and in peripheral blood mononuclear cells of Alzheimer's disease patients (Tacconi et al. 2004). The activities of caspases-8 and -9 were reported to be elevated in brain tissue from Parkinson's disease patients (Hartmann et al. 2001; Viswanath et al. 2001). Huntington's disease, another neurodegenerative disorder, is caused by the abnormal expansion of polyglutamine repeats in the Huntington protein, which recruits and activates caspase-8 (Sanchez et al. 1999). Caspase-10 has also been proposed to play a role in the pathological development of Huntington's disease, in a fashion similar to that of caspase-8 (U et al. 2001). The Bcl-2 gene has been implicated in a number of cancers, including melanoma, breast, prostate and lung carcinomas. It is also thought to confer cellular resistance to chemotherapy (Pusztai et al. 2004). Carcinogenesis has been linked to abnormalities in the apoptotic pathway, and many drugs that are targeted at different parts of this pathway are being developed.

Many promising drugs target the extrinsic death receptor pathway as well as the intrinsic mitochondrial apoptotic pathway. There are also developments in targeting initiator and effector caspases, as well as the death domains that are involved in transducing the apoptotic signals (Dlamini et al. 2005).

Caspase-like proteases and programmed cell death in plants

Observation of plant PCD

In plants, PCD plays an important role in development and in the responses to pathogens and abiotic stress (Wang et al. 1996a, 1998, 1999; Pennell & Lamb 1997; Beers & McDowell 2001; Jones 2001; Danon et al. 2004; Kuriyama & Fukuda 2002). Several examples demonstrate that PCD is an important process occurring in plants during gamete and embryo formation or during plant development or in response to pathogen attack.

The tapetum plays a crucial role in pollen development. This secretory tissue produces numerous nutritive proteins that are necessary for pollen maturation. The tapetum also produces exine that is the main structural component of the pollen wall (Ku et al. 2003; Kawanabe et al. 2006). The tapetum undergoes PCD during the later stages of pollen development (Wu & Cheung 2000; Papini et al. 1999; Wang et al. 1999). Premature PCD of

the tapetum causes failure in pollen development and is associated with male sterility (Ku et al. 2003).

During pollination, plants enforce self-incompatibility (SI) as an important means to prevent self-fertilization. Research on the corn poppy (*Papaver rhoeas*) has revealed that proteins in the pistil on which the pollen lands interact with pollen, and triggers PCD in incompatible (self) pollen. Thomas & Franklin-Tong (2004) found that the response involves rapid inhibition of pollen-tube growth, followed by PCD.

PCD is involved in the elimination of certain cells during plant embryogenesis, as was shown in Norway spruce somatic embryogenesis. Two successive waves of PCD are implicated in the transition from proliferating proembryogenic masses (PEMs) to somatic embryos and in correct embryonic pattern formation, respectively (Filonova et al. 2000). The first wave of PCD triggers the degradation of PEMs when they give rise to somatic embryos. The second wave of PCD eliminates terminally differentiated embryo-suspensor cells during early embryogenesis.

In barley androgenesis, PCD takes place during the transition from multicellular structures to globular embryos (Maraschin et al. 2005, chapter 3). PCD takes place in the small cell domain of the multicellular structures. The cell death of this domain marked the site of exine wall rupture. Chromatin condensation and DNA degradation preceded cell detachment and cytoplasm dismantling. This PCD was characterized by the formation of vesicles and vacuoles that contained cytoplasmic material. PCD was accompanied by an increase of activity of caspase-3-like proteases.

The endosperm of cereals functions as a storage tissue in which the majority of starch and seed storage proteins are synthesized (Young & Gallie 2000). During seed maturation, the endosperm degradation process is accompanied by typical PCD-related changes of cell morphology and internucleosomal DNA cleavage (Wojciechowska & Olszewska 2003).

The perforations in the leaf blades of *Monstera obliqua* (Araceae) arise through PCD early in leaf development because a subpopulation of cells undergoes PCD simultaneously (Gunawardena et al. 2005). DNA cleavage was demonstrated by TUNEL but was found to be randomly degraded but not as multiples of internucleosomal units. Cells were found to be misshapen with densely stained nuclei with condensed chromatin, disrupted vacuoles, and condensed cytoplasm.

During post-germinative seedling growth, the white spruce (*Picea glauca*) megagametophyte undergoes PCD (He & Kermode 2003a and 2003b). The death process is accompanied by internucleosomal DNA cleavage, activation of several nucleases and proteases.

During germination of barley grains, DNA fragmentation was observed in the aleurone by TUNEL staining accompanied by activation of hydrolytic enzymes such as alpha-amylase (Wang et al. 1996a).

During vascular development, xylem precursor cells give rise to tracheary elements (TE), xylem parenchyma cells and xylem fibres, which together form xylem. For maturition TE are emptied by the loss of all cell contents, including the nucleus, to form hollow xylem tubes. Several enzymes - such as cysteine proteases, serine proteases, RNases, S1-type nucleases, acid phosphatases and lipases (Demura et al. 2002) - are synthesized and then transported to the vacuole where they are activated (Funk et al. 2002). The autolysis of TE starts with the rupture of the vacuole (Groover et al. 1997; Kuriyama 1999; Obara et al. 2001).

Plants can recognize certain pathogens and activate defenses, called the resistance response, that result in the limitation of pathogen growth at the site of infection. One hallmark of the resistance response is the induction of a localized cell death response, called the hypersensitive response or HR, at the site of the infection. HR limits the pathogen's nutrient supply, since the dying tissue rapidly becomes dehydrated. The induction of HR by some pathogens and elicitors (molecules secreted by pathogens) is similar to apoptosis in animals, since apoptotic features - such as DNA breaks with 3'OH ends, blebbing of the plasma membrane as well as nuclear and cytoplasmic condensation - are present in some cells undergoing HR (Levine et al. 1996; Wang et al. 1996b; Ryerson & Heath 1996, Heath 2000). Many researchers have identified genes involved in the control and execution of HR. They, for example, identified mutant lines in which cell death is deregulated. These mutants (*acd2* for accelerated cell death 2 and *lsd* lesions simulating disease) are called lesion mimics because their phenotypes resemble pathogen-inducible HR cell death. They were classified into two groups: initiation mutants and feedback or propagation mutants (Pontier et al. 1998; Lorrain et al. 2003). This classification is based upon the assumption that two different mechanisms are involved in controlling cell death: a pathway to initiate PCD and a pathway to suppress PCD.

The examples given so far concern PCD during gamete, embryo or post embryo development. In natural environments plants are subjected to many environmental stresses - such as cold stress, light stress, mechanical stress and also stresses caused by bacterial and fungal pathogens - which in turn can cause secondary oxidative stress (Hippeli et al 1999). The excessive formation of reactive oxygen species (ROS) in response to the primary, environmental stress activates a signal transduction pathway that may be independent of or additive to the signals induced by the primary stress (Levine et al. 1996). The intensity of the secondary oxidative stress may vary from very mild to extreme, depending on the severity of

the primary stress. During mild stress, plants activate the antioxidant responses; more severe stress activates the PCD pathway, while extreme stress causes necrosis (Levine et al. 1994; Willekens et al. 1997).

Many examples demonstrate that PCD occurs in plant cells following abiotic stimuli. Heat-shock treatment triggers PCD as demonstrated in tobacco (Vacca et al. 2004), and in rice (chapter 4). DNA laddering was found in cucumber (Balk et al. 1999), nuclear condensation and cytoplasm shrinkage were found in carrot (Mc Cabe et al. 1997), and caspase-like activity was detected in tobacco (Tian et al. 2000) and in oat (Coffeen & Wolpert 2004) after heat-shock induction.

The apoptotic pathway

Concerning animals, the term apoptosis (Kerr et al. 1972) refers to a morphological type, often observed in PCD, that involves nuclear shrinkage and fragmentation, cellular shrinkage, DNA fragmentation, membrane blebbing, formation of apoptotic bodies, and digestion by macrophages (Wyllie 1980). Some elements of the same cell suicide mechanisms used in animal cells may be functionally conserved in plants. Though the biochemical mechanisms responsible for cell suicide in plants are largely unknown, a variety of reports suggest similarities to apoptosis that occurs in animal species. The morphological characteristics of plant cells undergoing PCD also bear some striking similarities to apoptosis in animals, though the presence of a cell wall around plant cells imposes certain differences.

Akin to animal cells, PCD in plants is associated with cytochrome c release, cell shrinkage, cytoplasmic condensation, chromatin condensation, and internucleosomal DNA fragmentation (DNA ladders). DNA fragmentation is a PCD hallmark. Salt stress, for instance, induces nuclear fragmentation and DNA degradation into oligonucleosomal fragments in barley roots (Katsuhara & Kawasaki 1996; Katsuhara 1997). Another example is DNA laddering in Arabidopsis roots and maize cultured cells induced by mannose (Stein & Hansen 1999). Ito and Fukuda (2002) reported nuclear degradation triggered by the collapse of the vacuole in tracheary elements of the xylem.

In various plant systems, the release of cytochrome c from mitochondria into the cytosol precedes cell death (Sun et al. 1999; Hansen 2000; Balk et al. 1999; Balk & Leaver 2001; Curtis & Wolpert 2002; Krause & Durner 2004; Tiwari et al. 2002). *In vivo*, cytochrome c release into the cytosol was observed as an early event during PCD in cucumber (Balk et al., 1999), maize suspension culture cells (Stein & Hansen 1999), tobacco protoplasts (Sun et al., 1999), and Arabidopsis suspension cells (Krause & Durner 2004).

In addition, evidence of the existence of a mitochondrial permeability transition (MPT) during PCD is accumulating in isolated plant mitochondria *in vitro* and plant tissue *in vivo* (Arpagaus et al. 2002; Curtis & Wolpert 2002; Tiwari et al. 2002; Yao et al. 2004). These findings indicate that mitochondrial function may be shared in a very similar way during PCD in both animals and plants.

Calcium is an almost universal intracellular messenger, controlling a broad range of cellular processes, including animal apoptosis. In plant PCD, Ca^{2+} has also been recognized as a ubiquitous signal. Elevated Ca^{2+} levels have been observed during tracheary element differentiation (Yu et al. 2002), aerenchyma formation (Bouranis et al. 2006), wheat aleurone differentiation (Kuo et al. 1996), HR (Mittler et al. 1999), and leaf senescence (Oh et al. 1996).

Ectopic expression of certain animal anti-apoptosis genes in transgenic plants has been demonstrated to provide protection from pathogens and other insults as a result of cell death suppression (Dickman et al. 2001; Mitsuhara et al. 1999). Conversely, expression of animal pro-apoptotic proteins such as Bax in plants can induce cell death mechanisms similar to endogenous programs for cell suicide (Lacomme & Santa Cruz 1999; Yoshinaga et al. 2005). Heterologous Bax induces PCD in a predominantly ROS-dependent manner and localizes to Arabidopsis mitochondria *in vivo* (Baek et al., 2004). Bax Inhibitor-1 (BI-1) is an anti-apoptotic protein which is conserved in both animal and plant species - including rice, Arabidopsis, barley, oilseed rape and tobacco - (Bolduc et al. 2003; Huckelhoven et al. 2003; Kawai et al. 1999; Kawai-Yamada et al. 2001; Lam et al. 2001; Sanchez et al. 2000; Watanabe & Lam 2006). Arabidopsis BI-1 has been shown to protect transgenic plants against cell death induced by ectopic expression of mammalian Bax (Kawai-Yamada et al. 2001; Baek et al. 2004), indicating an *in vivo* role for BI-1 in cytoprotective pathways in planta and suggesting that the biochemical mechanism regulated by BI-1 is evolutionary conserved. BI-1 overexpression also regulates resistance to fungal pathogens in barley, probably due to its cell death-suppressive effects (Huckelhoven et al. 2003). Antisense-mediated downregulation of BI-1 in tobacco BY-2 cells results in accelerated cell death upon carbon starvation (Bolduc & Brisson 2002). Endogenous expression of BI-1 is induced during wound-healing responses and upon exposure to certain pathogens in plants (Huckelhoven et al., 2001; Sanchez et al., 2000), suggesting that BI-1 may play a role in host defense mechanisms during times of stress. Thus, BI-1 represents the first endogenous gene to be identified that regulates cell death in both plant and animal cells.

As described previously, some common features of type I cell death or apoptosis are conserved in both plants and metazoa (Danon & Gallois 1998; Yao et al. 2004). Apoptosis, as it is in animals, apparently does not occur in plants. Plants do not have an immune system

with phagocytosis. For example, engulfment of apoptotic bodies and degradation in another cell is not found during plant PCD and the rigid and thick cell walls of plant cells do not help engulfment and degradation. PCD in plant cells mostly resembles that of type II or autophagic cell death in animals (van Doorn & Woltering 2005; Liu et al. 2005). Vacuolization of the cytoplasm through autophagy and vacuole disruption are observed in most cases of plant PCD: somatic embryogenesis, xylem differentiation, aleurone layer elimination during germination, and HR. The vacuole contains many of the hydrolytic activities that carry out PCD - including proteases, RNases and DNases - physically separated from their targets (Lam 2004; Ito & Fukuda 2002). The tonoplast (the vacuolar membrane) collapses by a mechanism that is still not understood, initiating the massive degradation of cellular contents.

The enzymes involved in plant PCD

In view of the strong conservation of the regulators and the executioners in animals, it was initially expected that the same actors would be involved in plant PCD. Indeed, caspase-like enzymatic activities were detected in plant tissues undergoing PCD. Different proteases were found to be associated with plant PCD, including senescence (Delorme et al. 2000; Schmid et al. 2001), oxidative stress (Solomon et al. 1999), seed development (Schmid et al. 1998, 1999; Wan et al. 2002), tracheary element development (Runeberg-Roos & Saarma 1998; Groover & Jones 1999), and the HR (Vera & Conejero 1988; D'Silva et al. 1998; Kruger et al. 2002). These proteases may be involved in the terminal decomposition of the dying cell, but not in the initiation or progression of PCD (Rotari et al. 2005).

Caspase-like activity associated with PCD was mentioned in several studies (del Pozo & Lam 1998; Lam & del Pozo 2000; Sun et al. 1999; Tian et al. 2000; de Jong et al. 2000; Mlejnek & Prochazka 2002; Danon et al. 2004; Belenghi et al. 2004; Maraschin et al. 2005; see also chapters 2, 3 and 4). Table 3 lists the various caspase-like activities detected in plants. Researchers who used synthetic caspase substrates and inhibitors have reported on different caspase-like proteases, such as -1, -3 and -6 (Chen et al. 2000; Bozhkov et al. 2004). Caspase-like activity was found during HR induced by a pathogen attack of tobacco leaves (del Pozo & Lam 1998), and during chemical and stress induced cell death of tobacco suspension cells and protoplasts (de Jong et al. 2000).

Caspase-like activities were measured with the caspase-specific substrate (Ac-DEVD-AMC) in the megagametophyte before seed germination (He & Kermode 2003a). These activities gradually increased after germination, until a certain length of the seeds radicle, hypocotyl and cotyledons was obtained. The activities were inhibited by the specific caspase-3 inhibitor (Ac-DEVD-CHO). Camptothecin-induced PCD in tomato suspension cells

can be inhibited with caspase-specific peptide inhibitors, which suggests that caspase-like proteases are involved in the death process (de Jong et al. 2000). Caspase-3 like activity has been detected in tobacco suspension cells after heat shock-induced apoptosis (Tian et al. 2000), and in embryonic suspension cells of barley (*Hordeum vulgare*) (Korthout et al. 2000). Both caspase-1 and caspase-3 like activities were observed in tomato suspension cells after chemically induced apoptosis (de Jong et al. 2000). Caspase-1 like activity has been detected in Arabidopsis suspension cultured cells after nitric oxide-induced cell death (Clarke et al. 2000), and in tobacco BY-2 cells after isopentenyladenosine-induced apoptosis (Mlejnek & Prochazka 2002).

Table 3: List of caspase-like activities in plants cells, adapted from Rotari et al. (2005).

Activity	Tissue	Buffer	Literature
Caspase-1 like (YVADase)	Tobacco leaf tissue	50mM HEPES, pH 7,5, 20% glycerol, 1mM EDTA, 1mM DTT, 1% BSA, 1mM PMSF	del Pozo & Lam (1998)
	Barley embryonic suspension cells	25mM HEPES -KOH, pH7.5, 10% sucrose,1mM DTT, 0.1% Triton X-100, 1mM PMSF	Korthout et al. (2000)
	Arabidopsis thaliana seedlings	50mM sodium acetate, pH5.0, 20% glycerol, 0.1% Triton, 10mM EDTA, 3mM DTT, 2mM PMSF	Danon et al. (2004)
	Germination of white spruce seeds	50mM sodium acetate pH5.5, 20% glycerol, 1mM EDTA, 1mM DTT, 0.2% BSA and 1mM PMSF	He & Kermode (2003)a and b
	Tobacco (BY2) suspension cells	50mM HEPES, pH7.2, 1mM EDTA, 0.2% CHAPS, 5mM DTT, protease inhibitor cocktail (Roche)	Mlejnek & Prochazka (2002)
	Pisum sativum shoots	20 mM MES pH6.6, 0.25 mM DTT, 100 mM NaCl, 2.5 mM EDTA,	Belenghi et al. (2004)
Caspase-3 like (DEVDase)	Rice suspension cells and Arabidopsis *sns* plant tissue	100mM HEPES, 10% sucrose, 0.1% CHAPS, 5mM DTT, 10^{-6}% Nonidet P-40, pH7.0,	Chapters 2,3,4 and 5
	Barley microspores	100mM HEPES, 10% sucrose, 0.1% CHAPS, 5mM DTT, 10^{-6}% Nonidet P-40, pH7.0,	Maraschin et al. (2005, chapter 3)
	Barley embryonic suspension cells	25mM HEPES -KOH, pH7.5, 10% sucrose,1mM DTT, 0.1% Triton X-100, 1mM PMSF	Korthout et al. (2000)
	Arabidopsis thaliana seedlings	50mM sodium acetate, pH5.0, 20% glycerol, 0.1% Triton, 10mM EDTA, 3mM DTT, 2mM PMSF	Danon et al. (2004)

Table 3: continued

Caspase-3 like (DEVDase)	Germination of white spruce (*Picea glauca*) seeds	50mM sodium acetate pH5.5, 20% glycerol, 1mM EDTA, 1mM DTT, 0.2% BSA and 1mM PMSF	He & Kermode (2003)a and b
	Tobacco (BY2) suspension cells	50mM HEPES, pH7.2, 1mM EDTA, 0.2% CHAPS, 5mM DTT, protease inhibitor cocktail (Roche)	Mlejnek & Prochazka (2002)
	Avena sativa leaves	20mM MOPS, pH7, 1mM DTT	Coffeen & Wolpert (2004)
	Tobacco (BY2) suspension cells	50mM HEPES, pH7.4, 100mM NaCl, 0.1% CHAPS,1mM DTT, 0.1mM EDTA, 10% glycerol	Tian et al. (2000)
	Embryogenic cell line of Norway spruce	100mM HEPES, 10% sucrose, 0.1% CHAPS, 5mM DTT, 10^{-6}% Nonidet P-40, pH7.0.	Bozhkov et al. (2004) Suarez et al. (2004)
	Papaver pollen	50mM HEPES pH7.4, 10mM NaCl, 0.1% CHAPS, 10mM DTT, 1mM EDTA, 10% glycerol	Thomas & Franklin-Tong (2004)
Caspase-6 like (VEIDase)	Rice suspension cells and Arabidopsis *sns* plant tissue	100mM HEPES, 10% sucrose, 0.1% CHAPS, 5mM DTT, 10^{-6}% Nonidet P-40, pH7.0,	Chapters 2, 3, 4 and 5
	Embryogenic cell line of Norway spruce	100mM HEPES, 10% sucrose, 0.1% CHAPS, 5mM DTT, 10^{-6}% Nonidet P-40, pH7.0	Bozhkov et al. (2004)
Caspase-8 like (IETDase)	*Arabidopsis thaliana* seedlings	50mM sodium acetate, pH5, 3mM DTT	Rotari et al. (2005)
	Avena sativa leaves	20mM MOPS, pH7, 1mM DTT	Coffeen & Wolpert (2004)
Saspase (VKMDase)	*Avena sativa* leaves	20mM MOPS, pH7, 1mM DTT	Coffeen & Wolpert (2004)
TATDase	Tobacco Xanthi, leaves	Buffer (?) at PH6.8, 1mM PMSF	Chichkova et al. (2004)

YVADase and DEVDase, known from animal studies as caspase-1 and caspase-3, were present in most plant PCD pathways (Woltering et al. 2002). Now research focuses on other activities: VEIDase, IETDase and TATDase. The activation of a protease or a group of proteases with the preferential cleavage of caspase-6 substrate Ac-VEID-AMC is associated with the Norway spruce embryo development (Bozhkov et al. 2004). A TATDase proteolytic activity was detected during the N gene-mediated HR in tobacco plants infected with the tobacco mosaic virus (TMV). Here ectopically expressed *Agrobacterium tumefaciens* VirD2 protein was used as a target, because according to prediction it was a substrate for human

caspase-3. A tetrapeptide aldehyde (biotinyl-TATD-CHO) was designed on the basis of the VirD2 cleavage site for plant caspase. The tetrapeptide aldehyde prevented cleavage of VirD2 by plant caspase, and it counteracted TMV triggered HR *in vivo* (Chichkova et al. 2004). To conclude, several caspase-like activities were measured in plants. Most of these activities have been detected in several species, and in various tissues or cell types (as shown in table 3).

Plant targets and caspase inhibitors

Animal caspases have many identified targets or 'death substrates' that are either deactivated - such as PARP1, nuclear lamin, gelsolin, Bcl-2, p53, pRb, FAK, STAT-1 and β-catenin - or activated - such as MEKK1, p21-activated kinase, protein kinase C and the ICAD/CAD complex - (Lopez-Otin & Overall 2002). Some of these substrates have plant orthologues, but at present, the only possible substrate for plant caspase-like activities is PARP1. Tobacco PARP1 is cleaved during PCD in tobacco protoplasts after menadione treatment (Sun et al. 1999), and in tobacco suspension cells after heat shock treatment (Tian et al. 2000). This cleavage was blocked by caspase inhibitors. A bovine PARP was cleaved in Thomas and Franklin-Tong's 2004 study of papaver pollen PCD during self-incompatible pollination. A DSVD site was conserved with the Arabidopsis AtPARP1 that is orthologous to the animal PARP1 (Doucet-Chabeaud et al. 2001). This would confirm AtPARP1 as a possible substrate for a DEVDase activity.

To conclude, PARP1 has been shown to be one possible substrate. This has been demonstrated in only a few studies. By contrast, many substrates have been found in animal studies. The substrates of the caspase-like proteases are mostly not known for plants. The substrates of plant caspase-like proteases are perhaps not similar to the substrates of animal caspases (Rotari et al. 2005). This is important because knowledge of the substrates would help to identify the plant caspase-like proteases. If it cannot be established that plant caspase-like proteases and animal caspases have the same substrates, other similarities can be taken into consideration. Do plant caspase-like proteases and animal caspases have similar substrate- and site-specificities?

A number of cysteine and serine protease inhibitors (table 2) can partially suppress cell death in plants or have no effect (Lam & Del Pozo 2000). In some cases, they block cell death but this requires high concentrations (Sun et al.1999; de Jong et al. 2000; Woltering et al. 2002). Animal caspase inhibitors have been found to inhibit cell death effectively at low concentrations. Both caspase-1 and caspase-3 inhibitors prevent cell death in various plants (del Pozo & Lam 1998; Clarke et al. 2000; de Jong et al. 2000; Korthout et al. 2000). PARP

cleavage and DNA fragmentation could be inhibited in tobacco suspension cells. Here PCD was induced by high concentrations of nicotinamide. PCD was inhibited by addition of the caspase-3 inhibitor Ac-DEVD-CHO (Zhang et al. 2003). A cell free system was used in another study. Here cytochrome c of animal origin was capable of activating plant caspase-like proteases in carrot cytoplasm. The cytoplasm could then degrade rat liver nuclei (Zhao et al. 1999). In this study, the formation of a DNA ladder was inhibited by the specific caspase-1 and caspase-3 inhibitors (Ac-YVAD-CHO and Ac-DEVD-CHO, respectively). Belenghi et al. (2004) found that caspase-3 like proteases play an important role in the elimination of secondary shoots of pea seedlings after removal of the epicotyl. The injection of the caspase-3 like inhibitor into the remainder of the epicotyl strongly inhibited the death of the secondary shoot, resulting in a seedling with two equal shoots. Bozhkov et al. (2004) found that during plant embryogenesis, caspase-6 like activity was the essential caspase-like activity involved in PCD. The study concerned embryonic pattern formation during shape remodeling. The use of caspase-6 inhibitor blocked the embryo-suspensor differentiation, disturbing embryo development. Sun et al (1999) found that with menadione-induced cell death in tobacco protoplasts, Ac-DEVD-CHO inhibits DNA laddering. In another study, the heat-shock induced cleavage of lamin-like proteins in tobacco protoplasts correlated with the proteolytic activity of caspase-6 like proteases (Chen et al. 2000). In this study the use of the animal caspase-6 inhibitor (Ac-VEID-CH0) inhibited the lamin cleavage. Del Pozo and Lam (1998) prevented tobacco mosaic virus–induced HR in *Nicotiana tabacum* leaves by a treatment with short peptide inhibitors. These inhibitors preferentially inhibit caspase-1 and caspase-3 proteases. De Jong et al. (2000) showed that PCD chemically induced by camptothecin in tomato suspension cells can be inhibited by caspase inhibitors. Elbaz et al. (2002) obtained similar results with caspase inhibitors that prevent or limit staurosporine-induced cell death. Mlejnek and Prochazka (2002) performed this study with isopentenyladenosine to induce cell death, with similar results. Korthout et al. (2000) demonstrated caspase-like activity in barley cell extracts. Here the activity could be inhibited by a caspase-3 inhibitor, but not by cysteine protease inhibitors. Most of the animal caspase inhibitors that were tested in plants are remarkably effective at suppressing cell death. There are some exceptions, though. Caspase-3 inhibitor had no effect on TMV-induced necrotic lesions in tobacco, whereas caspase-1 inhibitor did have an inhibition effect (Chichkova et al. 2004; Hatsugai et al. 2004). Caspase-1 inhibitor did not suppress cell death in papaver pollen tubes, in contrast to caspase-3 inhibitor (Thomas & Franklin-Tong 2004). In chapter 4, a study is described in which caspase-3 and caspase-6 like activities could be inhibited by animal caspase-3 and -6 inhibitors.

In these studies, it was shown that animal caspase inhibitors can inhibit PCD in plants. It can therefore be inferred that caspase-like proteases play a role in PCD in plants.

The other possible candidates

Although caspase-like activities seem to be involved in PCD in plants, it has become clear that orthologs of the animal genes for caspases are not present in plants. In the search for the proteases that are involved in plant PCD, other proteins have been found and described as playing a role in plant PCD. Those proteins are described here. If there is a main executioner of plant PCD with caspase-like activity, it could be one of those proteins.

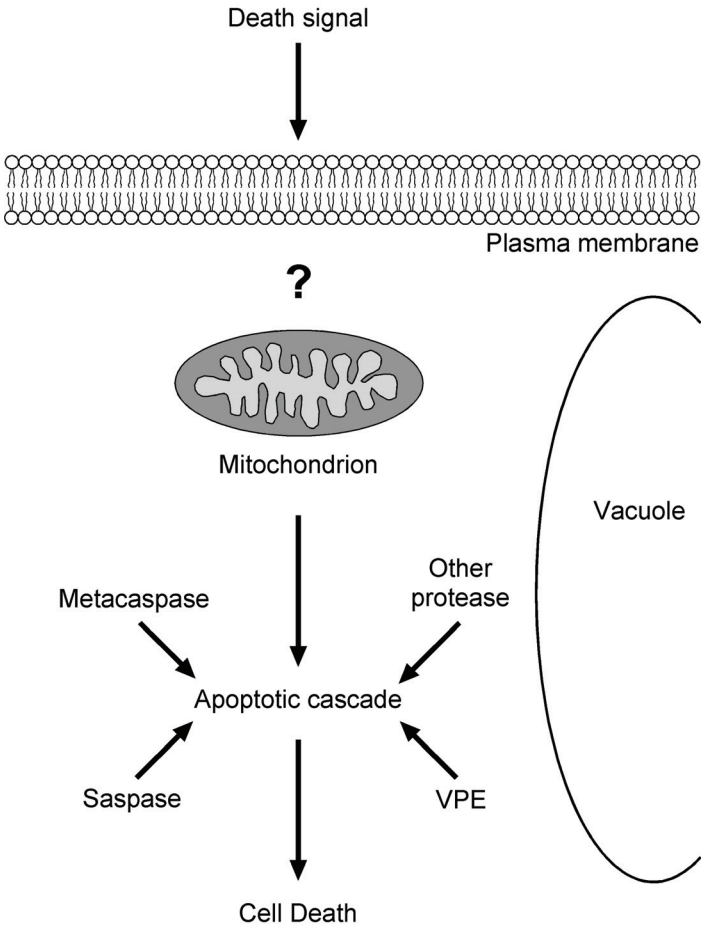

Figure 4: Caspase-like activities and PCD in plant cells. There are several proteases known to play a role during plant PCD. Those proteases are caspase-like candidates.

Metacaspases

Uren et al. (2000) found a family of distantly related caspase-like proteases - named metacaspases - in plants, fungi and Plasmodium. Depending on sequence similarities (within their caspase-like regions) and domain structure, the plant metacaspases can be divided in two classes (type I and II). Whether these metacaspases possess caspase-like proteolytic activity and are involved in plant PCD remains unknown (Woltering et al. 2002; Woltering 2004). Many investigations indicate that metacaspases can have a role in PCD.

Madeo et al. (2002) reported that the yeast metacaspase protein (YCA1) knockout is unable to complete PCD in the presence of H_2O_2. Hoeberichts et al. (2003b) have shown that mRNA levels of LeMCA1 - a tomato (*Lycopersicon esculentum*) type II metacaspase - increased upon infection of leaves with the fungal pathogen *Botrytis cinerea*. This increase correlates with the formation of primary necrotic lesions.

The protein mcII-Pa (plant metacaspase type II) was expressed during PCD in somatic embryogenesis in Norway spruce. *In situ* hybridization analysis showed mRNA accumulation in the part of embryogenic tissues and structures committed to die (Suarez et al. 2004). The activation of proteases cleaving the caspase-6 substrate (VEIDase activity) is essential for PCD and embryogenesis in Norway spruce (*Picea abies*) (Bozhkov et al. 2004). Silencing of the *P. abies* metacaspase gene *mcII-Pa* inhibited VEIDase activity, suppressed PCD in the embryos and blocked suspensor differentiation (Suarez et al. 2004). Immunolocalization analyses and functional assays showed that mcII-Pa accumulates in the nuclei of the suspensor cells and that it is directly involved in the execution of nuclear disassembly (Bozhkov et al. 2005). Watanabe and Lam (2005) found that two type I metacaspases (At5g64240 and At1g02170) were up-regulated in Arabidopsis plants after infiltration with a bacterial pathogen, whereas type II metacaspases were not significantly affected.

The metacaspases could be involved in a plant PCD cascade. Such a cascade occurs with caspase activation in animals. Thus, the metacaspases might activate the plant caspase-like proteases, as was suggested by Rotari et al. (2005).

Vacuolar processing enzyme

The vacuolar processing enzyme (VPE) was originally identified as a processing enzyme that is involved in the maturation of seed storage proteins (Hara-Nishimura et al. 1991; 1998; 2005). VPEs - VPE α, β, γ and δ - also promote the maturation and the activation of various vacuolar proteins in plants (Yamada et al. 1999; Shimada et al. 2003; Rojo et al. 2003; Gruis

et al. 2004). Their counterpart in animals similarly activates lysosomal proteins (Shirahama-Noda et al. 2003). Recent data suggested that VPEs might be key factors in vacuolar collapse-triggered cell death.

In vegetative tissues, the isoform VPEγ is more expressed than the other three. In those tissues, this isoform plays a role in protein degradation during senescence, a PCD pathway in plants. VPEγ is localized in precursor protease vesicles (PPVs), which are hydrolase-containing organelles that are associated with PCD processes (Schmid et al. 1999). VPEγ is also found in the vacuole, an organelle essential for cell dismantling during plant PCD (Lam 2004; Rojo et al. 2004).

VPEs might convert the hydrolytic enzymes that are involved in the disintegration of vacuoles from an inactive to their active forms. The enzyme conversion would initiate the proteolytic cascade in plant PCD. Arabidopsis VPE genes are up-regulated in dying cells during development and senescence of tissues (Kinoshita et al. 1999). There is no sequence similarity between VPEs and caspases. However, VPEs have a proteolytic activity toward a caspase-1 substrate, and VPE activity is inhibited by a caspase-1 inhibitor. Tobacco VPE exhibits the caspase-1 like activity that is required for the completion of cell death during TMV-induced HR in tobacco (Hatsugai et al. 2004).

Saspases

Substilisin-like proteases, named saspase-A and -B, belong to the class of serine proteases. Subtilisin-like proteases were identified in several plant species (Beers et al. 2000). Saspase-A and -B have been found to be involved in victorin-induced PCD in oat (*Avena sativa*) (Coffeen & Wolpert 2004). They were found to cleave caspase specific substrates and they were found to be inhibited by caspase-specific inhibitors. Coffeen and Wolpert (2004) reported that caspase-specific inhibitors prevented rubisco proteolysis during victorin-induced PCD. They also found that a caspase-like activity toward the pan-caspase substrate z-VAD-AFC was present in extracts from victorin-treated *A. sativa* leaves. The two oat saspases show hydrolytic activities for caspase-6, -8 and -9 substrates (VKMD, IETD, and LEHD, respectively) but not for DEVD and VEID. It is important to determine how saspases contribute to plant PCD and to the caspase-like activities.

Other protease(s)

By studying PCD in plants, still some other proteases were also found to be associated with PCD. For many of them, their characterization was done on the basis of inhibitors. As described in table 1, the inhibitors can help to determine the class of the protease that is involved in a particular process. Some examples are here described.

In soybean cells, some cysteine proteases are activated during oxidative stress-induced PCD (Solomon et al. 1999) and the activation of these proteases is required for PCD. Ectopic expression of cystatin, an endogenous cysteine protease inhibitor gene, prevented the increase in cysteine protease activity and blocked PCD triggered either by an avirulent strain of *Pseudomonas syringae pv glycinea* or directly by oxidative stress.

Xylogenesis in *Zinnia elegans* cell cultures can be prevented by the addition of inhibitors such as E-64 and PMSF. This suggests the involvement of some cysteine or serine proteases in this process of PCD (Minami & Fukuda 1995; Ye & Varner 1996; Beers & Freeman 1997).

PCD of the megagametophyte during post-germinative seedling growth of white spruce (*Picea glauca*) is associated with the induction of serine and cysteine proteases and caspase-like activity (He & Kermode 2003a). When germinated seeds were treated with a caspase-3 inhibitor, both the peak of the caspase-like activities and the death of megagametophyte cells were delayed.

A matrix metalloproteinase Cs1-MMP was proposed as a candidate involved in cucumber extracellular cell matrix degradation, and in PCD (Delorme et al. 2000). Cs1-MMP activity was completely inhibited by a hydroxamate-based inhibitor that binds at the active site of MMPs in a stereospecific manner. PCD in the corolla of tobacco (*Nicotiana tabacum*) flowers was inhibited by leupeptin, but not by PMSF, suggesting that a cysteine protease was important for this process (Serafini-Fracassini et al. 2002).

A barley vacuolar aspartic proteinase (phytepsin), highly homologous to mammalian lysosomal cathepsin D, was expressed at a high level, both during formation of tracheary elements and during autolysis of sieve cells (Runeberg-Roos & Saarma 1998). The enzymatic activity was completely inhibited by pepstatin - a specific inhibitor of aspartic proteinases (Sarkkinen et al. 1992). The protease may play a role in the active autolysis of plant cells.

In the endosperm of castor bean (*Ricans communis*), PCD is associated with the accumulation of papain-like propeptidase (Cys-EP) in ricinosomes during germination (Schmid et al. 1999). This process of PCD is also associated with the release of the peptidase from ricinosomes during cell collapse. In *Brassica napus*, a papain-like cysteine protease is associated with PCD of the inner integument of seed coat during early stages of seed development (Wan et al. 2002).

The proteases discussed above do not seem to be the main executioners of plant PCD in general. They participate in PCD in specific tissues only. It may be possible that these proteases are involved in the progression of PCD, but not in the initiation of PCD (Rotari et al. 2005).

Outline of the thesis

The development of multicellular organisms involves an important balance between cell growth, cell division and cell death. Programmed cell death (PCD) plays a key role in all animals, by forming and deleting structures, controlling cell numbers and eliminating abnormal damaged cells (Baehrecke 2002). Apoptosis is a genetically and morphologically encoded form of PCD (Kerr et al. 1972). Caspases were found to be the executioners of the apoptotic pathway.

In plants, PCD plays normal physiological roles in a variety of processes. Some processes in which PCD plays a role are: (i) the deletion of cells with temporary functions, such as the aleurone cells in seeds and the suspensor cells in embryos; (ii) the removal of unwanted cells, such as the root cap cells found in the tips of elongating plant roots and the stamen primordia cells in unisexual flowers; (iii) the deletion of cells during sculpting of the plant body and formation of leaf lobes and perforations; (iv) the death of cells during plant specialization, such as the death of TE cells which creates channels for water transport in vascular plants; (vi) leaf senescence; (vii) responses to plant pathogens and abiotic stresses (Pennell & Lamb 1997; Dangl & Jones 2001; Kuriyama & Fukuda 2002; Danon et al. 2004).

Some common features of apoptosis were found to be conserved in both plants and animals (Danon & Gallois 1998; Yao et al. 2004). These include cytoplasm shrinkage, cytochrome c leakage out of mitochondria, chromatin condensation, altered nuclear morphology, DNA fragmentation and DNA laddering. After the elucidation of the complete Arabidopsis genome, it has become clear that no genes for the caspases or for the apoptotic regulators of the IAP and Bcl-2 families are present in plants. However, animal Bcl-2 members have been found to modify cell death processes in plants (Lam et al. 1999; Baek et al. 2004). This indicates that a similar apoptotic machinery may still be present in plants.

At the start of the work described in this thesis, caspase-like activities had been found to be involved in PCD processes in plants. These activities were measured with animal caspase substrates and inhibited by animal caspase inhibitors. This suggested that a core mechanism is conserved in both animal and plant PCD. However, orthologs of the caspase genes turned out not to be present in the plant genomes. Thus, the researchers at that time wondered which plant protease was responsible for the caspase-like activity in plant extracts.

The aim of the research described in this thesis was to describe PCD in different plant systems (see below), and to identify the proteases in plant cells that show caspase-like activities during PCD.

Chapter 2 describes the Arabidopsis spontaneous necrotic spot (*sns*) mutant. The necrotic spots were visible on the mutant leaves after two or three weeks of growth,

resembling the lesions that accompany the hypersensitive response after a pathogen attack. The phenotype of the *sns* mutant plants was analyzed and evidence for the occurrence of PCD in the necrotic spots was obtained.

Chapter 3 describes the transition from multicellular structures to globular embryos during androgenesis in barley. In this plant system, the transition is possible since some cells - part of the small generative domain - will die at the site of the exine wall rupture. Typical features of plant PCD, in the transition process, were found.

C**hapter 4** describes cell death in rice suspension cells after heat-shock. Evidence for the occurrence of cell death by necrosis and PCD was found.

For chapters 2, 3 and 4, caspase-like activities during PCD were measured. This confirmed that caspase-like proteases are involved in plant PCD. **Chapter 5** describes the development and implementation of the protocol to purify plant caspase-3 like activity. This protocol was based on the one used to purify human caspase-3 with biotin-DEVD-CHO.

Chapter 6 comprises a summarizing general discussion.

Acknowledgments

For valuable discussion and critical reading of the manuscript I am grateful to Prof. Dr. Paul Hooykaas (Institute of Biology Leiden, Leiden University) and to Dr. Wouter-Jan Oosten (Sociotext Foundation). Mr Peter Hock was so friendly to finalize the figures. This work was financed by the BVS Foundation (Binair Vector Systeem).

References

Abraham MC and Shaham S. (2004) Death without caspases, caspases without death. Trends Cell Biol.14 (4): 184-193.

Adrain C, Martin SJ. (2001) The mitochondrial apoptosome: a killer unleashed by the cytochrome seas. Trends Biochem Sci. 26 (6): 390-397.

Arpagaus S, Rawyler A, Braendle R. (2002) Occurrence and characteristics of the mitochondrial permeability transition in plants. J Biol Chem. 277 (3): 1780-1787.

Ashkenaz A and Dixit VM. (1998) Death receptors: signaling and modulation. Science. 281 (5381): 1305-1308.

Baehrecke EH. (2002) How death shapes life during development. Nat Rev Mol Cell Biol. 3 (10): 779-787

Baek D, Nam J, Koo YD, Kim DH, Lee J, Jeong JC, Kwak SS, Chung WS, Lim CO, Bahk JD, Hong JC, Lee SY, Kawai-Yamada M, Uchimiya H and Yun DJ. (2004) Bax-induced cell death of Arabidopsis is meditated through reactive oxygen-dependent and -independent processes. Plant Mol Biol. 56 (1): 15-27.

Balk J, Leaver CJ and McCabe PF. (1999) Translocation of cytochrome c from the mitochondria to the cytosol occurs during heat-induced programmed cell death in cucumber plants. FEBS Lett. 463 (1-2): 151-154.

Balk J and Leaver CJ. (2001) The PET1-CMS mitochondrial mutation in sunflower is associated with premature programmed cell death and cytochrome c release. Plant Cell 13 (8): 1803-1818.

Beers EP and Freeman TB. (1997) Proteinase activity during tracheary element differentiation in Zinnia mesophyll cultures. Plant Physiol. 113 (3): 873-880

Beers EP and McDowell JM. (2001) Regulation and execution of programmed cell death in response to pathogens, stress and developmental cues. Curr Opin Plant Biol. 4 (6): 561-567.

Beers EP, Woffenden BJ and Zhao C. (2000) Plant proteolytic enzymes: possible roles during programmed cell death. Plant Mol Biol. 44 (3): 399-415.

Belenghi B, Salomon M and Levine A. (2004) Caspase-like activity in the seedlings of *Pisum sativum* eliminates weaker shoots during early vegetative development by induction of cell death. J Exp Bot. 55 (398): 889-897.

Bolduc N and Brisson LF. (2002) Antisense down regulation of NtBI-1 in tobacco BY-2 cells induces accelerated cell death upon carbon starvation. FEBS Lett. 532 (1-2): 111-114.

Bolduc N, Ouellet M, Pitre F and Brisson LF. (2003) Molecular characterization of two plant BI-1 homologues which suppress Bax-induced apoptosis in human 293 cells. Planta. 216 (3): 377-386.

Bouranis DL, Chorianopoulou SN, Kollias C, Maniou P, Protonotarios VE, Siyiannis VF and Hawkesford MJ. (2006) Dynamics of Aerenchyma distribution in the cortex of sulfate-deprived adventitious roots of maize. Ann Bot (Lond). 97 (5): 695-704.

Bozhkov PV, Filonova LH, Suarez MF, Helmersson A, Smertenko AP, Zhivotovsky B and von Arnold S. (2004) VEIDase is a principal caspase-like activity involved in plant programmed cellc death and essential for embryonic pattern formation. Cell Death Differ. 11 (2): 175-182.

Bozhkov PV, Suarez MF, Filonova LH, Daniel G, Zamyatnin AA Jr, Rodriguez-Nieto S, Zhivotovsky B, Smertenko A. (2005) Cysteine protease mcII-Pa executes programmed cell death during plant embryogenesis. Proc Natl Acad Sci USA. 102 (40): 14463-14468.

Bras M, Queenan B and Susin SA. (2005) Programmed cell death via mitochondria: different modes of dying. Biochemistry (Mosc). 70 (2): 231-239.

Broker LE, Kruyt FA and Giaccone G. (2005) Cell death independent of caspases: a review. Clin Cancer Res. 11 (9): 3155-3162.

Bursch W, Ellinger A, Gerner C, Frohwein U and Schulte-Hermann R. (2000) Programmed Cell Death (PCD). Apoptosis, autophagic PCD, or others? Ann NY Acad Sci. 926: 1-12.

Cerretti DP, Kozlosky CJ, Mosley B, Nelson N, Van Ness K, Greenstreet TA, March CJ, Kronheim SR, Druck T, Cannizzaro LA, et al. (1992) Molecular cloning of the interleukin-1 beta converting enzyme. Science 256 (5053): 97-100.

Chandra D, Bratton SB, Person MD, Tian Y, Martin AG, Ayres M, Fearnhead HO, Gandhi V and Tang DG. (2006) Intracellular nucleotides act as critical prosurvival factors by binding to cytochrome C and inhibiting apoptosome. Cell. 125 (7): 1333-1346.

Chang HY and Yang X. (2000) Proteases for cell suicide: functions and regulation of caspases. Microbiol Mol Biol Rev. 64 (4): 821-846.

Chen HM, Zhou J and Dai YR. (2000) Cleavage of lamin-like proteins in *in vivo* and *in vitro* apoptosis of tobacco protoplasts induced by heat shock. FEBS Lett. 480 (2-3): 165-168.

Chichkova NV, Kim SH, Titova ES, Kalkum M, Morozov VS, Rubtsov YP, Kalinina NO, Taliansky ME and Vartapetian AB. (2004) A plant caspase-like protease activated during the hypersensitive response. Plant Cell. 16 (1): 157-171.

Chinnaiyan AM. (1999) The apoptosome: heart and soul of the cell death machine. Neoplasia. 1 (1): 5-15.

Chipuk JE and Green DR. (2004) Cytoplasmic p53: bax and forward. Cell Cycle. 3 (4): 429-431.

Clarke A, Desikan R, Hurst RD, Hancock JT and Neill SJ. (2000) NO way back: nitric oxide and programmed cell death in Arabidopsis thaliana suspension cultures. Plant J. 24 (5): 667-677.

Clarke PG. (1990) Developmental cell death: morphological diversity and multiple mechanisms. Anat Embryol. 181(3):195-213.

Coffeen WC and Wolpert TJ. (2004) Purification and characterization of serine proteases that exhibit caspase-like activity and are associated with programmed cell death in *Avena sativa*. Plant Cell. 6 (4): 857-873.

Cohen GM. (1997) Caspases: the executioners of apoptosis. Biochem J. 326 (1): 1-16.

Costantini P, Bruey JM, Castedo M, Metivier D, Loeffler M, Susin SA, Ravagnan L, Zamzami N, Garrido C and Kroemer G. (2002) Pre-processed caspase-9 contained in mitochondria participates in apoptosis. Cell Death Differ. 9 (1): 82-88.

Curtis MJ and Wolpert TJ. (2002) The oat mitochondrial permeability transition and its implication in victorin binding and induced cell death. Plant J. 29 (3): 295-312.

Danial NN and Korsmeyer SJ. (2004). Cell death: critical control points. Cell. 116 (2): 205-219.

Dangl JL and Jones JD. (2001) Plant pathogens and integrated defence responses to infection. Nature. 411 (6839): 826-833.

Danon A, Rotari VI, Gordon A, Mailhac N and Gallois P. (2004) Ultraviolet-C overexposure induces programmed cell death in Arabidopsis, which is mediated by caspase-like activities and which can be suppressed by caspase inhibitors, p35 and Defender against Apoptotic Death. J Biol Chem. 279 (1): 779-787.

Danon A and Gallois P. (1998) UV-C radiation induces apoptotic-like changes in *Arabidopsis thaliana*. FEBS Lett. 437 (1-2): 131-136.

Degterev A, Boyce M and Yuan J. (2003) A decade of caspases. Oncogene. 22(53): 8543-8567.

De Jong AJ, Hoeberichts FA, Yakimova ET, Maximova E, Woltering EJ. (2000) Chemical-induced apoptotic cell death in tomato cells: involvement of caspase-like proteases. Planta.211 (5): 656-662.

Delorme VG, McCabe PF, Kim DJ and Leaver CJ. (2000) A matrix metalloproteinase gene is expressed at the boundary of senescence and programmed cell death in cucumber. Plant Physiol. 123 (3): 917-927.

Del Pozo O and Lam E. (1998) Caspases and programmed cell death in the hypersensitive response of plants to pathogens. Curr Biol. 8 (20): 1129-1132.

Demura T, Tashiro G, Horiguchi G, Kishimoto N, Kubo M, Matsuoka N, Minami A, Nagata-Hiwatashi M, Nakamura K, Okamura Y, Sassa N, Suzuki S, Yazaki J, Kikuchi S and Fukuda H. (2002) Visualization by comprehensive microarray analysis of gene expression programs during transdifferentiation of mesophyll cells into xylem cells. Proc. Natl Acad. Sci. USA. 99 (24): 15794-15799.

Dickman MB, Park YK, Oltersdorf T, Li W, Clemente T and French R. (2001) Abrogation of disease development in plants expressing animal antiapoptotic genes. Proc Natl Acad Sci USA. 98 (12): 6957-6962.

Dlamini Z, Mbita Z and Ledwaba T. (2005) Can targeting apoptosis resolve the cancer saga? Future Oncol. 1(3):339-349.

Doorn van WG and Woltering EJ. (2005) Many ways to exit? Cell death categories in plants. Trends Plant Sci. 10(3): 117-122.

Doucet-Chabeaud G, Godon C, Brutesco C, de Murcia G and Kazmaier M. (2001) Ionising radiation induces the expression of PARP-1 and PARP-2 genes in Arabidopsis. Mol Genet Genomics. 265 (6): 954-963.

D'Silva I, Poirier GG, Heath MC. (1998) Activation of cysteine proteases in cowpea plants during the hypersensitive response - a form of programmed cell death. Exp Cell Res 1998; 245 (2): 389-399.

Earnshaw WC, Martins LM and Kaufmann SH. (1999) Mammalian caspases: Structure, activation, substrates, and functions during apoptosis. Annu Rev Biochem. 68: 383-424.

Elbaz M, Avni A and Weil M. (2002) Constitutive caspase-like machinery executes programmed cell death in plant cells. Cell Death Differ. 9 (7): 726-733.

Estrov Z, Black RA, Sleath PR, Harris D, Van Q, LaPushin R, Estey EH and Talpaz M. (1995) Effect of interleukin-1 beta converting enzyme inhibitor on acute myelogenous leukemia progenitor proliferation. Blood. 86 (12): 4594-4602.

Fan TJ, Xia L and Han YR. (2001) Mitochondrion and apoptosis. Acta Biochim Biophys Sin. 33 (1): 7-12.

Fan TJ, Han LH, Cong RS and Liang J. (2005) Caspase family proteases and apoptosis. Acta Biochim Biophys Sin. 37(11): 719-727.

Fernandes-Alnemri T, Litwack G and Alnemri ES. (1994) CPP32, a novel human apoptotic protein with homology to *Caenorhabditis elegans* cell death protein Ced-3 and mammalian interleukin-1 beta-converting enzyme. J Biol Chem. 269 (49): 30761-30764.

Ferri KF and Kroemer G. (2001) Organelle-specific initiation of cell death pathways. Nat Cell Biol. 3 (11): E255-63.

Fesik SW and Shi Y. (2001) Structural biology. Controlling the caspases. Science. 294 (5546): 1477-1478.

Fietta P. (2006) Many ways to die: passive and active cell death styles. Riv Biol. 99 (1): 69-83.

Filonova LH, Bozhkov PV, Brukhin VB, Daniel G, Zhivotovsky B and von Arnold S. (2000) Two waves of programmed cell death occur during formation and development of somatic embryos in the gymnosperm, Norway spruce. J Cell Sci. 113 (24): 4399-4411.

Fischer U, Janicke RU and Schulze-Osthoff K. (2003) Many cuts to ruin: a comprehensive update of caspase substrates. Cell Death Differ. 10(1):76-100.

Formigli L, Papucci L, Tani A, Schiavone N, Tempestini A, Orlandini GE, Capaccioli S and Orlandini SZ. (2000) Aponecrosis: morphological and biochemical exploration of a syncretic process of cell death sharing apoptosis and necrosis. J Cell Phys. 182 (1): 41-49.

Forte M, Bernardi P. (2005) Genetic dissection of the permeability transition pore. J Bioenerg Biomembr. 37 (3): 121-128.

Fu YF and Fan TJ. (2002) Bcl-2 family proteins and apoptosis. Acta Biochim Biophys Sin. 34 (4): 389-394.

Funk V, Kositsup B, Zhao C and Beers EP (2002) The *Arabidopsis* xylem peptidase XCP1 is a tracheary element vacuolar protein that may be a papain orthology. Plant Physiol. 128 (1): 84-94.

Gozuacik D and Kimchi A. (2004) Autophagy as a cell death and tumor suppressor mechanism. Oncogene. 23 (16): 2891-2906.

Graybill TL, Dolle RE, Helaszek CT, Miller RE and Ator MA. (1994) Preparation and evaluation of peptidic aspartyl hemiacetals as reversible inhibitors of interleukin-1 beta converting enzyme (ICE). Int. J. Pept. Protein Res. 44 (2): 173-182.

Green DR, Kroemer G. (2004) The pathophysiology of mitochondrial cell death. Science. 305 (5684): 626-629.

Groover A, DeWitt N, Heidel A and Jones A. (1997) Programmed cell death of plant tracheary elements differentiating *in vitro*. Protoplasma. 196: 197-211.

Groover A and Jones AM. (1999) Tracheary element differentiation uses a novel mechanism coordinating programmed cell death and secondary cell wall synthesis Plant Physiol. 119 (2): 375-384.

Gross A, McDonnell JM and Korsmeyer SJ. (1999) BCL-2 family members and the mitochondria in apoptosis. Genes Dev. 13 (15): 1899-1911.

Gruis D, Schulze J and Jung R. (2004) Storage protein accumulation in the absence of the vacuolar processing enzyme family of cysteine proteases. Plant Cell. 16 (1): 270-290

Gu Y, Sarnecki C, Aldape RA, Livingston DJ and Su MS. (1995) Cleavage of poly(ADP-ribose) polymerase by interleukin-1*β* converting enzyme and its homologs TX and Nedd-2. J. Biol. Chem. 270(32): 18715-18718.

Gunawardena AH, Sault K, Donnelly P, Greenwood JS and Dengler NG. (2005) Programmed cell death and leaf morphogenesis in *Monstera obliqua* (Araceae). Planta. 221 (5): 607-618.

Hansen G. (2000) Evidence for Agrobacterium-induced apoptosis in maize cells. Mol Plant Microbe Interact. 13 (6): 649-657.

Hara-Nishimura I, Hatsugai N, Nakaune S, Kuroyanagi M and Nishimura M. (2005) Vacuolar processing enzyme: an executor of plant cell death. Curr Opin Plant Biol. 8 (4): 404-408.

Hara-Nishimura I, Inoue K and Nishimura M. (1991) A unique vacuolar processing enzyme responsible for conversion of several proprotein precursors into the mature forms. FEBS Lett. 294 (1-2): 89-93.

Hara-Nishimura I, Kinoshita T, Hiraiwa N and Nishimura M. (1998) Vacuolar processing enzymes in protein-storage vacuoles and lytic vacuoles. J Plant Physiol. 152: 668-674.

Hartmann A, Troadec JD, Hunot S, Kikly K, Faucheux BA, Mouatt-Prigent A, Ruberg M, Agid Y and Hirsch EC. (2001) Caspase-8 is an effector in apoptotic death of dopaminergic neurons in Parkinson's disease, but pathway inhibition results in neuronal necrosis. J Neurosci 21 (7): 2247-2255.

Hatsugai N, Kuroyanagi M, Nishimura M and Hara-Nishimura I. (2006) A cellular suicide strategy of plants: vacuole-mediated cell death. Apoptosis. 11 (6): 905-911.

Hatsugai N, Kuroyanagi M, Yamada K, Meshi T, Tsuda S, Kondo M, Nishimura M and Hara-Nishimura I. (2004) A plant vacuolar protease, VPE, mediates virus-induced hypersensitive cell death. Science. 305 (5685): 855-858.

He X and Kermode AR. (2003 a) Proteases associated with programmed cell death of megagametophyte cells after germination of white spruce (Picea glauca) seeds. Plant Mol Biol. 52 (4): 729-744.

He X and Kermode AR. (2003 b) Nuclease activities and DNA fragmentation during programmed cell death of megagametophyte cells of white spruce (Picea glauca) seeds. Plant Mol Biol. 51 (4): 509-521.

Heath MC. (2000) Hypersensitive response-related death. Plant Mol Biol. 44 (3): 321-334.

Hengartner MO. (2000) The biochemistry of apoptosis. Nature. 407 (6805): 770-776.

Hippeli S, Heiser I and Elstner EF. (1999) Activated oxygen and free oxygen radicals in pathology: New insights and analogies between animals and plants. Plant Physiol Biochem. 37 (3): 167-178.

Ho PK and Hawkins CJ. (2005) Mammalian initiator apoptotic caspases. FEBS J. 272 (21): 5436-5453.

Hoeberichts FA and Woltering EJ. (2003a) Multiple mediators of plant programmed cell death: interplay of conserved cell death mechanisms and plant-specific regulators. BioEssay. 25 (1): 47-57.

Huckelhoven R, Dechert C and Kogel KH. (2003) Overexpression of barley BAX inhibitor 1 induces breakdown of mlo-mediated penetration resistance to *Blumeria graminis*. Proc Natl Acad Sci USA. 100 (9): 5555-5560.

Huckelhoven R, Dechert C, Trujillo M and Kogel KH. (2001) Differential expression of putative cell death regulator genes in near-isogenic, resistant and susceptible barley lines during interaction with the powdery mildew fungus. Plant Mol Biol. 47 (6): 739-748.

Ito J and Fukuda H. (2002) ZEN1 is a key enzyme in degradation of nuclear DNA during programmed cell death of tracheary elements. Plant Cell 14 (12): 3201-3211.

Jin Z and El-Deiry WS. (2005) Overview of cell death signaling pathways. Cancer Biol Ther. 4 (2): 139-163.

Jones AM. (2001) Programmed cell death in development and defense. Plant Physiol. 125 (1): 94-97.

Katsuhara K (1997) Apoptosis-like cell death in barley roots under salt stress. Plant Cell Physiol 38: 1091-1093.

Katsuhara K and Kawasaki T (1996) Salt stress induced nuclear and DNA degradation in meristematic cells of barley roots. Plant Cell Physiol 37: 169-173.

Kawai M, Pan L, Reed JC and Uchimiya H. (1999) Evolutionally conserved plant homologue of the Bax inhibitor-1 (BI-1) gene capable of suppressing Bax-induced cell death in yeast. FEBS Lett. 464 (3): 143-147.

Kawai-Yamada M, Jin L, Yoshinaga K, Hirata A and Uchimiya H. (2001) Mammalian Bax-induced plant cell death can be down-regulated by overexpression of Arabidopsis Bax Inhibitor-1 (AtBI-1). Proc Natl Acad Sci USA. 98 (21): 12295-12300.

Kawanabe T, Ariizumi T, Kawai-Yamada M, Uchimiya H and Toriyama K. (2006) Abolition of the tapetum suicide program ruins microsporogenesis. Plant Cell Physiol. 47 (6): 784-787.

Kerr JF, Wyllie AH and Currie AR. (1972) Apoptosis: a basic biological phenomenon with wide-ranging implications in tissue kinetics. Br J Cancer. 26(4): 239-257

Kim JS, He L and Lemasters JJ. (2003) Mitochondrial permeability transition: a common pathway to necrosis and apoptosis. Biochem Biophys Res Commun. 304 (3): 463-470.

Kim R (2005) Recent advances in understanding the cell death pathways activated by anticancer therapy. Cancer 103 (8): 1551-1560.

Kinoshita T, Yamada K, Hiraiwa N, Kondo M, Nishimura M and Hara-Nishimura I. (1999) Vacuolar processing enzyme is up-regulated in the lytic vacuoles of vegetative tissues during senescence and under various stressed conditions. Plant J. 19(1):43-53.

Korthout HA, Berecki G, Bruin W, Van Duijn B and Wang M. (2000) The presence and subcellular localization of caspase 3-like proteinases in plant cells. FEBS Lett. 475 (2): 139-144.

Krause M and Durner J. (2004) Harpin inactivates mitochondria in Arabidopsis suspension cells. Mol Plant Microbe Interact. 17 (2): 131-139.

Kroemer G and Martin SJ. (2005) Caspase-independent cell death. Nat Med. 11 (7): 725-730.

Kruger J, Thomas CM, Golstein C, Dixon MS, Smoker M, Tang S, Mulder L and Jones JD. (2002) A tomato cysteine protease required for Cf-2-dependent disease resistance and suppression of autonecrosis. Science. 296 (5568): 744-747.

Ku S, Yoon H, Suh HS and Chung YY. (2003) Male-sterility of thermosensitive genic male-sterile rice is associated with premature programmed cell death of the tapetum. Planta. 217 (4): 559-565.

Kuo A, Cappelluti S, Cervantes-Cervantes M, Rodriguez M, Bush DS. (1996) Okadaic acid, a protein phosphatase inhibitor, blocks calcium changes, gene expression, and cell death induced by gibberellin in wheat aleurone cells. Plant Cell. 8 (2): 259-269.

Kuriyama H and Fukuda H. (2002) Developmental programmed cell death in plants. Curr Opin Plant Biol. 5 (6): 568-573.

Kuriyama H. (1999) Loss of tonoplast integrity programmed in tracheary element differentiation. Plant Physiol. 121 (3): 763-774.

Lacomme C and Santa Cruz S. (1999) Bax-induced cell death in tobacco is similar to the hypersensitive response. Proc Natl Acad Sci USA. 96 (14): 7956-7961.

Lam E. (2004). Controlled cell death, plant survival and development. Nat. Rev. Mol. Cell Biol. 5 (4): 305-315.

Lam E, Kato N and Lawton M. (2001) Programmed cell death, mitochondria and the plant hypersensitive response. Nature. 411 (6839): 848-853.

Lam E and del Pozo O. (2000) Caspase-like protease involvement in the control of plant cell death. Plant Mol Biol. 44: 417-428.

Lam E, del Pozo O and Pontier D. (1999) BAXing in the hypersensitive response. Trends Plant Sci. 4(11): 419-421.

Launay S, Hermine O, Fontenay M, Kroemer G, Solary E and Garrido C. (2005) Vital functions for lethal caspases. Oncogene. 24 (33): 5137-5148.

Lawen A. (2003) Apoptosis-an introduction. Bioessays. 25 (9): 888-896.

Lazebnik YA, Kaufmann SH, Desnoyers S, Poirier GG and Earnshaw WC. (1994) Cleavage of poly(ADP-ribose) polymerase by a proteinase with properties like ICE. Nature. 371 (6495): 346-347.

Leist M, Single B, Castoldi AF, Kuhnle S and Nicotera P. (1997) Intracellular adenosine triphosphate (ATP) concentration: a switch in the decision between apoptosis and necrosis. J Exp Med. 185 (8): 1481-1486.

Leist M. and Jaattela M. (2001) Four deaths and a funeral: from caspases to alternative mechanisms. Nature Rev Mol Cell Biol. 2 (8): 589-598.

Levine B and Klionsky DJ. (2004) Development by self-digestion: molecular mechanisms and biological functions of autophagy. Dev Cell. 6 (4): 463-477.

Levine A, Pennell RI, Alvarez ME, Palmer R and Lamb C. (1996) Calcium-mediated apoptosis in a plant hypersensitive disease resistance response. Curr Biol. 6 (4): 427-437.

Levine A, Tenhaken R, Dixon R and Lamb C. (1994) H_2O_2 from the oxidative burst orchestrates the plant hypersensitive disease resistance response. Cell. 79 (4): 583-593.

Li P, Nijhawan D, Budihardjo I, Srinivasula SM, Ahmad M, Alnemri ES and Wang X. (1997) Cytochrome c and dATP-dependent formation of Apaf-1/caspase-9 complex initiates an apoptotic protease cascade. Cell. 91(4): 479-489.

Liu QA and Hengartner MO. (1999) The molecular mechanism of programmed cell death in *C. elegans*. Ann NY Acad Sci. 887:92-104.

Liu Y, Schiff M, Czymmek K, Talloczy Z, Levine B and Dinesh-Kumar SP. (2005) Autophagy regulates programmed cell death during the plant innate immune response. Cell. 121 (4): 567-577.

Lockshin RA and Zakeri Z. (2002) Caspase-independent cell deaths. Curr Opin Cell Biol. 14 (6): 727-733.

Lockshin RA, Zakeri Z. (2004) Apoptosis, autophagy, and more. Int J Biochem Cell Biol. 36 (12): 2405-2419.

Lopez-Otin C and Overall CM. (2002) Protease degradomics: a new challenge for proteomics. Nat Rev Mol Cell Biol. 3 (7): 509-519.

Lorrain S, Vailleau F, Balague C and Roby D. (2003) Lesion mimic mutants: keys for deciphering cell death and defense pathways in plants? Trends Plant Sci. 8(6): 263-271.

Lü CX, Fan TJ, Hu GB and Cong RS. (2003) Apoptosis-inducing factor and apoptosis. Acta Biochim Biophys Sin. 35 (10): 881-885.

McCabe PF, Levine A, Meijer P-J, Tapon NA and Pennell RI. (1997) A programmed cell death pathway activated in carrot cells cultured at low cell density. Plant J. 12: 267-280.

Madeo F, Herker E, Maldener C, Wissing S, Lachelt S, Herlan M, Fehr M, Lauber K, Sigrist SJ, Wesselborg S and Frohlich KU. (2002) A caspase-related protease regulates apoptosis in yeast. Mol Cell. 9 (4): 911-917.

Maraschin SF, Gaussand G, Pulido A, Olmedilla A, Lamers GEM, Korthout H, Spaink HP and Wang M. (2005) Programmed cell death during the transition from multicellular structures to globular embryos in barley androgenesis. Planta. 221 (4): 459-470.

Meier P, Finch A and Evan G. (2000) Apoptosis in development. Nature. 407 (6805): 796-801.

Milosevic J, Hoffarth S, Huber C and Schuler M. (2003) The DNA damage-induced decrease of Bcl-2 is secondary to the activation of apoptotic effector caspases. Oncogene. 22 (44): 6852-6856.

Minami A and Fukuda H. (1995) Transient and specific expression of a cysteine endopeptidase associated with autolysis during differentiation of Zinnia mesophyll cells into tracheary elements. Plant Cell Physiol. 36 (8): 1599-1606.

Mitsuhara I, Malik KA, Miura M and Ohashi Y. (1999) Animal cell-death suppressors Bcl-x(L) and Ced-9 inhibit cell death in tobacco plants. Curr Biol. 9 (14): 775-778.

Mittler R, Lam E, Shulaev V and Cohen M. (1999) Signals controlling the expression of cytosolic ascorbate peroxidase during pathogen-induced programmed cell death in tobacco. Plant Mol Biol. 39 (5): 1025-1035.

Mlejnek P and Prochazka S. (2002) Activation of caspase-like proteases and induction of apoptosis by isopentenyladenosine in tobacco BY-2 cells. Planta. 215 (1): 158-166.

Momoi T. (2004) Caspases involved in ER stress-mediated cell death. J Chem Neuroanat. 28 (1-2): 101-105.

Nicholson DW. (1999) Caspase structure, proteolytic substrates, and function during apoptotic cell death. Cell Death Differ. 6 (11): 1028-1042.

Nicholson DW, Ali A, Thornberry NA, Vaillancourt JP, Ding CK, Gallant M, Gareau Y, Griffin PR, Labelle M, Lazebnik YA, Munday NA, Raju SM, Smulson ME, Yamin TT, Yu VL and Miller DK. (1995) Identification and inhibition of the ICE/CED-3 protease necessary for mammalian apoptosis. Nature. 376 (6535): 37-43.

Nicotera P, Leist M, and Ferrando-May E. (1998) Intracellular ATP, a switch in the decision between apoptosis and necrosis. Toxicol Lett. 102-103: 139-142

Nunez G, Benedict MA, Hu Y and Inohara N. (1998) Caspases: the proteases of the apoptotic pathway. Oncogene. 17 (25): 3237-3245.

Obara K, Kuriyama H and Fukuda H. (2001) Direct evidence of active and rapid nuclear degradation triggered by vacuole rupture during programmed cell death in *Zinnia*. Plant Physiol. 125 (2): 615-626.

Oh SA, Lee SY, Chung IK, Lee CH and Nam HG. (1996) A senescence-associated gene of Arabidopsis thaliana is distinctively regulated during natural and artificially induced leaf senescence. Plant Mol Biol. 30 (4): 739-754.

Papini A, Mosti S and Brighigna L. (1999) Programmed-cell-death events during tapetum development of angiosperms. Protoplasma 207: 213-221.

Pennell RI and Lamb C. (1997) Programmed cell death in plants. Plant Cell 9 (7): 1157-1168.

Plomp PJ, Gordon PB, Meijer AJ, Hoyvik H and Seglen PO. (1989) Energy dependence of different steps in the autophagic-lysosomal pathway. J Biol Chem. 264 (12): 6699-6704.

Pontier D, Balague C and Roby D. (1998) The hypersensitive response. A programmed cell death associated with plant resistance. C R Acad Sci III. 321 (9):721-734.

Pusztai L, Krishnamurti S, Perez Cardona J, Sneige N, Esteva FJ, Volchenok M, Breitenfelder P, Kau SW, Takayama S, Krajewski S, Reed JC, Bast RC Jr and Hortobagyi GN. (2004) Expression of BAG-1 and BcL-2 proteins before and after neoadjuvant chemotherapy of locally advanced breast cancer. Cancer Invest. 22 (2): 248-256.

Putcha GV and Johnson EM Jr. (2004) Men are but worms: neuronal cell death in *C. elegans* and vertebrates. Cell Death Differ. 11 (1): 38-48.

Riedl SJ and Shi Y. (2004) Molecular mechanisms of caspase regulation during apoptosis. Nat Rev Mol Cell Biol. 5 (11): 897-907.

Rohn TT, Head E, Nesse WH, Cotman CW and Cribbs DH (2001) Activation of caspase-8 in the Alzheimer's disease brain. Neurobiol Dis. 8 (6): 1006-1016.

Rohn TT, Rissman RA, Davis MC, Kim YE, Cotman CW and Head E (2002) Caspase-9 activation and caspase cleavage of tau in the Alzheimer's disease brain. Neurobiol Dis. 11(2): 341-354.

Rojo E, Zouhar J, Carter C, Kovaleva V and Raikhel NV. (2003) A unique mechanism for protein processing and degradation in Arabidopsis thaliana. Proc. Natl. Acad. Sci. USA 100 (12): 7389-7394.

Rojo E, Martin R, Carter C, Zouhar J, Pan S, Plotnikova J, Jin H, Paneque M, Sanchez-Serrano JJ, Baker B, Ausubel FM, Raikhel NV. (2004) VPE gamma exhibits a caspase-like activity that contributes to defense against pathogens. Curr Biol. 14 (21): 1897-1906.

Rotari VI, HE R and Gallois P. (2005) Death by proteases in plants: whodunit. Physiologia plantarum. 123 (4): 376-385.

Ruchaud S, Korfali N, Villa P, Kottke TJ, Dingwall C, Kaufmann SH and Earnshaw WC. (2002) Caspase-6 gene disruption reveals a requirement for lamin A cleavage in apoptotic chromatin condensation. EMBO J. 21 (8): 1967-1977.

Runeberg-Roos P and Saarma M. (1998) Phytepsin, a barley vacuolar aspartic proteinase, is highly expressed during autolysis of developing tracheary elements and sieve cells. Plant J. 15 (1): 139-145.

Ryerson DE and Heath MC. (1996) Cleavage of nuclear DNA into oligonucleosomal fragments during cell death induced by fungal infection or by abiotic treatments. Plant Cell. 8 (3): 393-402.

Sanchez P, de Torres Zabala M and Grant M. (2000) AtBI-1, a plant homologue of Bax inhibitor-1, suppresses Bax-induced cell death in yeast and is rapidly upregulated during wounding and pathogen challenge. Plant J. 21 (4): 393-399.

Sanchez I, Xu CJ, Juo P, Kakizaka A, Blenis J and Yuan J (1999) Caspase-8 is required for cell death induced by expanded polyglutamine repeats. Neuron. 22 (3): 623-633.

Sarkkinen P, Kalkkinen N, Tilgmann C, Siuro J, Kervinen J and Mikola L. (1992) Aspartic proteinase from barley grains is related to mammalian lysosomal cathepsin D. Planta. 186 (3): 317-323.

Schmid M, Simpson D and Gietl C. (1999) Programmed cell death in castor bean endosperm is associated with the accumulation and release of a cysteine endopeptidase from ricinosomes. Proc Natl Acad Sci USA. 96 (24): 14159-14164.

Schmid M, Simpson D, Kalousek F and Gietl C. (1998) A cysteine endopeptidase with a C-terminal KDEL motif isolated from castor bean endosperm is a marker enzyme for the ricinosome, a putative lytic compartment. Planta. 206 (3): 466-475.

Schmid M, Simpson DJ, Sarioglu H, Lottspeich F and Gietl C. (2001) The ricinosomes of senescing plant tissue bud from the endoplasmic reticulum. Proc Natl Acad Sci USA. 98 (9): 5353-5358.

Schreiber V, Molinete M, Boeuf H, de Murcia G and Menissier-de Murcia J. (1992) The human poly (ADP-ribose) polymerase nuclear localization signal is a bipartite element functionally separate from DNA binding and catalytic activity. EMBO J. 11(9): 3263–3269

Serafini-Fracassini D, Del Duca S, Monti F, Poli F, Sacchetti G, Bregoli AM, Biondi S and Della Mea M. (2002) Transglutaminase activity during senescence and programmed cell death in the corolla of tobacco (*Nicotiana tabacum*) flowers. Cell Death Differ. 9 (3): 309-321.

Shimada T, Yamada K, Kataoka M, Nakaune S, Koumoto Y, Kuroyanagi M, Tabata S, Kato T, Shinozaki K, Seki M, Kobayashi M, Kondo M, Nishimura M, Hara-Nishimura I. (2003) Vacuolar processing enzymes are essential for proper processing of seed storage proteins in *Arabidopsis thaliana*. J Biol Chem. 278 (34): 32292-32299.

Shirahama-Noda K, Yamamoto A, Sugihara K, Hashimoto N, Asano M, Nishimura M and Hara-Nishimura I. (2003) Biosynthetic processing of cathepsins and lysosomal degradation are abolished in asparaginyl endopeptidase-deficient mice. J Biol Chem. 278 (35): 33194-33199.

Solomon M, Belenghi B, Delledonne M, Menachem E and Levine A. (1999) The involvement of cysteine proteases and protease inhibitor genes in the regulation of programmed cell death in plants. Plant Cell. 11 (3): 431-444.

Stein JC and Hansen G. (1999) Mannose induces an endonuclease responsible for DNA laddering in plant cells. Plant Physiol 121 (1): 71-80.

Steller H. (1995) Mechanisms and genes of cellular suicide. Science. 267 (5203): 1445-1449.

Stennicke HR and Salvesen GS. (2000) Caspase assays. Methods Enzymol. 322: 91-100.

Suarez MF, Filonova LH, Smertenko A, Savenkov EI, Clapham DH, von Arnold S, Zhivotovsky B and Bozhkov PV. (2004) Metacaspase-dependent programmed cell death is essential for plant embryogenesis. Curr biol. 14 (9): R339–R340.

Sun YL, Zhao Y, Hong X and Zhai ZH. (1999) Cytochrome c release and caspase activation during menadione-induced apoptosis in plants. FEBS Lett. 462 (3): 317-321.

Tacconi S, Perri R, Balestrieri E, Grelli S, Bernardini S, Annichiarico R, Mastino A, Caltagirone C and Macchi B. (2004) Increased caspase activation in peripheral blood mononuclear cells of patients with Alzheimer's disease. Exp Neurol. 190 (1): 254-262.

Tewari M, Quan LT, O'Rourke K, Desnoyers S, Zeng Z, Beidler DR, Poirier GG, Salvesen GS and Dixit VM. (1995) Yama/CPP32 beta, a mammalian homolog of CED-3, is a CrmA-inhibitable protease that cleaves the death substrate poly (ADP-ribose) polymerase. Cell. 81 (5): 801-809.

Thomas SG and Franklin-Tong VE. (2004) Self-incompatibility triggers programmed cell death in Papaver pollen. Nature. 429 (6989): 305-309.

Thompson CB. (1995) Apoptosis in the pathogenesis and treatment of disease. Science. 267 (5203): 1456-1462.

Thornberry NA, Bull HG, Calaycay JR, Chapman KT, Howard AD, Kostura MJ, Miller DK, Molineaux SM, Weidner JR, Aunins J, Elliston KO, Ayala JM, Casano FJ, Chin J, Ding GJF, Egger LA, Gaffney EP, Limjuco G, Palyha OC, Raju SM, Rolando AM, Salley JP, Yamin TT, Lee TD, Shively JE, Maccross M, Mumford RA, Schmidt JA and Tocci MJ. (1992) A novel heterodimeric cysteine protease is required for interleukin-1 beta processing in monocytes. Nature 356 (6372): 768-774.

Thornberry NA and Lazebnik Y. (1998) Caspases: enemies within. Science. 281 (5381): 1312-1316.

Tian R, Zhang G, Yan C and Dai Y. (2000) Involvement of poly (ADP-ribose) polymerase and activation of caspase-3- like protease in heat shock-induced apoptosis in tobacco suspension cells. FEBS Lett. 474 (1): 11-15.

Tiwari BS, Belenghi B and Levine A. (2002) Oxidative stress increased respiration and generation of reactive oxygen species, resulting in ATP depletion, opening of mitochondrial permeability transition, and programmed cell death. Plant Physiol. 128 (4): 1271-1281.

U M, Miyashita T, Ohtsuka Y, Okamura-Oho Y, Shikama Y and Yamada M. (2001) Extended polyglutamine selectively interacts with caspase-8 and -10 in nuclear aggregates. Cell Death Differ. 8 (4): 377-386.

Uren AG, Coulson EJ and Vaux DL. (1998) Conservation of baculovirus inhibitor of apoptosis repeat proteins (BIRPs) in viruses, nematodes, vertebrates and yeasts. Trends Biochem Sci. 23 (5): 159-162

Uren AG, O'Rourke K, Aravind LA, Pisabarro MT, Seshagiri S, Koonin EV, Dixit VM. (2000) Identification of paracaspases and metacaspases: two ancient families of caspase-like proteins, one of which plays a key role in MALT lymphoma. Mol Cell. 6 (4): 961-967.

Vacca RA, de Pinto MC, Valenti D, Passarella S, Marra E and De Gara L. (2004) Production of reactive oxygen species, alteration of cytosolic ascorbate peroxidase, and impairment of mitochondrial metabolism are early events in heat shock-induced programmed cell death in tobacco Bright-Yellow 2 cells. Plant Physiol. 134 (3): 1100-1112.

Vaux DL, Cory S and Adams JM. (1988) Bcl-2 gene promotes haemopoietic cell survival and cooperates with c-myc to immortalize pre-B cells. Nature. 335 (6189): 440-442.

Vera P and Conejero V. (1988) Pathogenesis-related proteins of tomato : P-69 as an alkaline endoproteinase. Plant Physiol. 87 (1): 58-63.

Viswanath V, Wu Y, Boonplueang R, Chen S, Stevenson FF, Yantiri F, Yang L, Beal MF and Andersen JK. (2001) Caspase-9 activation results in downstream caspase-8 activation and bid cleavage in 1-methyl-4-phenyl-1,2,3,6-tetrahydropyridine-induced Parkinson's disease. J Neurosci. 21 (24): 9519-9528.

Wan L, Xia Q, Qiu X and Selvaraj G. (2002) Early stages of seed development in *Brassica napus*: a seed coat-specific cysteine proteinase associated with programmed cell death of the inner integument. Plant J. 30 (1): 1-10.

Wang M, Oppedijk BJ, Lu X, van Duijn B and Schilperoort RA. (1996a) Apoptosis in barley aleurone during germination and its inhibition by abscisic acid. Plant Mol Biol 32: 1125-1134.

Wang H, Li J, Bostock RM and Gilchrist DG. (1996b) Apoptosis: A functional paradigm for programmed plant cell death induced by a host-selective phytotoxin and invoked during development. Plant Cell 8 (3): 375-391.

Wang M, Oppedijk BJ, Caspers MPM, Lamers GEM, Boot MJ, Geerlings DNG, Bakhuizen B, Meijer AH and van Duijn B. (1998) Spatial and temporal regulation of DNA fragmentation in the aleurone of germinating barley. J Exp Bot 325: 1293-1301.

Wang M, Hoekstra S, van Bergen S, Lamers GE, Oppedijk BJ, van der Heijden MW, de Priester W and Schilperoort RA. (1999) Apoptosis in developing anthers and the role of ABA in this process during androgenesis in Hordeum vulgare L. Plant Mol Biol. 39 (3): 489-501.

Watanabe N and Lam E. (2005) Two Arabidopsis metacaspases AtMCP1b and AtMCP2b are arginine/lysine-specific cysteine proteases and activate apoptosis-like cell death in yeast. J Biol Chem. 280 (15): 14691-14699.

Watanabe N and Lam E. (2006) Arabidopsis Bax inhibitor-1 functions as an attenuator of biotic and abiotic types of cell death. Plant J. 45 (6): 884-894.

Willekens H, Chamnongpol S, Davey M, Schraudner M, Langebartels C, Van Montagu M, Inze D and Van Camp W. (1997) Catalase is a sink for H2O2 and is indispensable for stress defence in C3 plants. EMBO J. 16 (16): 4806-4816.

Wojciechowska M and Olszewska MJ. (2003) Endosperm degradation during seed development of *Echinocystis lobata* (Cucurbitaceae) as a manifestation of programmed cell death (PCD) in plants.Folia Histochem Cytobiol. 41 (1): 41-50.

Wolf BB and Green DR. (1999) Suicidal tendencies: apoptotic cell death by caspase family proteinases. J Biol Chem. 274 (29): 20049-20052.

Woltering EJ, van der Bent A and Hoeberichts FA. (2002) Do plant caspases exist? Plant Physiol. 130 (4): 1764-1769.

Woltering EJ. (2004) Death proteases come alive. Trends Plant Sci. 9 (10): 469-472.

Wu H and Cheung AY. (2000) Programmed cell death in plant reproduction. Plant Mol Biol. 44: 267-281.

Wyllie AH. (1980) Glucocorticoid-induced thymocyte apoptosis is associated with endogenous endonuclease activation. Nature. 284 (5756): 555-556.

Yamada K, Shimada T, Kondo M, Nishimura M, Hara-Nishimura I. (1999) Multiple functional proteins are produced by cleaving Asn-Gln bonds of a single precursor by vacuolar processing enzyme. J Biol Chem. 274 (4): 2563-2570.

Yao N, Eisfelder BJ, Marvin J and Greenberg JT. (2004) The mitochondrion – an organelle commonly involved in programmed cell death in *Arabidopsis thaliana*. Plant J. 40 (4): 596-610.

Ye ZH and Varner JE. (1996) Induction of cysteine and serine proteases during xylogenesis in *Zinnia elegans*. Plant Mol Biol. 30 (6): 1233-1246.

Yew DT, Ping Li W and Liu WK (2004) Fas and activated caspase 8 in normal, Alzheimer and multiple infarct brains. Neurosci Lett 367 (1): 113-117.

Yoshinaga K, Arimura SI, Hirata A, Niwa Y, Yun DJ, Tsutsumi N, Uchimiya H and Kawai-Yamada M. (2005) Mammalian Bax initiates plant cell death through organelle destruction. Plant Cell Rep. 24 (7): 408-417.

Young TE and Gallie DR. (2000) Programmed cell death during endosperm development. Plant Mol Biol. 44 (3): 283-301.

Yu XH, Perdue TD, Heimer YM and Jones AM. (2002) Mitochondrial involvement in tracheary element programmed cell death. Cell Death Differ. 9 (2): 189-198.

Yuan J, Shaham S, Ledoux S, Ellis HM and Horvitz HR. (1993) The *C. elegans* cell death gene ced-3 encodes a protein similar to mammalian interleukin-b-converting enzyme. Cell 75 (4): 641-652.

Zamzami N, Brenner C, Marzo I, Susin SA and Kroemer G. (1998) Subcellular and submitochondrial mode of action of Bcl-2-like oncoproteins. Oncogene. 16 (17): 2265-2282.

Zhang X, Shan P, Sasidhar M, Chupp GL, Flavell RA, Choi AM and Lee PJ. (2003) Reactive oxygen species and extracellular signal-regulated kinase 1/2 mitogen-activated protein kinase mediate hyperoxia-induced cell death in lung epithelium. Am J Respir Cell Mol Biol. 28 (3): 305-315.

Zhao Y, Jiang ZF, Sun YL and Zhai ZH. (1999) Apoptosis of mouse liver nuclei induced in the cytosol of carrot cells. FEBS Lett. 448 (1): 197-200.

Zhivotovsky B. (2003) Caspases: the enzymes of death. Essays Biochem. 39: 25-40.

Chapter 2

Programmed cell death in the leaves of the *Arabidopsis* spontaneous necrotic spot (*sns*) mutant

Gwénaël M.D.J-M Gaussand, Eric van der Graaff, Gerda E.M. Lamers, Paul F. Fransz, B. Sylvia de Pater and Paul J.J. Hooykaas

Abstract

A pool of transgenic Arabidopsis plants harboring the activator T-DNA construct pSDM1550 was screened for altered phenotypes. One of the transgenic plants identified was the spontaneous necrotic spots (*sns)* mutant which develops necrotic spots during development. Those spots are visible on the leaves after two or three weeks of growth, resembling the lesions that accompany the hypersensitive response after a pathogen attack. Both the T-DNA and the binary vector are inserted in the 3'UTR of the gene At1g13020 which encodes a putative eukaryotic translation initiation factor, eIF4B5. Heterozygous hygromycin-resistant progeny and hygromycin-sensitive progeny showed a ratio of 2:1, which suggests that *sns* homozygous plants are embryo lethal, and that the *sns* mutation is dominant or leads to haplo-insufficiency. The present study attempted to establish whether the Arabidopsis *sns* mutant is a lesion mimic mutant in which PCD occurs. Therefore, the phenotype of the *sns* mutant plants was analyzed in detail in order to explain the effect of the mutation on the leaves. By use of TUNEL analysis DNA fragmentation was found in the nuclei of cells in the necrotic spots. In addition a significant increase of caspase-3 and -6 like activities was found in *sns* leaf extracts. This indicates that the mutation causes local cell death by PCD.

As a consequence of the T-DNA and binary vector integration, the expression level of some genes in the vicinity of the insertion site was changed. Because the insertion could not be precisely mapped by rescue of border fragments, a FISH study was done to localize the T-DNA and the binary vector insertion. This revealed that, due to the insertion, a chromosomal rearrangement had occurred on chromosome I.

Introduction

Cell death may occur via the process of necrosis or as programmed cell death (PCD). Necrosis is a consequence of persistent trauma and is not considered to be genetically coordinated (Gilchrist 1998; Pasqualini et al. 2003). PCD is genetically controlled and is characterized by cell shrinkage, cytoplasmic condensation, chromatin condensation, and DNA fragmentation. In plants, PCD is a normal process involved in development of anthers, megagametophytes, and vascular tissues (Jones & Dangl 1996; Pennell & Lamb 1997; Wang et al. 1999), in senescence and pollination (Wang et al. 1996a; Groover et al. 1997; Yen & Yang 1998; Panavas et al. 2000; Wu & Cheung 2000) as well as in seed germination (Wang et al. 1996b; 1998). Plants also employ PCD as a controlled response to different biotic and

abiotic stresses (Greenberg & Ausubel 1993; Greenberg et al. 1994; Ryerson & Heath 1996; McCabe et al. 1997; Solomon et al. 1999; Huh et al. 2002).

In response to pathogen attacks plants have developed complex signaling and defense mechanisms. One of the most efficient and immediate resistance mechanisms is the hypersensitive response (HR), which is characterized by the rapid death of the plant cells directly in contact with, or close to the pathogen. Several studies have shown that the death of plant cells during HR in the incompatible plant-pathogen interaction results from the activation of a PCD pathway in cells at the infection site (Greenberg et al. 1994; Wang et al. 1996c; Lorrain et al. 2003).

Researchers have made considerable efforts to identify genes involved in the control and execution of the hypersensitive cell death. They, for example, identified mutant lines in which cell death is deregulated. These mutants are called lesion mimics because their phenotypes resemble those of plants in which HR cell death is invoked by a pathogen. Many mutants exhibiting spontaneous cell death were initially isolated in maize (Hoisington et al. 1982). They have also been identified in other plants, including rice (Takahashi et al. 1999), barley (Wolter et al. 1993) and Arabidopsis (Greenberg & Ausubel 1993; Dietrich et al. 1994; Greenberg et al. 1994). Lesion mimic mutants show different lesion phenotypes with respect to the timing and conditions of lesion appearance, and with respect to the color and the size of the lesions. They are classified into two groups: initiation mutants and feedback or propagation mutants (Lorrain et al. 2003). This classification is based upon the assumption that two different mechanisms are involved in controlling cell death: a pathway to initiate PCD and a pathway to suppress PCD. Initiation mutants form localized necrotic spots of determinate size, whereas propagation mutants are unable to control the rate and extent of the lesions.

Agrobacterium-mediated plant transformation is the most popular and reliable method to introduce foreign genes into plants. During the *Agrobacterium* infection a segment of the tumor-inducing (Ti) plasmid, which is delimited by two short border sequences and which is called the T-region, is transferred to the plant cell nucleus. The segment is transferred in a single-stranded linear form (T-strand) which in the plant cell nucleus is integrated into the host genome in a random fashion (Vergunst et al. 2000). The *Agrobacterium* plant vector system allows the transfer of any DNA segment to plant cells, provided that the segment is surrounded by the 24 bp T-DNA border repeats. To accommodate plant genetic engineering, plant binary vectors were developed in which the T-DNA is present on a small replicon (Hoekema et al. 1984). According to several reports, not only the T-DNA but also vector parts are sometimes transferred from *Agrobacteria* that carry such binary vectors (Martineau et al. 1994; van der Graaff et al. 1996). A pool of transgenic

Arabidopsis plants harboring the activator T-DNA construct pSDM1550 was screened in the laboratory for altered phenotypes. To establish whether an altered phenotype was linked to the T-DNA insert, putative lines exhibiting such a mutant phenotype were analyzed. One of those lines identified was the spontaneous necrotic spots (*sns*) mutant which develops necrotic spots during development.

The present study attempted to establish whether the Arabidopsis *sns* mutant is a lesion mimic mutant in which PCD occurs. The phenotype of the *sns* mutant plants was analyzed in detail, and also biochemical analyses were done for caspase-like activity and DNA fragmentation. Furthermore, the consequences of T-DNA and binary vector integration for the expression level of the genes surrounding the insertion were studied. Finally, the genomic rearrangement in the *sns* mutant plants was analyzed by the FISH technique.

Material and methods

Plant material and microscopy

Arabidopsis thaliana (ecotype C24) wild-type and *sns* (van der Graaff, 1997) seeds were sterilized by incubation during 1 minute in 70% ethanol, then 30 minutes in 1% hypochlorite, followed by four rinses with sterile water. Seeds were imbibed on solidified ½ MS medium, in the dark, for two to four days at 4°C. The seeds were then placed in a culture chamber (21°C, sixteen hours of light/eight hours of dark, 3000 lux) to germinate. The transgenic plants were selected by germination on hygromycin-containing medium (Duchefa Biochemie, The Netherlands, 10 mg/l). Hygromycin-resistant seedlings were scored 2 weeks after germination. All microscopic images of the wild-type and *sns* plants were recorded with a Leica MZ12 stereomicroscope (Leica Microsystems, The Netherlands), equipped with a Sony DKC-5000 camera, and compiled with Adobe Photoshop 6.0.

Scanning electron microscopy (SEM)

One and five weeks old wild-type and *sns* seedlings were fixed in a mixture of 2% (w/v) paraformaldehyde and 2.5% (v/v) glutaraldehyde in 0.1 M sodium cacodylate buffer, pH 7.3, for three hours at room temperature. Samples were dehydrated through a graded series of 50%, 70%, 90%, 96% and 100% (v/v) acetone and then dried with a Bal-Tec CPD 030 critical point drier (The Netherlands). The samples were then mounted on stubs, coated with gold on a Polaron SEM coating unit E5100 and observed by use of a Jeol 6400 scanning electron microscope (Japan). SEM pictures were used to estimate the number of stomata on both adaxial and abaxial sides of wild-type and *sns* leaves. The number of stomata was estimated

on several regions of 100 µm x 100 µm leaf tissues of one week old cotyledons and five weeks old leaves. The number of stomata was estimated on 2 leaves per plant and tested on 5 plants.

Crude protein extraction and caspase assays

Ten plants of about five weeks old were ground in 10 ml ice-cold extraction buffer containing 100 mM HEPES (pH 7.2), 10% (w/v) sucrose, 0.1% (w/v) CHAPS, 5 mM DTT and 10^{-6} % (v/v) NP40 with an Ultrathurrax (three pulses at 24000 rpm of 30 seconds each with 30 seconds intervals, on ice). Subsequently, the homogenate was incubated on ice for 15 minutes. Then the homogenate was centrifuged to pellet cell debris at 2000 g for 5 minutes. The supernatant of the previous centrifugation was centrifuged to pellet cell debris and microsomal fraction for 10 minutes at 100000 g at 4°C. The lipid layer was removed from the surface by sucking with a needle and a syringe. The soluble protein extract was filtered over a 0.22 µm Millex syringe driven filter unit (Millipore Corporation, USA). Protein concentrations were determined using the Bradford method (Bio-Rad, USA) with BSA as the standard (Bradford 1977). In a 96-well plate, 75 µl of soluble protein extract containing 5 µg of proteins were mixed with 25 µl of the synthetic fluorogenic caspase-3 or caspase-6 substrates (Ac-DEVD-AMC or Ac-VEID-AMC, respectively, 75 µM final concentration in assay, Calbiochem, USA). The specificity was measured by addition of caspase-3 or caspase-6 inhibitor (Ac-DEVD-CHO or Ac-VEID-CHO respectively, 250 µM final concentration in assay). During two hours, the proteolytic activity was measured every 10 minutes at room temperature in triplicates per sample. Substrate cleavage was detected in a fluorescence spectrometer LS50B (Perkin Elmer, USA) at an excitation wavelength of 380 nm and an emission wavelength of 460 nm. The standard setting chosen was an excitation and an emission slit value of 5.0. Kinetics of substrate hydrolysis was tested to be linear throughout two hours of reaction. The caspase-like activity was calculated in fluorescence units (relative fluorescence units correlated with substrate hydrolysis) per µg protein per hour. The data presented were representative of three independent experiments (n = 3) with three different extracts and the data were represented as mean ± SD.

Terminal deoxynucleotidyl transferase-mediated dUTP nick end labeling (TUNEL)

Five weeks old wild-type or *sns* leaves were fixed in 2% (w/v) glutaraldehyde in 10 mM NaH_2PO_4, 120 mM NaCl, 2.7 mM KCl, pH 7.4 (phosphate-buffered saline, PBS) overnight at room temperature. After dehydration at room temperature in a graded series of 70%, 90%, 96% and 100% (v/v) ethanol, samples were embedded in Technovit (Heraeus Kulzer, Germany). Sections (2 µm) were attached on Biobond (Biocell, UK) coated slides. Terminal

deoxynucleotidyl transferase-mediated dUTP nick end labeling (TUNEL) assay was done with an *in situ* cell death detection kit (Roche, Germany) according to the manufacturer's instructions. Following TUNEL reaction, Sytox orange nuclear staining was performed as described (Maraschin et al. 2005). Samples were observed by use of a Zeiss Axioplan confocal microscope (The Netherlands) with a MRC 1024 ES Biorad module. An Argon/Krypton laser (488/568nm) was used to visualize the TUNEL (Ex 488 nm, Em 522 DF 32) and the Sytox orange (Ex 568, Em 605 DF 32) signals. The images were compiled with Adobe Photoshop 6.0.

Total RNA isolation and northern blot analysis

Total RNA was isolated from entire wild-type and *sns* plants or from separate organs (flowers, leaves or roots) with an RNeasy Plant Mini Kit (Qiagen, USA) according to the instructions of the manufacturer and then treated with RNase free DNase (Promega, USA). Of the total RNA sample, 10 µg was separated electrophoretically along with a RNA marker (GibcoBRL, USA) in a 1.5% (w/v) agarose gel containing 2% (v/v) formaldehyde, 20 mM 3-(N-morpholino) propanesulfonic acid, 8 mM sodium acetate, 10 mM EDTA, pH 7.0; blotted with 50 mM Na-phosphate buffer pH6.5 and 5 mM EDTA onto hybond-N (Amersham Biosciences, Sweden) membranes and hybridized with ^{32}P-labeled cDNA probes as described previously (Menke et al. 1999). To generate radioactively labeled [32P]dCTP probes the following gene fragments were used: At1g12980 (AP2 domain-containing transcription factor, putative/enhancer of shoot regeneration); At1g12990 (glycosyl transferase family 17 protein); At1g13000 (unknown protein); At1g13020 (eukaryotic translation initiation factor, putative eIF4B5 eukaryotic initiation factor 4B); At1g13030 (unknown protein, possible sphere organelles protein-related). Each gene fragment was amplified from cDNA with primers (5'-GCCTCACCTGTTAGCCGCAACCGC-3') and (5'-CGAGAGGAACACGAGGCGTCGCG-3') for At1g12980; (5'-GAAGACTGATGATATCTGCGG-3') and (5'-CGCCAAGATTTCATCAGACTGTCG-3') for At1g12990; (5'-GCATACATGGTCATCTAGGGGTCCG-3') and (5'-GCAGGCTGCGATATCTCTAGACCG-3') for At1g13000; (5'-GAGGGAGAGAGGATGTTGAAGG-3') and (5'-CCATCCTTCCCTTGCTGACG-3') for At1g13020; (5'-CTTGGACACCCGAGGTTTCC-3') and (5'-CCATGAGCCTCCACTTGAACTCCC-3') for At1g13030, respectively. The primers (5'-CGGGAAGGATCGTGATGGA-3') and (5'-CCAACCTTCTCGATGGCCT-3') were used to amplify a 400 bp fragment from the cyclophilin cDNA (AtROC1, At4g38740). PCR conditions were as follows: 2 minutes at 95°C, 35 cycles (30 for AtROC1) of 30 seconds at 95°C, 30 seconds at 60°C and 2 minutes at 72°C, followed by 5 minutes at 72°C. The corresponding cDNA fragments were purified from agarose gels using Qiaquick Gel Extraction kit (Qiagen, USA) according to the

manufacturer's instructions. cDNA probes were labeled with Prime a Gene labeling system kit (Promega, USA) and purified by use of ProbeQuant G-50 micro columns (Amersham Biosciences, Sweden) according to the manufacturer's instructions.

Fluorescence in situ hybridization (FISH)

Flower buds were used as a source for nuclei preparations. Tissue fixation, cell spreading and screening for appropriate stages have been described by Schubert et al. (2001). Selected nuclei preparations were used for fluorescence *in situ* hybridization (FISH) as described by Schubert et al. (2001). BAC F3F19 and BAC F13K23 are adjacent on the chromosome I and located near the T-DNA and vector integration. The BAC regions on the chromosome I were hybridized with F3F19 and F13K23 sequences labeled with biotin-dUTP and digoxigenin-dUTP, and detected with rhodamine-labeled streptavidin (red fluorescence) and fluorescein isothiocyanate-labeled anti-digoxigenin (green fluorescence), respectively. The preparations were counterstained and mounted in 1 mg/ml 4', 6-diamidino-2-phenylindole (DAPI) in Vectashield (Vecta Laboratories, UK). Preparations were analyzed with a microscope (model BH2-RFC; Olympus, Japan) equipped with a 100 W mercury lamp. Images were acquired with a cooled CCD camera (Astromed; Astrocam, UK).

Experimental data

Significance of the differences in mean values of the specific caspase-3 or caspase-6 like activities and the number of stomata in 10000 μm^2 cotyledon or leaf tissue were tested with a Student's *t*-test.

Results

Characterization of the mutant

A pool of transgenic Arabidopsis plants harboring the activator T-DNA construct pSDM1550 was previously screened for altered phenotypes in the laboratory (van der Graaff & Hooykaas 1998). One of those transgenic lines is the Arabidopsis *sns* mutant which shows spontaneous necrotic spots on the leaves. Southern analysis demonstrated that only one T-DNA was integrated. The right end of the T-DNA insert was obtained by sequencing the result of the plasmid rescue for which the carbenicillin resistance gene was used. The sequencing revealed that the T-DNA was transferred with the complete binary vector sequences (van der Graaff et al. 1996). Plasmid rescue with the kanamycin resistance marker of the binary vector

resulted in the isolation of about 2 kbp of plant DNA that flanks the integrated binary vector sequence and the right border sequence that is involved in T-DNA transfer.

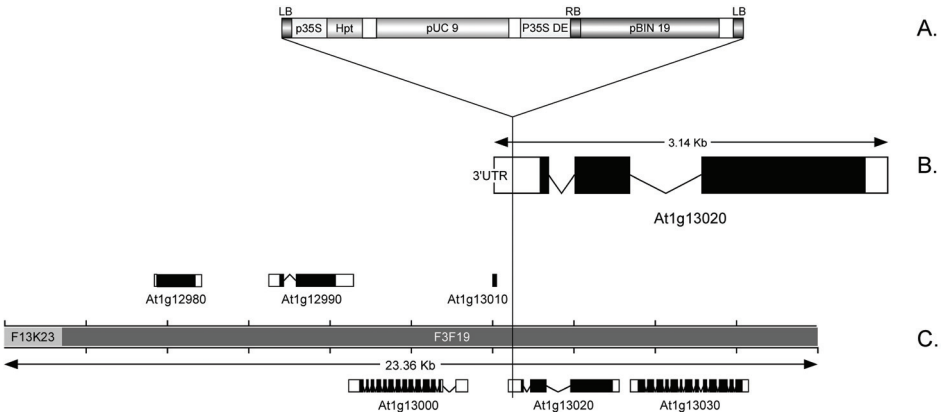

Figure 1: Schematic representation of the T-DNA and binary vector (A) inserted in the 3'UTR of the gene At1g13020 encoding an eukaryotic translation initiation factor, eIF4B5 (B) and the surrounding genes on chromosome I (C) (At1g12980 AP2 domain-containing transcription factor, putative/enhancer of shoot regeneration (ESR1); At1g12990 glycosyl transferase family 17 protein; At1g13000 expressed unknown protein; At1g13010 tRNA-Arg; At1g13030 unknown protein, possible sphere organelles protein-related). The T-DNA construct was made by cloning the pUC9 vector containing the 35S double enhancer and the AMV (Alfalfa Mosaic Virus) 5'leader and the hygromycin resistance marker between the synthetic borders of the pBIN19 derived pSDM14 vector using the unique XhoI site. pUC9: complete pUC9 cloning vector, p35S: CaMV 35S promoter, p35S DE: 35S CaMV promoter with doubled enhancer, Hpt: hygromycin resistance marker, RB: right T-DNA border repeat, LB: left T-DNA border repeat, F13K23 and F3F19: BAC regions on chromosome I.

After sequence analysis of the flanking plant DNA, database searches revealed that these flanking plant DNA sequences were derived from the Arabidopsis gene At1g13020. This gene encodes the eukaryotic translation initiation factor eIF4B5. The large insert was located in the 3'UTR of the gene At1g13020 (figure 1). To obtain the plant DNA sequences flanking the left border of the T-DNA, the genomic DNA sequences from the total DNA of hygromycin-resistant plants were amplified by thermal asymmetric interlaced (TAIL) PCR. However, the fragment flanking the 3'end of the inserted element could not be amplified. Specific primers located downstream of At1g13020 in combination with primers in the 35S promoter did not result in any PCR product. Thus, the precise insertion site could not be mapped.

The T-DNA vector contains a hygromycin phosphotransferase (HPT) gene that confers resistance to the antibiotic hygromycin. A total of 435 F2 individuals was tested and 291 hygromycin resistant individuals were seen to segregate from 144 hygromycin-sensitive individuals at a 2:1 ratio, respectively (χ^2 test). This ratio suggests the possibility that

homozygosity for the T-DNA may be lethal. Indeed empty spaces were seen in the siliques, representing aborted embryos.

Description of the leaf phenotype

The *sns* seedlings displayed a specific phenotype visible after two or three weeks of growth on solidified $^1/_2$ MS medium in the culture chamber. Necrotic spots were seen to form on the leaves. It was not possible to differentiate the wild-type and the mutant at an early stage after germination. As shown in figure 2, neither necrotic spots nor differences in morphology were visible on cotyledons or on the first leaves of one week old seedlings. After two weeks *sns* seedlings showed necrotic spots (figure 2, G-H) on their old leaves, whereas the wild-type seedlings cultured in the same way did not show such spots (figure 2, E-F). In addition, the *sns* mutant plants remained smaller than the wild-type. The differences between wild-type (figure 2, I-J) and *sns* mutant (figure 2, K-N) were more pronounced after five weeks. Two groups of equal ratio were distinguished among the *sns* mutant plants: a group with big leaves which are rather green (figure 2, K-L) and a group with smaller and coiled leaves which are rather necrotic (figure 2, M-N). Both types of *sns* mutant seedlings were smaller than the wild-type. Also the shoots of the *sns* mutant plants remained smaller than those of the wild-type. The roots of the mutant line exhibited the formation of shorter root hairs. Many of the *sns* mutant plants died before a proper inflorescence could be formed.

To characterize further possible differences between the *sns* mutant and the wild-type, analysis of the leaves was performed with SEM. No difference between the wild-type and the *sns* mutant were observed in their early stages of development. The adaxial and abaxial sides of the cotyledons of one week old wild-type seedlings (figure 3, B and C) and those of one week old *sns* mutant seedlings (figure 3, K and L) look identical. However, SEM analysis of five weeks old seedlings showed differences between the wild-type and the *sns* mutant plants on both sides of the leaves (figure 3).

The epidermal cells were less developed and appeared compressed in the case of the mutant, not only in the necrotic spots but also elsewhere on the leaf. By comparison with the wild-type (figure 3, D-I), the epidermal cells of *sns* mutant leaves were flattened on both adaxial and abaxial sides (figure 3, M-R). The pattern of the internal cell layers was slightly distorted compared to wild-type leaves.

Moreover, the number of stomata in the *sns* mutant leaves was changed. Stomata were counted on adaxial and on abaxial sides, of cotyledons and of five weeks old plant leaves per 10000 μm^2 (table 1). With both wild-type and *sns* plants, the stomata were more abundant on the abaxial side of the cotyledons than on the adaxial side. Compared to the wild-type, the *sns* mutant had less stomata on cotyledons. After five weeks, more stomata

were counted on the adaxial side of the leaves of the *sns* mutant compared to that of the wild-type (5.5 ± 1.1 for *sns* adaxial side of mutant leaf versus 2.9 ±1.1 for adaxial side of wild-type leaf). The wild-type leaves were more expanded, but the size of the cells was identical to that of the cells of *sns* leaves. Thus there are more cells in wild-type leaves.

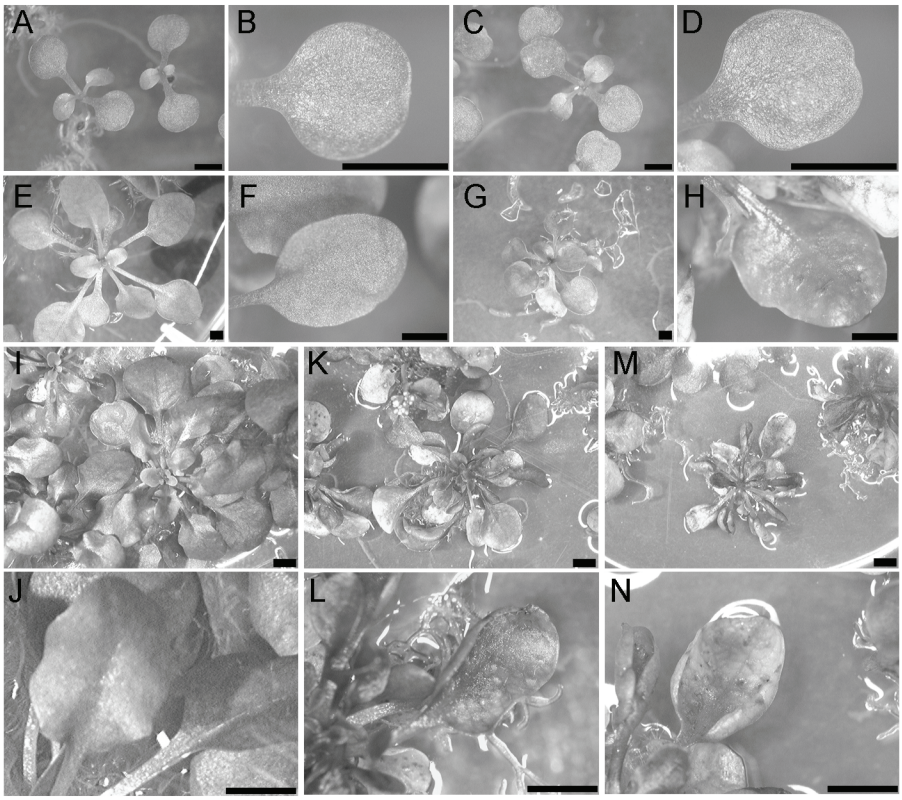

Figure 2: Phenotype of *sns* mutant plants and development of necrotic spots on the leaves. Leaves and cotyledons of one week old wild-type (A-B) and *sns* (C-D) seedlings, 3 weeks old wild-type (E-F) and *sns* (G-H) seedlings, and 5 weeks old wild-type (I-J) and *sns* (K-N) seedlings. Among the *sns* mutant plants, 2 groups are distinguished: a group with big leaves, rather green (K-L) and a group with smaller and coiled, necrotic leaves (M-N). Bars are 2 mm.

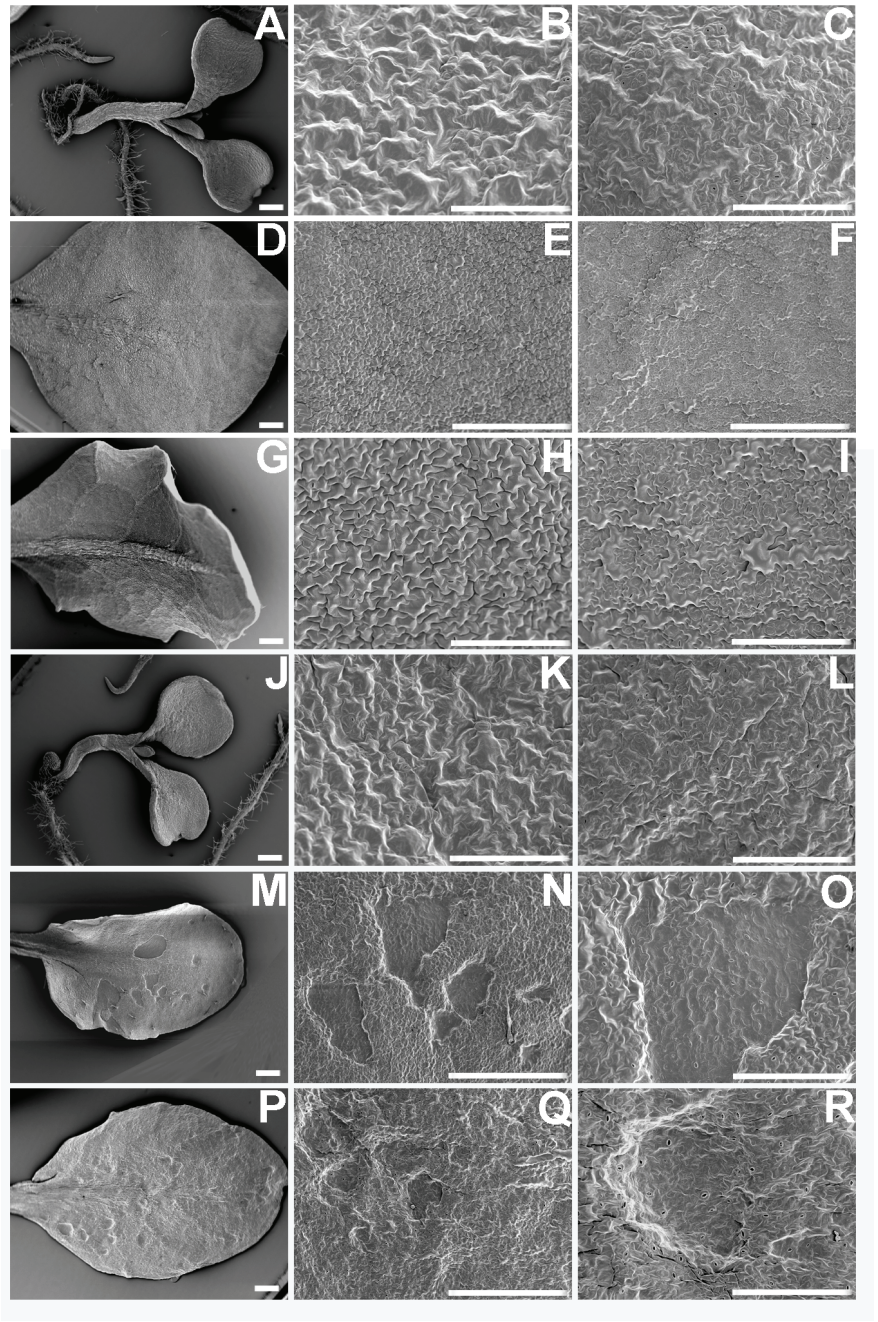

Figure 3: SEM analysis of leaves and cotyledons of one week old wild-type (A-C) and *sns* (J-L) seedlings, and 5 weeks old wild-type (D-I) and *sns* (M-R) seedlings. In B, D, E, F, K, M, N and O adaxial sides of cotyledons or leaves are represented and in C, G, H, I, L, P, Q and R abaxial sides of cotyledons or leaves. Bars in A, D, G, J, M and P are 500 µm and in the others 200 µm.

Table 1: Number of stomata in wild-type and *sns* on adaxial and abaxial sides of cotyledons and on adaxial and abaxial sides of leaves of five weeks old plants in 100x100 µm tissue.

Number of stomata on 10000 µm^2 tissue	Cotyledon	Leaf
sns adaxial	4.2 ± 1.5	5.5 ± 1.1
sns abaxial	6.3 ± 1.1	6.1 ± 1.4
wt adaxial	5.3 ± 1.6	2.9 ± 1.1
wt abaxial	7.2 ± 3.2	5.2 ± 1.2

Caspase-like activities and TUNEL

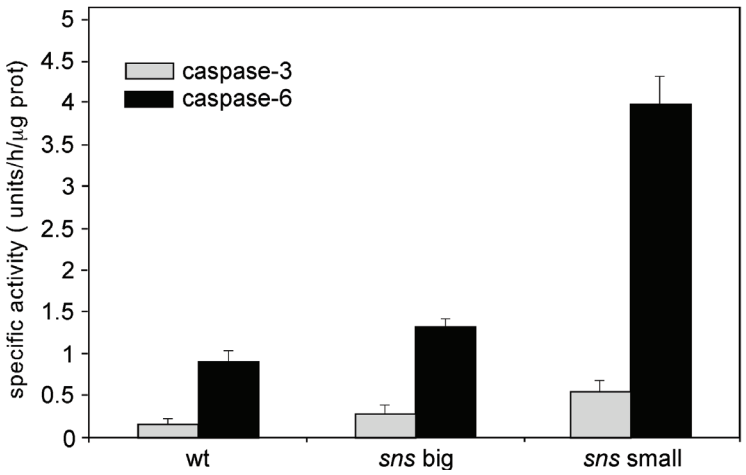

Figure 4: Specific caspase-3 and -6 like activities measured in leaf extract of 5 weeks old wild-type plants and of 5 weeks old *sns* mutant plants (2 groups: big and small plants).

Analysis of the mutant leaves suggests that the epidermal cells and the internal cell layers in the necrotic spots die. Cell death takes place in plants as necrosis or programmed cell death (PCD). With the Arabidopsis *sns* mutant, the occurrence of PCD markers, such as activation of caspase-like proteases and DNA cleavage, was investigated. Caspase-3 and -6 like activities were measured in leaf extracts by use of the synthetic fluorogenic caspase-3 substrate Ac-DEVD-AMC and the synthetic fluorogenic caspase-6 substrate Ac-VEID-AMC, respectively. An increase of the caspase-3-like activity was measured in *sns* leaf extracts (figure 4, grey columns) for both big and small leaf phenotypes. Caspase-3 like activity was

about 3-fold higher in *sns* big leaf and about 6-fold higher in *sns* small leaf. A similar observation was made with caspase-6 like activity (figure 4, black columns). Caspase-6 like activity was about 1.5-fold higher in *sns* big leaf and 4.5-fold higher in *sns* small leaf. The *sns* plants of a small leaf phenotype have more caspase-3 like and caspase-6 like activities, measured in leaf extract, than wild-type and *sns* plants of a big leaf phenotype.

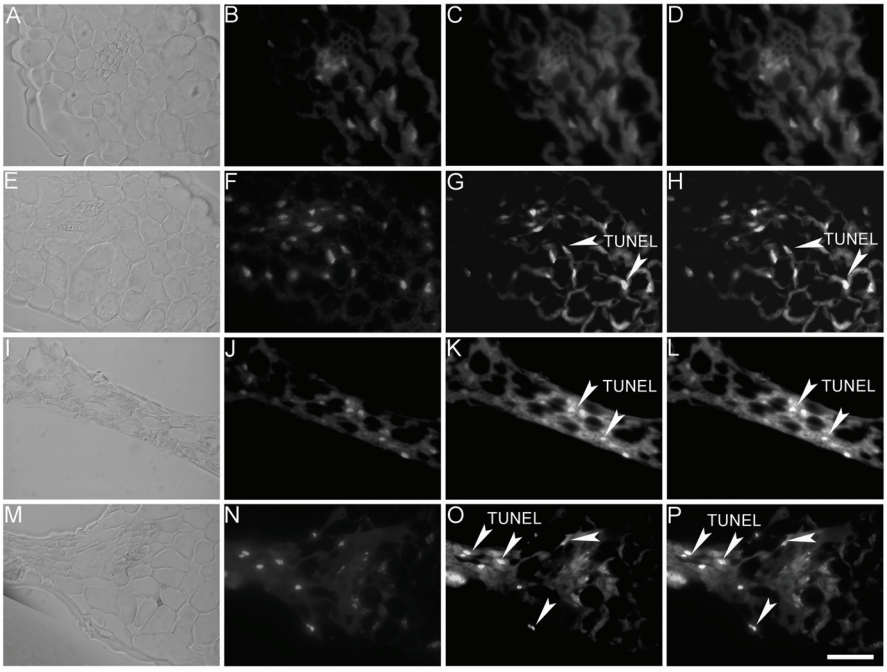

Figure 5: Detection of DNA fragmentation in necrotic spots with TUNEL staining. Transmitted light image (A, E, I, M), sytox orange nuclear staining (B, F, J, N) and TUNEL staining (C, G, K, O) on cross-sections of 5 weeks old C24 leaf (A-D) and DNase I-treated cross-sections of 5 weeks old C24 leaf (E-H) and on cross-sections of 5 weeks old *sns* leaf (I-L) and DNase I-treated cross-sections of 5 weeks old *sns* leaf (M-P). (D, H, L and P) are merged images of (B, C), (F, G), (J, K) and (N, O), respectively. TUNEL-positive nuclei are indicated by arrows. Bar is 25 µm.

DNA cleavage, one of the PCD markers of which the occurrence was investigated, was visualized by TUNEL assay. The wild-type did not show TUNEL-positive nuclei (figure 5, A-D), whereas pre-incubation with DNase I prior to TUNEL reaction induced DNA cleavage everywhere on the leaf (figure 5, E-H). The *sns* mutant showed TUNEL-positive nuclei in the cells of the necrotic spots, whereas no TUNEL signal was found outside the necrotic spots (figure 5, I-L). With transmitted light image the necrotic spots appeared like as a brown zone of collapsed cells. Sytox orange was used to detect all nuclei on cross-sections of five weeks old *sns* leaves. Pre-incubation with DNAse I prior to TUNEL reaction induced DNA cleavage everywhere on the leaf (figure 5, M-P), whereas no TUNEL signal was found in negative

controls when the transferase was omitted from the TUNEL reaction (data not shown). To conclude, the *in situ* detection of DNA fragmentation by TUNEL analysis of the leaves showed that many epidermal cells in the necrotic spots contain fragmented DNA, one of the hallmarks of PCD.

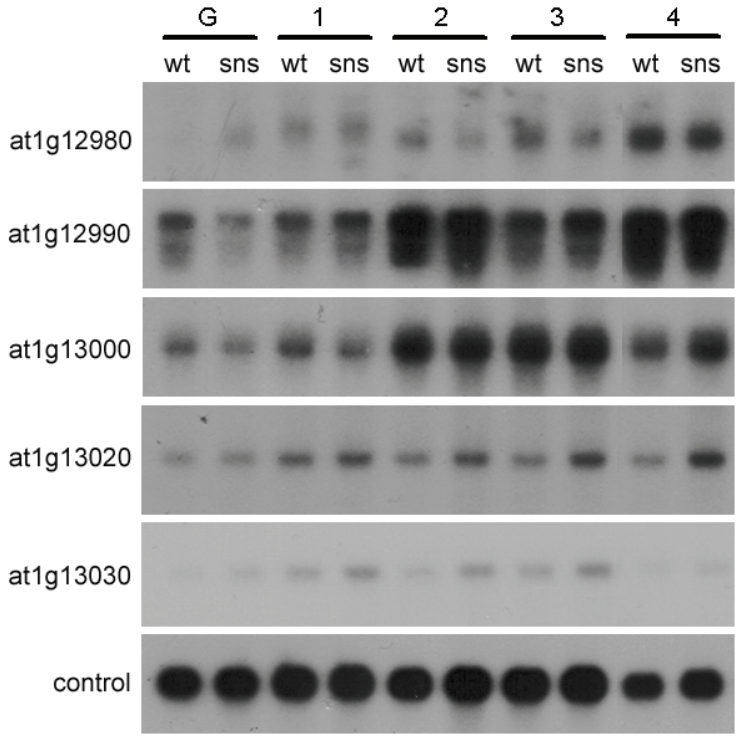

Figure 6: Northern blot analysis of the genes located near the T-DNA insertion in the *sns* mutant at different growth stages (G: just germinated, 1: 1 week after germination, 2: 2 weeks after germination, 3: 3 weeks after germination, 4: 4 weeks after germination). RNA from wild-type (wt) and *sns* mutant (*sns*) was hybridized with different probes: At1g12980, At1g12990, At1g13000, At1g13020 and At1g13030. Equal loading of RNA was checked by hybridization with At4g38740 (cyclophilin).

Expression level of the genes located near the T-DNA insertion

The T-DNA and the binary vector were inserted in the 3'UTR of the gene At1g13020 in the *sns* mutant. The T-DNA is an activation tagging T-DNA that contains a 35S enhancer. Northern blot analysis was performed to determine whether At1g13020 and genes located upstream and downstream were expressed differently in wild-type and *sns* mutant plants. Plants of different growth stages were used for the analysis. As compared to the level in the wild-type, the expression level of At1g13020 was higher in the *sns* mutant plants at later stages of development (weeks 2 to 4) (figure 6).

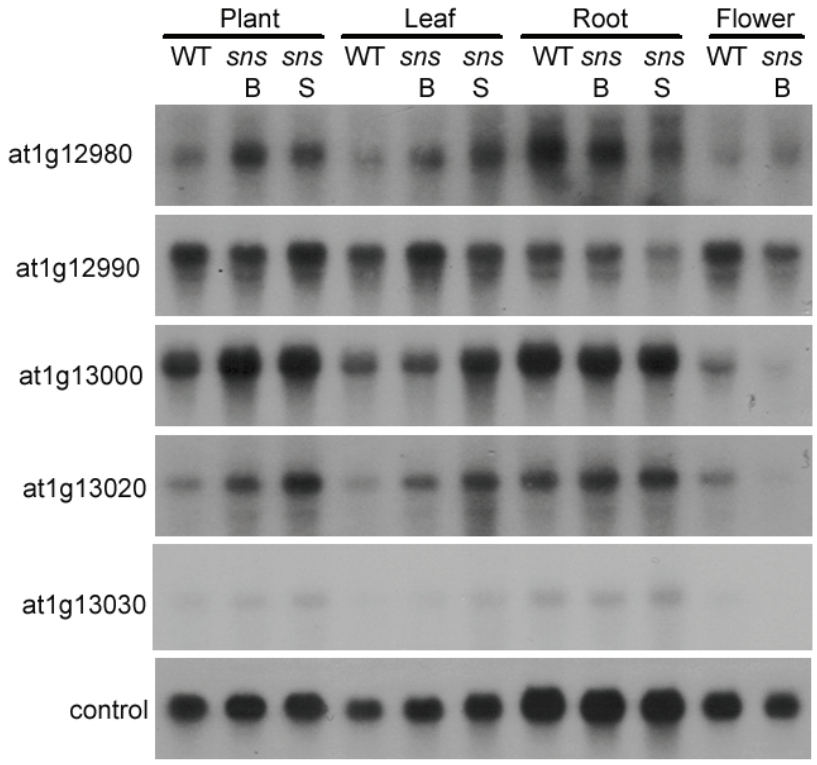

Figure 7: Northern blot analysis of the genes located near the T-DNA insertion in *sns* in different tissues (whole plant, leaf, root and flower). RNA from 5 weeks old wild-type plants, and big and small *sns* plants was hybridized with different probes: At1g12980, At1g12990, At1g13000, At1g13020 and At1g13030. Equal loading of RNA was checked by hybridization with At4g38740 (cyclophilin). Flower analysis only concerned flowers of wild-type and *sns* big leaf plants, because the *sns* small leaf plants did not produce flowers.

There is a correlation between the higher expression level of At1g13020 and the appearance of necrotic spots after two weeks of germination. Changes in expression level were also seen for the upstream and downstream genes at different time points after germination. However, these changes correlated less well with the appearance of necrotic spots.

After five weeks of growth two groups of *sns* mutant plants could be distinguished: a group with rather green and big leaves, and a group with smaller and coiled, rather necrotic leaves (shown in figure 2). To find out whether the expression level of At1g 13020 correlated with the severity of the phenotype, the expression levels of the set of genes, mentioned previously, were also analyzed for separate organs (leaf, root and flower) for five weeks old wild-type, small leaf and big leaf *sns* mutant plants. Although the loading was not completely identical in all lanes, it was clear that At1g13020 was expressed in leaves and that its

expression levels were higher in leaf tissue of *sns* plants and the highest in the plants with small necrotic leaves (figure 7).

Therefore, an increased expression of At1g13020 may underlie the phenotype seen in the *sns* mutant. However, as there are many other changes in gene expression seen, the phenotype may also be due to a change in expression of one of the other genes or a combination of genes.

Fluorescence in situ hybridization

The fluorescence *in situ* hybridization (FISH) technique was used to investigate the genomic organization of the region where the T-DNA/binary vector had integrated in the *sns* mutant plants. This technique was used because the integration of one T-DNA end could not be mapped by PCR or TAIL-PCR. As shown in figure 1, the insertion of the T-DNA and the binary vector are in the 3'UTR of the gene At1g13020 on chromosome I in the genomic sequence located on BAC clone F3F19.

Wild-type and *sns* nuclei were hybridized with BAC clones F3F19 (red signal) and F13K23 (green signal) as probes. BAC F3F19 and BAC F13K23 are adjacent on the chromosome I. The interphase wild-type nuclei (figure 8A) showed overlapping red and green signals, which is expected as the two BAC sequences are from adjacent segments of chromosome I.

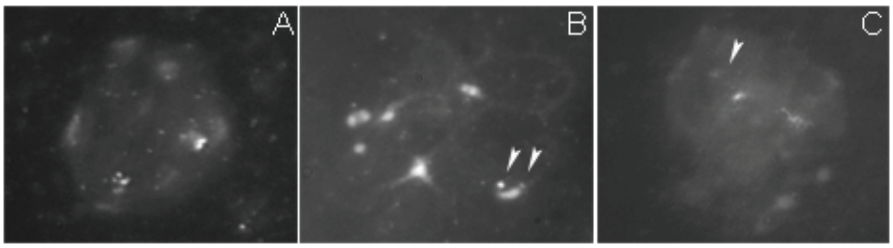

Figure 8: Chromosomal rearrangement shown by fluorescence in situ hybridization (FISH). Nuclei were stained with DAPI and interphase wild-type nucleus (A) and *sns* (B pachytene and C interphase) nuclei were hybridized with BAC F3F19 (red signal) and F13K23 (green signal) probes. Arrows indicate the red signal in *sns* nuclei on the rearranged chromosome.

The *sns* mutant nuclei showed overlapping red and green signals on one of the chromosomes I, but discontinuous red and green signals on the other chromosome I (figures 8B and C). Especially in pachytene cells with fully paired homologous chromosomes, we observed discontinuity between the two BAC signals, visualized by two red signals instead of one. This suggests a chromosomal rearrangement involving chromosome I (figure 8B). Such

chromosome mutation, which could affect many genes, could also explain the phenotype of the *sns* plants. In that case the phenotype could be due not only to a change in expression of a gene or genes located in the vicinity of the integration site, but also to changes in expression of distant genes.

Discussion

T-DNA insertion and chromosomal rearrangement

After two or three weeks of growth, the *sns* mutant displayed a specific phenotype in that necrotic spots formed on the leaves. The epidermal cells of *sns* mutant leaves were flattened in the area of the necrotic spots on both leaf sides. The phenotype reported in this study is clearly a consequence of the T-DNA integration and the associated chromosomal rearrangement. A wide range of chromosomal defects have been observed in populations of Arabidopsis subjected to T-DNA mutagenesis (Tax et al. 2001). Different chromosome mutations have been seen in those populations, ranging from small insertions and deletions of a few bases (Negruk et al. 1996; Noguchi et al. 1999) to larger rearrangements and chromosomal translocations (Gheysen et al. 1991; Castle et al. 1993; Nacry et al. 1998; Laufs et al. 1999). The single T-DNA insert studied here appeared to be the result of transfer of both the complete binary vector sequence and the T-region (van der Graaff et al. 1996). Sequence analysis of the flanking plant DNA at the right end of the T-DNA revealed that these flanking plant DNA sequences were derived from the Arabidopsis gene At1g13020, which encodes an eukaryotic translation initiation factor eIF4B5, and that the T-DNA was located in the 3'UTR of the gene At1g13020. No fragment could be obtained from the plant DNA flanking the T-DNA at the other left end of the T-DNA, neither by plasmid rescue nor by thermal asymmetric interlaced (TAIL) PCR.

The difficulty to map the precise location of the T-DNA insertion might be due to the large chromosomal rearrangements that apparently accompanied this T-DNA integration event. Evidence for such chromosomal rearrangements was obtained by FISH on *sns* nuclei. The detection signal for the fluorescent probe in the nuclei of pachytene cells of the wild-type with fully paired homologous chromosomes is one red signal. In this study, two red signals were visible in the nuclei instead of one, which suggested a discontinuity between the two BAC signals. FISH is an effective tool for the analysis of transgene organization (Fransz et al. 1996).

The sns mutation

After selfing, hygromycin-resistant progeny and hygromycin sensitive progeny were recovered in a ratio of approximately 2:1. After five weeks, two groups were distinguished among the hygromycin resistant *sns* mutant plants: a group with big leaves which are rather green and a group with smaller and coiled leaves which are rather necrotic. The plants with small necrotic and coiled leaves died during development and they did not form a proper inflorescence, so no seeds could be obtained. The *sns* plants with big leaves, however, matured normally and produced seeds. The offspring of these plants included both hygromycin resistant and sensitive seedlings in a ratio of 2:1. This shows that the *sns* mutation is dominant. It is possible that the *sns* mutation is (partially) embryo-lethal. Indeed empty spaces were seen in the siliques of *sns* plants. The small *sns* plants may also represent plants that are homozygous for the *sns* mutation. The T-DNA insertion landed in the 3'end of the gene At1g13020. Therefore the *sns* phenotype may be due to a change in expression of the At1g13020 gene. However as an activation tag T-DNA was used, changes in expression of some of the neighboring genes may underlie the phenotype. Finally, the phenotype may be due to the alterations of gene expression that are a consequence of chromosomal rearrangement. The fact that the mutation is dominant suggests gene dosage effects such as overdoses or haplo-insufficiency. In order to find more molecular evidence for this, northern blot analyses were performed to determine whether At1g13020 and genes located upstream and downstream were expressed differently in wild-type and *sns* mutant plants. The expression levels of several genes were found to be affected in the area of the T-DNA integration. The expression level of At1g13020 was higher in the *sns* mutant plants at later stages of development, correlating with the appearance of the necrotic spots. At1g13020 encodes the eukaryotic initiation factor eIF4B5. The initiation of protein synthesis in eukaryotes is a complicated process. This initiation requires at least 8-10 eukaryotic initiation factors (eIFs) to properly align the initiation codon of messenger RNA on the 40S ribosome and to join with the 60S ribosome at the initiation codon of mRNA (Pestova et al. 2001). The cap-binding complex eIF4F and the factors eIF4A and eIF4B are required to bind 43S complexes (comprising a 40S subunit, eIF2/GTP/Met-tRNAi and eIF3) to the 5'end of capped mRNA, but they are not sufficient to promote ribosomal scanning to the initiation codon. Regulation of protein synthesis at the level of translation initiation is of fundamental importance to the control of cell proliferation under normal physiological conditions. If the translation is deregulated, this can have major consequences like the ones observed in *sns*. In mammals, deregulation of translation is associated with a wide range of cancers (Calkhoven et al. 2002; Watkins & Norbury 2002).

The expression levels of neighbouring genes were also altered in the *sns* mutant. This may contribute to the *sns* phenotype. The LETTUCE mutant has leafy petioles in which the phenotype is due to the increased expression of two genes VAS and LEP (van der Graaf et al. 2002).

At1g13000 and At1g13030 encode proteins of unknown functions. At1g12980 was already described as one of the genes identified to control shoot meristem development in Arabidopsis, the Dornröschen/enhancer of shoot regeneration1, encoding an AP2/ERF transcription factor (Banno et al. 2001; Kirch et al. 2003). At1g12990 encodes an acetylglucosaminyltransferase. The homologue of this gene was found in cucumber by the mRNA RT-PCR differential display technique during identification of genes involved in Systemic Acquired Resistance (Bovie et al. 2004). The acetylglucosaminyltransferase protein is reported to be one of the components of signal transduction pathways in mammals and plants.

Other T-DNA insertion mutants with T-DNA inserted in the studied genes (SM-3-35017, Sail 310-G09, Sail 398-F05 and Salk 010395 for the corresponding genes At1g12980, At1g13000, At1g13020 and At1g13030 respectively) were analyzed (unpublished results). Here, no specific *sns* phenotype was seen (data not shown). Possible explanations are that a single mutation is not enough to result in the phenotype, or that only increased expression (*via* 35S) results in the phenotype. Moreover, the expression level of the tRNA-Arg (At1g13010), also located in the proximity of the T-DNA insertion, was not determined.

Necrotic spots and programmed cell death

The *sns* mutant was characterized by the formation of necrotic spots on the leaves after two weeks of seedling development. The necrotic spots observed in the *sns* mutant were similar to those observed during the hypersensitive response (HR) involved in pathogen defense. PCD markers such as DNA cleavage and activation of caspase-like proteases were used to find out if PCD took place in the necrotic spots in the Arabidopsis *sns* mutant. The TUNEL labeling is considered as a good marker to indicate PCD both in animals and plants. DNA fragmentation is one of the hallmarks of PCD. This fragmentation is demonstrated with the TUNEL reaction by labeling the free 3'-OH DNA extremities of DNA breaks. In the *sns* mutant, many epidermal cells within the necrotic spots contained fragmented DNA. The occurrence of DNA fragmentation is frequently reported in a variety of senescing plant tissues by TUNEL labeling of degrading nuclei (Orzaez & Granell 1997; Kawai & Uchimiya 2000; Pasqualini et al. 2003).

The discovery of the CED9/CED4/CED3 pathway in *Caenorhabiditis elegans* and its machinery conserved in other animal species, such as humans and Drosophila,

demonstrated that this apoptotic death pathway is highly conserved in metazoans (Ameisen 2004; Hoeberichts & Woltering 2003; Jin and& Reed 2002; Lam 2004; Lam et al. 2001). By use of fluorogenic substrates for caspase-1, -3 and -6, increases of caspase-like activities were found to occur in dying plant cells (del Pozo & Lam 1998; Sun et al. 1999; de Jong et al. 2000; Bozhkov et al. 2004). In both plants with big and small leaf phenotypes, significant increases of caspase-3 and -6 like activities were measured in *sns* leaf extracts. The increase is more pronounced with the small leaf mutant line. The results of this study confirmed that the necrotic spots in the Arabidopsis *sns* mutant are not due to cells that are dying by necrosis but by PCD (TUNEL and caspase-like activities).

After the elucidation of the complete Arabidopsis genome, it has become clear that no genes for caspases are present in plants. Plants might use other proteases that exhibit a caspase-like activity that underlies PCD. Identification of such proteases is essential to reveal the molecular mechanism that operates in plant PCD and to provide some insights into differences between plant and animal PCD. In oat (*Avena sativa*), serine proteinases exhibit caspase-like activities, and these activities increase during PCD induced by the fungal toxin victorin (Coffeen & Wolpert 2004). Homology searches reveal the existence of several metacaspases in plants and fungi (Uren et al. 2000). The silencing of a metacaspase gene reduced one caspase-like activity and abolished developmental cell death in Norway spruce (Suarez et al. 2004). These results imply that proteases exhibiting caspase-like activities are involved in plant PCD.

The phenotype of the *sns* mutant resembles the phenotype of senescing leaf or the lesion phenotype of a leaf affected by a pathogen during the hypersensitive response. Both processes involve the induction of pathogenesis-related genes and the accumulation of salicylic acid and reactive oxygen species (Quirino et al. 2000). The appearance of lesions is, in most cases, accompanied by a constitutive expression of markers associated with pathogen infection: auto-fluorescent phenolic compound accumulation, deposition of callose, production of reactive oxygen intermediates (ROIs), constitutive expression of defense marker genes, and production of elevated levels of salicylic acid (Brodersen et al. 2002). It would be interesting to analyze these markers in the *sns* mutant.

Many accelerated-cell-death mutants have cell-death lesions that appear in aged leaves. Those mutants have been isolated and well characterized according to their defense phenotype (Shirasu & Schulze-Lefert 2000). Some of these mutants have defects in the senescence program. After their mutation many genes result in a lesion-mimic phenotype. The isolation of those genes was mostly realized from *Arabidopsis thaliana* (Lorrain et al. 2003). Those genes do not resemble the genes described in the case of the *sns* mutant. The

sns mutant might be used to study PCD markers and to help analyze expression levels of genes that are related to PCD or, more specifically, to hypersensitive response.

Acknowledgments

We are grateful to Dr. Wouter-Jan Oosten (Sociotext Foundation) for critical reading of the manuscript. We are grateful to the Arabidopsis Biological Resource Center for providing seeds of the mutant lines (SM-3-35017, Sail 310-G09, Sail 398-F05 and Salk 010395) and the BAC clones (F3F19 and F13K23), and to Peter Hock for the lay-out of the figures. This work was financed by Stichting BVS (Binair Vector Systeem).

References

Ameisen JC (2004) Looking for death at the core of life in the light of evolution. Cell Death Differ. 11(1): 4-10.

Banno H, Ikeda Y, Niu QW and Chua NH. (2001) Overexpression of Arabidopsis ESR1 induces initiation of shoot regeneration. Plant Cell. 13: 2609-2618.

Bovie C, Ongena M, Thonart P and Dommes J. (2004) Cloning and expression analysis of cDNAs corresponding to genes activated in cucumber showing systemic acquired resistance after BTH treatment. BMC Plant Biol. 4: 15.

Bozhkov PV, Filonova LH, Suarez MF, Helmersson A, Smertenko AP, Zhivotovsky B and von Arnold S (2004). VEIDase is a principal caspase-like activity involved in plant programmed cell death and essential for embryonic pattern formation. Cell Death Differ. 11(2): 175-182.

Brodersen P, Petersen M, Pike HM, Olszak B, Skov S, Odum N, Jorgensen LB, Brown RE and Mundy J. (2002) Knockout of Arabidopsis accelerated-cell-death11 encoding a sphingosine transfer protein causes activation of programmed cell death and defense. Genes Dev. 16(4): 490-502.

Calkhoven CF, Muller C and Leutz A. (2002) Translational control of gene expression and disease. Trends Mol Med. 8(12): 577-583.

Castle LA, Errampalli D, Atherton TL, Franzmann LH, Yoon ES and Meinke DW. (1993) Genetic and molecular characterization of embryonic mutants identified following seed transformation in Arabidopsis. Mol Gen Genet. 241(5-6): 504-514.

Coffeen WC and Wolpert TJ. (2004). Purification and characterization of serine proteases that exhibit caspase-like activity and are associated with programmed cell death in Avena sativa. Plant Cell. 16 (4): 857–873.

del Pozo O and Lam E. (1998) Caspases and programmed cell death in the hypersensitive response of plants to pathogens. Curr Biol. 8(20): 1129-1132.

Dietrich RA, Delaney TP, Uknes SJ, Ward ER, Ryals JA and Dangl JL. (1994) Arabidopsis mutants simulating disease resistance response. Cell. 77(4): 565–577.

Fransz PF, Alonso-Blanco C, Liharska TB, Peeters AJ, Zabel P, de Jong JH. (1996) High-resolution physical mapping in *Arabidopsis thaliana* and tomato by fluorescence in situ hybridization to extended DNA fibers. Plant J. 9(3): 421-430.

van der Graaff E. (1997) Developmental mutants of *Arabidopsis thaliana* obtained after T-DNA transformation. PhD Thesis Leiden University.

van der Graaff E and Hooykaas PJ. (1998) Transformation of *Arabidopsis thaliana* C24 leaf discs by *Agrobacterium tumefaciens*. Methods Mol Biol. 82: 245-258.

van der Graaff E, den Dulk-Ras A and Hooykaas PJ. (1996) Deviating T-DNA transfer from *Agrobacterium tumefaciens* to plants. Plant Mol Biol. 31(3): 677-681.

Gheysen G, Villarroel R and Van Montagu M. (1991) Illegitimate recombination in plants: a model for T-DNA integration. Genes Dev. 5(2): 287-297.

Gilchrist DG. (1998) Programmed cell death in plant disease: the possible and promise of cellular suicide. Annu. Rev. Phytopathol. 36: 393-414.

Greenberg JT and Ausubel FM (1993). Arabidopsis mutants compromised for the control of cellular damage during pathogenesis and aging. Plant J. 4(2): 327–341.

Greenberg JT, Guo A, Klessig DF and Ausubel FM (1994). Programmed cell death in plants: a pathogen-triggered response activated co-ordinately with multiple defense functions. Cell. 77(4): 551-563.

Groover A, De Witt N, Heidel A and Jones A. (1997) Programmed cell death of plant tracheary elements differentiating in vitro. Protoplasma 196: 197-211.

Hoeberichts FA and Woltering EJ. (2003) Multiple mediators of plant programmed cell death: interplay of conserved cell death mechanisms and plant-specific regulators. BioEssay. 25(1): 47-57.

Hoekema A, Hooykaas PJ and Schilperoort RA. (1984) Transfer of the octopine T-DNA segment to plant cells mediated by different types of Agrobacterium tumor- or root-inducing plasmids: generality of virulence systems. J Bacteriol. 158(1): 383-385.

Hoisington DA, Neuffer MG and Walbot V. (1982) Disease lesion mimics in maize. Effect of genetic background, temperature, developmental age, and wounding on necrotic spot formation with Les1. Dev. Biol. 93(2): 381-388.

Huh GH, Damaz B, Matsumoto T, Reddy MP, Rus AM, Ibeas JI, Narasimhan ML, Bressan RA and Hasegawa PM. (2002) Salt causes ion disequilibrium-induced programmed cell death in yeast and plants. Plant J. 29(5): 649-659.

Jin C and Reed JC. (2002) Yeast and apoptosis. Nat. Rev. Mol. Cell Biol. 3(6): 453-459.

Jones AM and Dangl JL. (1996) Logjam at the Styx: programmed cell death in plants. Trends Plant Sci 1: 114-119.

De Jong AJ, Hoeberichts FA, Yakimova ET, Maximova E and Woltering EJ. (2000) Chemical-induced apoptotic cell death in tomato cells: involvement of caspase-like proteases. Planta. 211(5): 656-662.

Kawai M and Uchimiya H (2000). Coleoptile senescence in rice (*Oryza sativa L.*) Ann Bot. 86: 405-414.

Kirch T, Simon R, Grünewald M and Werr W. (2003) The DORNRÖSCHEN/ ENHANCER OF SHOOT REGENERATION1 Gene of Arabidopsis Acts in the Control of Meristem Cell Fate and Lateral Organ Development. Plant Cell. 15(3): 694-705.

Lam E. (2004) Controlled cell death, plant survival and development. Nat Rev MolCell Biol. 5(4): 305-315.

Lam E, Kato N and Lawton M. (2001) Programmed cell death, mitochondria and the plant hypersensitive response. Nature. 411(6839): 848-853.

Laufs P, Autran D and Traas J. (1999) A chromosomal paracentric inversion associated with T-DNA integration in Arabidopsis. Plant J. 18(2): 131-139.

Lorrain S, Vailleau F, Balague C and Roby D. (2003) Lesion mimic mutants: keys for deciphering cell death and defense pathways in plants? Trends Plant Sci. 8(6): 263-271.

McCabe PF, Levine A, Meijer P-J, Tapon NA and Pennell RI. (1997) A programmed cell death pathway activated in carrot cells cultured at low cell density. Plant J. 12: 267-280.

Maraschin SF, Gaussand G, Pulido A, Olmedilla A, Lamers GEM, Korthout H, Spaink HP and Wang M. (2005) Programmed cell death during the transition from multicellular structures to globular embryos in barley androgenesis. Planta. 221(4): 459-470.

Martineau B, Voelker TA and Sanders RA. (1994) On defining T-DNA. Plant Cell. 6(8): 1032-1033.

Menke FLH, Parchmann S, Mueller MJ, Kijne JW and Memelink J. (1999) Involvement of the octadecanoid pathway and protein phosphorylation in fungal elicitor-induced expression of terpenoid indole alkaloid biosynthetic genes in *Cataranthus roseus*. Plant Physiol. 119(4): 1289-1296.

Nacry P, Camilleri C, Courtial B, Caboche M and Bouchez D. (1998) Major chromosomal rearrangements induced by T-DNA transformation in Arabidopsis. Genetics. 149(2): 641-650.

Negruk V, Eisner G and Lemieux B. (1996) Addition-deletion mutations in transgenic *Arabidopsis thaliana* generated by the seed co-cultivation method. Genome. 39(6): 1117-1122.

Noguchi S, Tajima T, Yamamoto Y, Ohno T and Kubo T. (1999) Deletion of a large genomic segment in tobacco varieties that are resistant to potato virus Y (PVY). Mol Gen Genet. 262(4-5): 822-829.

Orzaez D and Granell A. (1997) The plant homologue of the defender against apoptotic death gene is down-regulated during senescence of flower petals. FEBS Letters 404(2-3): 275-278.

Panavas T, LeVangie R, Mistler J, Reid PD and Rubinstein B. (2000) Activities of nucleases in senescing daylily petals. Plant Physiol Biochem 39: 837–843.

Pasqualini S, Piccioni C, Reale L,Ederli L, Della Tore G and Ferranti F. (2003) Ozone-induced cell death in tobacco cultivar Bel W3 plants. The role of programmed cell death in lesion formation. Plant Physiol. 133(3): 1122-1134.

Pestova TV, Kolupaeva VG, Lomakin IB, Pilipenko EV, Shatsky IN, Agol VI, and Hellen CU. (2001) Molecular mechanisms of translation initiation in eukaryotes. Proc Natl Acad Sci USA. 98(13): 7029-7036.

Pennell RI and Lamb C. (1997) Programmed cell death in plants. Plant Cell. 9(7): 1157-1168.

Quirino BF, Noh YS, Himelblau E and Amasino RM. (2000) Molecular aspects of leaf senescence. Trends Plant Sci. 5(7): 278-282.

Ryerson DE and Heath MC. (1996) Cleavage of nuclear DNA into oligonucleosomal fragments during cell death induced by fungal infection or by abiotic treatments. Plant Cell. 8(3): 393-402.

Schubert I, Fransz PF, Fuchs J and de Jong JH. (2001) Chromosome painting in plants. Methods Cell Sci. 23(1-3): 57-69.

Shirasu K and Schulze-Lefert P. (2000) Regulators of cell death in disease resistance. Plant Mol Biol. 44(3): 371-385.

Solomon M, Belenghi B, Delledonne M, Menachem E and Levine A. (1999) The involvement of cysteine protease inhibitor genes in the regulation of programmed cell death in plants. Plant Cell 11(3):B 431-443.

Suarez MF, Filonova LH, Smertenko A, Savenkov EI, Clapham DH, von Arnold S, Zhivotovsky B and Bozhkov PV. (2004) Metacaspase-dependent programmed cell death is essential for plant embryogenesis. Curr Biol. 14(9): R339–340.

Sun YL, Zhao Y, Hong X and Zhai ZH. (1999) Cytochrome c release and caspase activation during menadione-induced apoptosis in plants. FEBS Lett. 462(3): 317-321.

Takahashi A, Kawasaki T, Henmi K, Shil K, Kodama O, Satoh H and Shimamoto K. (1999) Lesion mimic mutants of rice with alterations in early signaling events of defense. Plant J. 17(5): 535-545.

Tax FE and Vernon DM. (2001) T-DNA-associated duplication/translocations in Arabidopsis. Implications for mutant analysis and functional genomics. Plant Physiol. 126(4): 1527-1538.

Uren AG, O'Rourke K, Aravind L, Pisabarro TM, Seshagiri S, Koonin EV and Dixit VM. (2000) Identification of paracaspases and metacaspases: two ancient families of caspase-like proteins, one of which plays a key role in MALT lymphoma. Mol Cell. 6(4): 961-967.

Vergunst AC, Jansen LE, Fransz PF, de Jong JH and Hooykaas PJ. (2000) Cre/lox-mediated recombination in Arabidopsis: evidence for transmission of a translocation and a deletion event. Chromosoma. 109(4): 287-297.

Wang H, Wu HM and Cheung AY. (1996a) Pollination induces mRNA poly(A) tail-shortening and cell deterioration in flower transmitting tissue. Plant J. 9(5): 715-727.

Wang M, Oppedijk BJ, Lu X, van Duijn B and Schilperoort RA. (1996b) Apoptosis in barley aleurone during germination and its inhibition by abscisic acid. Plant Mol Biol 32: 1125-1134.

Wang H, Li J, Bostock RM and Gilchrist DG (1996c). Apoptosis: a functional paradigm for programmed cell death induced by a host-selective phytotoxin and invoked during development. Plant Cell. 8(3): 375-391.

Wang M, Oppedijk BJ, Caspers MPM, Lamers GEM, Boot MJ, Geerlings DNG, Bakhuizen B, Meijer AH and van Duijn B. (1998) Spatial and temporal regulation of DNA fragmentation in the aleurone of germinating barley. J Exp Bot 325: 1293-1301.

Wang M, Hoekstra S, van Bergen S, Lamers GEM, Oppedijk BJ, van der Heijden MW, de Priester W and Schilperoort RA. (1999) Apoptosis in developing anthers and the role of ABA in this process during androgenesis in *Hordeum vulgare* L. Plant Mol Biol 39: 489-501.

Watkins SJ and Norbury CJ. (2002) Translation initiation and its deregulation during tumorigenesis. Br J Cancer. 86(7): 1023-1027.

Wolter M, Hollricher K, Salamini F and Schulze-Lefert P. (1993) The mlo resistance alleles to powdery mildew infection in barley trigger a developmentally controlled defence mimic phenotype. Mol Gen Genet. 239(1-2): 122-128.

Wu H-M and Cheung AY. (2000) Programmed cell death in plant reproduction. Plant Mol Biol. 44(3): 267-281.

Yen CH and Yang CH. (1998) Evidence for programmed cell death during leaf senescence in plants. Plant Cell Physiol. 39: 922-927.

Chapter 3

Programmed cell death during the transition from multicellular structures to globular embryos in barley androgenesis

Simone de Faria Maraschin*, Gwénaël Gaussand*, Amada Pulido, Adela Olmedilla, Gerda EM Lamers, Henrie Korthout, Herman P Spaink, Mei Wang (2005) Programmed cell death during the transition from multicellular structures to globular embryos in barley androgenesis. Planta, 221(4):459-70.

*Both authors contributed equally to this work.

Abstract

Androgenesis represents one of the most fascinating examples of cell differentiation in plants. In barley, the conversion of stressed uninucleate microspores into embryo-like structures is highly efficient. One of the bottlenecks in this process is the successful release of embryo-like structures out of the exine wall of microspores. In the present work, morphological and biochemical studies were performed during the transition from multicellular structures to globular embryos. Exine wall rupture and subsequent globular embryo formation were observed only in microspores that divided asymmetrically. Independent divisions of the generative and the vegetative nuclei gave rise to heterogeneous multicellular structures, which were composed of two different cellular domains: small cells with condensed chromatin structure and large cells with normal chromatin structure. During exine wall rupture, the small cells died and their death marked the site of exine wall rupture. Cell death in the small cell domain showed typical features of plant programmed cell death. Chromatin condensation and DNA degradation preceded cell detachment and cytoplasm dismantling, a process that was characterized by the formation of vesicles and vacuoles that contained cytoplasmic material. This morphotype of programmed cell death was accompanied by an increase in the activity of caspase-3-like proteases. The orchestration of such a death program culminated with the elimination of the small generative domain, and further embryogenesis was carried out by the large vegetative domain. To date, this is the first report to show evidence that programmed cell death takes part in the development of microspore-derived embryos.

Introduction

The life cycle of flowering plants alternates the dominant diploid sporophytic phase with the short-lived, small-sized structures of the haploid female and male gametophytes, represented by the embryo sac and pollen grains. Microspores, or young pollen grains, have the remarkable ability to switch from their normal gametophytic development towards a sporophytic route. This fascinating example of phase transition during the alternation of generations in plants is called androgenesis (Raghavan, 1986). Androgenesis can be efficiently triggered in several plant species by means of stress treatment around the first pollen mitosis. Androgenic microspores under specific culture conditions are capable to form multicellular structures (MCSs), which differentiate into embryo-like structures (ELSs) (Touraev et al., 1997). The successive ELS developmental stages are known to parallel

somatic and zygotic embryogenesis, providing advantages for both fundamental and applied research (Wang et al., 2000).

The initial steps of microspore embryogenesis are, however, unusual to any other embryogenic system, since MCS formation takes place inside the exine wall of microspores (Mordhorst et al., 1997). During the initial phase of microspore embryogenesis, several patterns of cell division have been identified to take place inside the exine wall. The asymmetric division of the microspore nucleus resulting in a generative and a vegetative cell characterizes the A-pathway. In the A-pathway, MCSs are formed from repeated divisions of the vegetative cell, while the generative cell or its derivatives degenerate and die (Sunderland, 1974). This is the most widely spread mechanism of MCS formation during androgenesis and it has been described in several plant species, including most cereals (Raghavan, 1986). In the B pathway, it is the symmetric division of the microspore nucleus that gives rise to MCSs (Sunderland, 1974). The B-pathway is known to play a major role in rapeseed (*Brassica napus* L.), potato (*Solanum tuberosum* L.), tobacco (*Nicotiana tabacum* L) and wheat (*Triticum aestivum* L.) microspore embryogenesis (Zaki and Dickinson, 1991; Říhová and Tupý, 1999; Touraev et al., 1996; Indrianto et al., 2001), and it has been also described among barley MCSs (Sunderland and Evans, 1980). An alternative route to androgenesis is defined by the independent divisions of the generative and vegetative cells, giving rise to MCSs with heterogeneous compositions. This modified version of the A-pathway, also termed E pathway (Raghavan, 1986), has been described in barley, maize, tobacco and pepper (*Capsicum annum* L) MCSs (Sunderland et al., 1979; Pretova et al., 1993; Touraev et al., 1996; Kim et al., 2004). Conversely to the known A and B pathways, in which the roles of the generative and vegetative cell are clearer, in this modified version of the A pathway both generative and vegetative cell appear to contribute equally to embryo formation (Raghavan, 1986).

What leads microspores to give preference to a particular division sequence is not yet clear. Different developmental pathways have been reported to vary according to plant species, and in response to different stress treatments and the microspore developmental stage (Raghavan, 1986; Sunderland et al., 1979; Říhová and Tupý, 1999; Kasha et al., 2001; Kim et al., 2004). In barley, a model species for androgenesis studies, a correlation between the yield of ELSs and the presence of heterogeneous MCSs has been reported in anther cultures of cold-stressed spikes (Sunderland and Huang, 1985). Nevertheless, no link has been established between the microspore developmental pathways that ultimately lead to barley ELSs formation. Recently, the development of mannitol-stressed barley microspores into ELSs has been monitored by time-lapse tracking (Maraschin et al., 2004). Following osmotic and starvation stress, 50 % of the microspores were triggered to divide and to form

MCSs, however only 20 % of the MCSs further developed into ELSs. The development of ELSs was conditioned to a specific type of MCSs that released ELSs characteristically at the opposite side of the pollen germ pore, a process that was marked by the death of the cells situated at exine wall rupture. The elimination of a specific cell type during the transition phase from MCSs to ELSs suggests that this might be an active cell death process.

Programmed cell death (PCD) is a genetically programmed process of cell death that occurs during development and in response to environmental triggers in a wide variety of biological systems, including higher plants (Raff, 1998; Lam, 2004). Despite the nature of the PCD signal, animal and plant cells undergoing PCD show several common cytological features that include activation of specific proteases, condensation of chromatin, DNA cleavage into ~180bp internucleosomal fragments and loss of cell shape and integrity (Pennel and Lamb, 1997). In animal cells, PCD is regulated by a conserved family of cysteine proteases that specifically cleave target proteins after an Asp residue. The most prevalent executioner caspase in animal cells is caspase-3 (Thornberry and Lazebnik, 1998). Although caspase-3 proteases have not been yet identified in plants, caspase-3-like activity towards the synthetic fluorogenic caspase-3 substrate *N*-acetyl-DEVD-7-amino-4-methylcoumarin (Ac-DEVD-AMC) has been described and related to PCD (Korthout et al., 2000; Lam and del Pozo, 2000).

In order to investigate whether PCD takes place during the transition from MCSs into ELSs, biochemical and morphological markers for PCD were assayed. During the transition of MCSs into ELSs, the death of the cells at the site of rupture was used as a marker for embryogenic development. With the help of this marker, the developmental pathways that lead to ELS formation during barley androgenesis were investigated. Our results indicate that embryogenic MCSs are formed by the modified A-pathway, and therefore are composed of two different cellular domains, displaying generative and vegetative characteristics. During exine wall rupture, the small cell domain derived from the generative cell was eliminated by PCD, while the large cell domain derived from the vegetative cell contributed to globular embryo formation. This is the first report to show that PCD takes place during the transition from MCSs into ELSs in barley androgenesis.

Materials and methods

Androgenesis induction and microspore culture

Donor plants of barley (*Hordeum vulgare* L. cv Igri, Landbouw Bureau Wiersum, The Netherlands) were grown in a phytotron under conditions described previously (Hoekstra et

al., 1992). Pre-treatment consisted of incubation of anthers containing mid-late to late uninucleate microspores in 0.37 M mannitol solution for 4 days in the dark, at 25°C (Hoekstra et al., 1992). After pre-treatment, microspores were isolated as described previously (Maraschin et al., 2003; 2004). The enlarged microspores were plated in medium I (Hoekstra et al., 1992) at a density of 2.10^4 enlarged microspores. ml^{-1} and cultured for 0-14 days for MCS and ELS development (Hoekstra et al., 1993). Cultures were sieved through appropriate nylon mesh sizes and dividing MCSs and ELSs were collected as previously described (Maraschin et al., 2003).

DAPI staining of nuclei

Nuclear evolution of isolated-microspore cultures was followed by 4',6-diamidino-2-phenylindole (DAPI) staining (Vergne et al., 1987). Fresh MCSs were briefly fixed in Carnoy (70% ethanol (v/v): acetic acid, 3:1), after which they were rinsed in 70% (v/v) ethanol and stained for 10 min in $1mg.ml^{-1}$ DAPI aqueous solution containing 1% (v/v) Triton X-100. Squashed material was studied under UV light with a Zeiss Axioplan microscope.

Cell viability and cell death staining of MCSs

MCSs and ELSs at different stages of culture were stained for cell death with Sytox orange (Molecular Probes) and for cell viability with fluorescein-diacetate (FDA, Sigma) as described previously (Maraschin et al., 2004). MCSs were observed using a Leica DM IRBE confocal microscope. An argon (488nm) and a krypton (568 nm) laser were used for visualization of the FDA (Ex 488nm, Em 502-540) and the Sytox orange (Ex 568, Em 570-610) signals, respectively. The percentage of ELSs released out of the exine wall was determined in three (*n*=3) independent experiments by estimating the relative amount of ELSs which showed FDA/ Sytox orange positive domains within 300 MCSs per experiment (Maraschin et al., 2004).

Terminal deoxynucleotidyl transferase-mediated dUTP nick end labelling (TUNEL)

MCSs and ELSs from different developmental stages were fixed in 2% (w/v) glutaraldehyde in 10 mM NaH_2PO_4, 120 mM NaCl, 2.7 mM KCl, pH 7.4 (phosphate-buffered saline, PBS) overnight at room temperature. After dehydration at room temperature in a graded series of 70 %, 90 %, 96 % and 100 % (v/v) ethanol, samples were embedded in Technovit (Heraeus Kulzer). Sections (2 µm) were attached on Biobond (Biocell) coated slides. TUNEL assay was done using an *in situ* cell death detection kit (Roche) according to manufacturer's instructions. Following TUNEL reaction, cross-sections were stained with Sytox orange for visualization of nuclei (Maraschin et al., 2004). Samples were observed using a Zeiss

Axioplan confocal microscope with a MRC 1024 ES Biorad module. An argon/ krypton laser (488/568nm) was used for the visualization of the TUNEL (Ex 488 nm, Em 522 DF 32) and the Sytox orange (Ex 568, Em 605 DF 32) signals.

DNA isolation and electrophoresis

Genomic DNA was isolated from MCSs and ELSs from different developmental stages that were frozen in liquid nitrogen immediately after sampling. Samples were ground with a mortar and pestle to a fine powder and DNA was isolated as described previously (Wang et al., 1999). Five µg of genomic DNA/ lane were separated on a 2 % (w/v) agarose gel containing 1 % (w/v) ethidium bromide in 0.2 M tris-acetate, 0.05 M EDTA pH 8.3 at 50 V for 4 h, along with a Smart DNA ladder (Eurogentec).

Protein isolation and caspase-3-like assay

MCSs and ELSs at different time points of culture were frozen in liquid nitrogen and were used to obtain cytosolic protein extracts. Samples were ground in 500 µl ice-cold extraction buffer containing 100 mM HEPES (pH 7.2), 10% (w/v) sucrose, 0.1% (w/v) CHAPS, 5 mM DTT and 10^{-6} % (v/v) NP40 using a glass mortar and pestle. Subsequently, the homogenate was incubated on ice for 15 min and centrifuged two times for 10 min at 13000 rpm at 4°C to pellet cell debris. The supernatant was cleared by filtration over a 0.22 µm Millex syringe driven filter unit (Millipore). For *in vitro* caspase-3-like activity, 75 µl of cytosolic extracts containing 5 µg of proteins were mixed to 25 µl of the synthetic fluorogenic caspase-3 substrate *N*-acetyl-DEVD-7-amino-4-methylcoumarin (Ac-DEVD-AMC, 75 µM) or with a mix of caspase-3 substrate Ac-DEVD-AMC and inhibitor (Ac-DEVD-CHO, 250 µM). The measurements were performed every 10 min for 2 h at room temperature in triplicates for each sample in three independent experiments (*n*=3). Substrate cleavage was detected in a Perkin Elmer fluorescence spectrometer LS50B at an excitation wavelength of 380 nm and an emission wavelength of 460 nm. The standard setting used an excitation and an emission slit value of 5.0. Kinetics of substrate hydrolysis was tested to be linear throughout the 2 h reactions.

Transmission electron microscopy (TEM)

MCSs and ELSs fixation, dehydration and embedding procedures were performed as described previously (Maraschin et al., 2004). Ultrathin sections were made using an ultramicrotome (Ultracut, Leica), stained for 10 min in 2 % (w/v) uranyl acetate in 50 % (v/v) ethanol, and for 10 min in 0.4 % (w/v) lead citrate, followed by thorough washes in deionized filtered water. Electron micrographs were made using a Jeol 100 CX electron microscope.

Pictures were taken at 60 kV on a FGP- film (Kodak 5302).

Scanning electron microscopy (SEM)

MCSs and ELSs from different developmental stages were fixed in a mixture of 2 % (w/v) paraformaldehyde and 2.5 % (v/v) glutaraldehyde in 0.1 M sodium cacodylate buffer, pH 7.3, for 3 h at room temperature. Samples were dehydrated through a graded series of 50 %, 70 %, 90 %, 96 % and 100 % (v/v) acetone and dried using a Bal-Tec CPD 030 critical point drier. The samples were then mounted on stubs, coated with gold on a Polaron SEM coating unit E5100 and observed using a Jeol 6400 scanning electron microscope.

Experimental data

Data presented on morphological analysis of developing MCSs were representative of at least 300 MCSs observed per time point in three independent experiments (n=3). Mean values ± SD of the daily frequencies of exine wall rupture were calculated as percentages. Significance of the differences in mean values of the specific caspase-3-like activities was tested with a Student's t-test.

Results

Mannitol treatment induces the formation of homogeneous and heterogeneous MCSs with different fates in culture

In order to investigate the developmental pathways by which mannitol-treated barley microspores develop into MCSs, the degree of DNA condensation in the nucleus was used as a marker to distinguish cells with vegetative and generative origins (Sunderland, 1974). During pollen and androgenic development, the generative cells are located opposite to the germ pore at the edge of the structure, connected to the intine (Huang, 1986; Sunderland et al., 1979). In the first day of culture, DAPI nuclear staining revealed that both symmetric and asymmetric divisions characterized the initial phase of MCSs formation. While symmetric divisions gave rise to two nuclei with normal chromatin structure (Fig. 1a), asymmetric divisions gave rise to two nuclei with different degrees of chromatin structure (Fig. 1b). In asymmetrically dividing microspores, the small nucleus with intense DAPI staining indicates the generative cell, and the large nucleus with weaker DAPI staining indicates the vegetative cell. Based on these DAPI-staining properties, MCSs with both homogeneous and heterogeneous nuclei composition were observed in 3 days-old cultures (Fig. 1c, indicated by arrows). A close-up of an heterogeneous MCSs shows that the small condensed nuclei

formed a file at the edge of the exine wall.

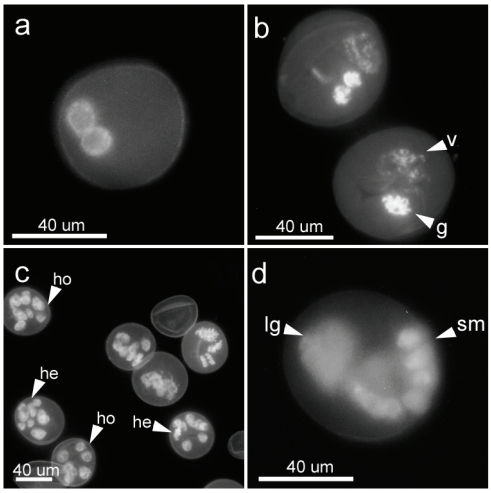

Figure 1. DAPI staining of nuclei in the first days of culture. (a,b) enlarged microspores at the first day of culture illustrating symmetric and asymmetric division of nuclei. (c,d) 3 day-old MCSs with homogeneous and heterogeneous composition. *g* generative nucleus, *lg* large nuclei with normal chromatin structure, *he* heterogeneous, *ho* homogenous, *sm* small condensed nuclei, *v* vegetative nucleus.

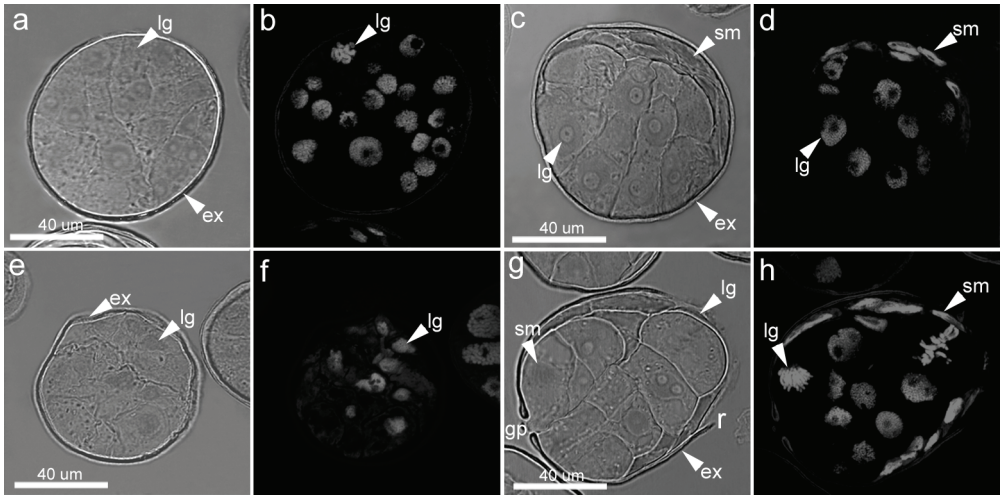

Figure 2. Cross-sections illustrating morphology of homogeneous and heterogeneous 5 and 7 days-old MCSs visualized by DIC and confocal microscopy stained by Sytox orange. (a,b) Homogeneous 5 days-old MCS composed of large cells with round nuclei. (c,d) Heterogeneous 5 days-old MCS displaying two cellular domains. (e,f) Homogeneous 7 days-old MCS displaying shrinkage at the time of exine wall rupture. (g,h) Exine wall rupture in heterogeneous MCS at the site of the small cell domain. *ex* exine wall, *gp* germ pore, *lg* large cell domain, *r* exine wall rupture, *sm* small cell domain.

The degree of chromatin condensation and the position at the edge of the exine wall point out their generative cell origin. At this stage, they divided more frequently than the large nuclei (Fig. 1d).

To better understand the morphology and the fate of the homogeneous and heterogeneous MCSs during the transition phase between MCSs and ELSs, cross-sections of homogeneous and heterogeneous MCSs were analyzed using differential interference contrast (DIC) microscopy and Sytox orange nuclear staining. Prior to exine wall rupture, 5 days-old homogeneous MCSs were composed of cells of equal size with rounded nuclei (Fig. 2a, b). In contrast, in 5 days-old heterogeneous MCSs, the generative domain was composed of small, compact cells with vermiform nuclei showing condensed chromatin structure and dense cytoplasm, while the vegetative domain was composed of large cells with round nuclei and normal chromatin structure (Fig. 2c, d). At the time of exine wall rupture, 7 days-old homogeneous MCSs appeared shrunken and did not develop further (Fig. 2e, f). Interestingly, only heterogeneous MCSs ruptured the exine wall after 7 days of culture. Heterogeneous MCSs displayed exine rupture exclusively at the domain composed of small cells, opposite to the pollen germ pore (Fig. 2g). At the exine wall rupture site, the small cell domain fell apart, while cell divisions were clearly observed within the large cell domain (Fig. 2h).

During microspore embryogenesis, exine wall rupture has been demonstrated to be accompanied by cell death at the site of rupture (Maraschin et al., 2004). In order to establish a link between the localization of the two different morphological domains in heterogeneous MCSs and the dying cells described previously in embryogenic MCSs, cell viability (FDA) and cell death (Sytox orange) staining were performed around the time of exine wall rupture (Fig. 3a-d). During the transition from MCSs to ELSs in 5-7 days-old cultures, Sytox orange-stained cells were located at the edge of the MCSs, at the site of exine wall rupture. This was the same localization as the domain composed of small cells in heterogeneous MCSs with ruptured exine (Fig. 2g, h). This indicates that the small cell domain dies at the time of exine wall rupture. At later stages, few dead cells were observed at the periphery of 9 days-old ELSs, and in most of the 11 days-old ELSs they had been completely eliminated (Fig. 3c, d).

Elimination of the small cell domain by PCD during exine wall rupture

The first PCD marker investigated during exine wall rupture was DNA cleavage. Assessment of *in situ* DNA cleavage was done by TUNEL assay. In liquid cultures, 5 days-old MCS had not yet come out of the exine wall (Fig. 3a). At this stage, some MCSs already showed signs of DNA degradation, as TUNEL-positive nuclei were observed in the small cells with condensed chromatin structure of nuclei. No TUNEL signal was found in the large cell

domain (Fig. 3e-h). After 7 days of culture, most of the MCSs had already ruptured the exine wall. The small cells appeared attached to the boundaries of the ruptured exine and their nuclei were heavily labeled by TUNEL (Fig. 3i-l). Pre-incubation with DNase I prior to TUNEL reaction induced DNA cleavage in both small and large cell domains (Fig. 3m-p), whereas no TUNEL signal was found in negative controls when the transferase was omitted in the TUNEL reaction (data not shown).

In order to investigate the time course analysis of DNA degradation, genomic DNA from 1-8 days-old MCSs was extracted and separated by conventional agarose gel electrophoresis. Extensive DNA degradation could be detected on gel in 7 days-old MCSs and 8 days-old ELSs (Fig. 4a). The apparent 2-days delay in detecting DNA fragmentation on gel compared to the detection of TUNEL-positive nuclei indicates that massive cell death takes place around 7-8 days of culture. In order to determine the dynamics of exine wall rupture, the daily frequency of ELSs released out of the exine wall was determined (Fig. 4b, open bars). An average of 50 ± 1.52 % (n=3) of the ELSs were released out of the exine after 7 days of culture, overlapping with the extensive DNA degradation observed in 7 and 8 days-old cultures (Fig. 4a).

To better understand the events leading to DNA degradation during PCD of the small cell domain, caspase-3-like activity towards the synthetic fluorogenic caspase-3 substrate Ac-DEVD-AMC was assayed (Fig. 4b, black bars). A significant increase of the caspase-3-like activity measured in 1-3 days-old MCSs was observed after 4 days of culture (P< 0.0004), whereas TUNEL positive nuclei were only detected after 5 days of culture (Fig. 3e-h). The increase in the caspase-3-like activity in 4 and 5 days-old MCSs showed a peak at 6 days of culture (P<0.000002) and significantly decreased thereafter.

The peak of the caspase-3-like activity measured in 6 days-old MCSs extracts preceded the DNA degradation observed after 7 and 8 days of culture (Fig. 4a) and the peak of exine wall rupture in 7 days-old MCSs (Fig. 4b, open bars). The caspase-3-like activity was efficiently inhibited by the specific mammalian caspase-3 inhibitor Ac-DEVD-CHO (Fig. 4b, gray bars). These results suggest that developing barley MCSs contain a caspase-3-like protease or a group of related proteases with the substrate preference and inhibitor specificity similar of mammalian caspase-3.

Morphology of cell dismantling

Since PCD involves specific cellular changes during cell dismantling, the ultrastructure of cell death was investigated by TEM in MCSs and ELSs around the time of exine wall rupture.

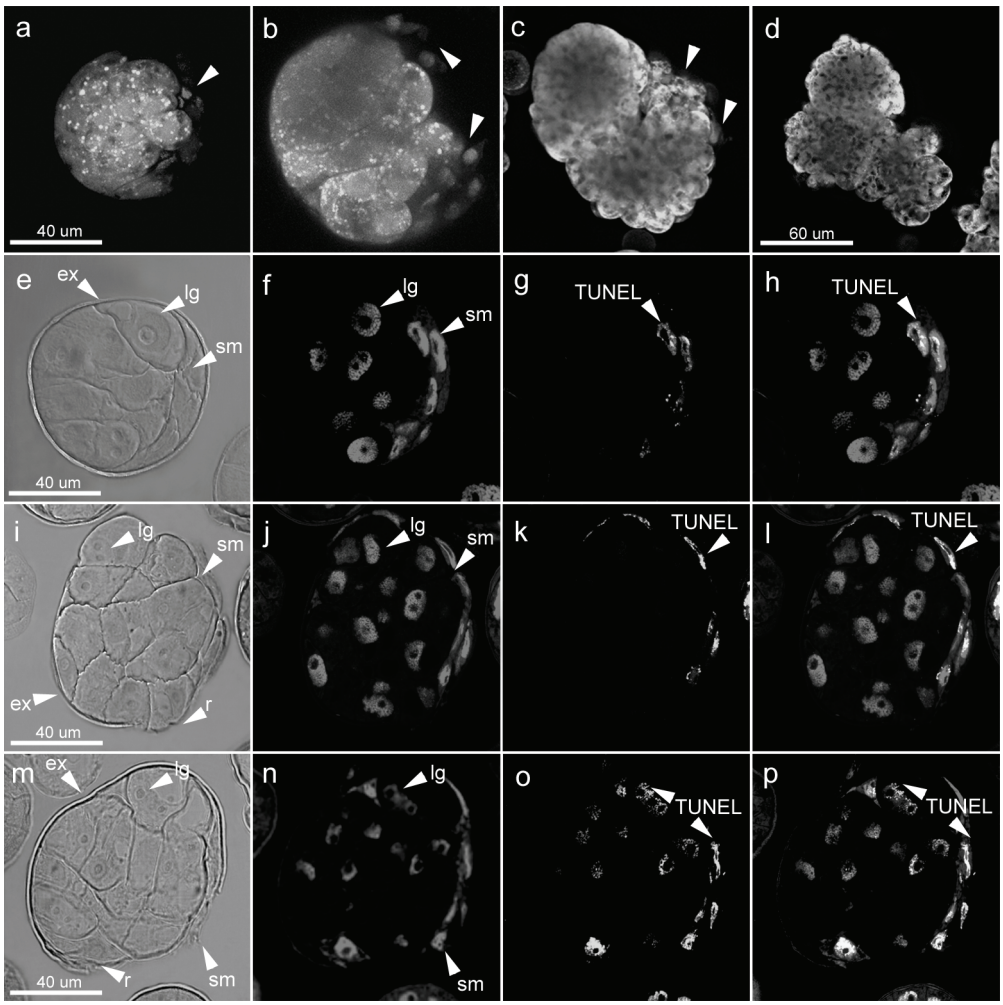

Figure 3. Fate of the different cellular domains during exine wall rupture visualized by FDA/ Sytox orange staining and TUNEL. (a) 5 days-old MCS, (b) 7 days-old MCS, (c) 9 days-old ELS and (d) 11 days-old ELS showing viability of the large cell domain as indicated by FDA staining, whereas the small cells are stained by Sytox orange and are progressively eliminated from the ELS (indicated by arrows). (e-h) Transmitted light image, Sytox orange nuclear staining and TUNEL signal on cross-sections of 5 days-old MCS and (i-l) 7 days-old MCS. (h,l) Are merged images of (f,g) and (j,k), respectively. (m-p) Transmitted light image, Sytox orange nuclear staining and TUNEL signal on a DNase I-treated cross-section of 7 days-old MCS. (p) Is a merged image of (n,o). TUNEL-positive nuclei in the small cell domain are indicated by arrows. *ex* exine wall, *lg* large cell domain, *r* exine wall rupture, *sm* small cell domain.

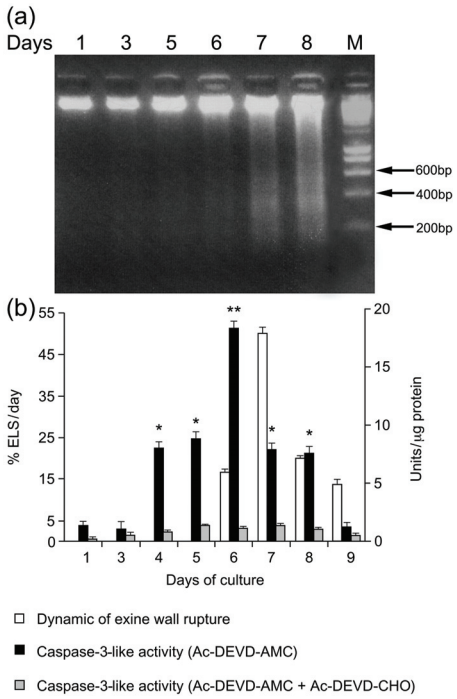

Figure 4. Time course analysis of DNA degradation, exine wall rupture dynamics and caspase-3-like activity. (a) Conventional DNA gel electrophoresis in 1-8 days-old MCSs and ELSs. DNA degradation is observed in 7 days-old MCSs and 8 days-old ELSs. *M*, marker DNA. (b) Dynamics of exine wall rupture (open bars) and caspase-3-like activity in total protein extracts of 1-9 days-old MCSs and ELSs in liquid culture (black bars). (*) Mean value significantly different than value measured at 1 day of culture (P<0.0004). (**) Mean value significantly different from values obtained in all the other samples measured (P<0.000002). Cleavage of the specific animal fluorogenic caspase-3 substrate (Ac-DEVD-AMC) was measured at 460 nm and was efficiently inhibited by the caspase-3 inhibitor (Ac-DEVD-CHO, gray bars) (n=3).

One of the most striking differences between the two cellular domains was the electron-dense cytoplasm of the small cells in 5 days-old MCSs prior to exine wall rupture (Fig. 5a). Due to the high density of the cytoplasm, few organelles could be distinguished at this stage. Among these, amyloplasts filled with starch granules, lipid bodies and mitochondria could be recognized. The nucleus showed a very condensed chromatin structure, and the nucleolus was very dense, characteristic of cells with little transcription activity (Fig. 5b).

The first ultrastructural change associated with PCD visualized in the nucleus was the formation of patches of condensed chromatin (Fig. 5c), which differed from the regular organized condensed chromatin structure (Fig. 5b). In the cytoplasm, mitochondria became less electron-dense (Fig. 5c). After exine wall rupture in 7 days-old MCSs, osmiophilic bodies were observed near the cell membranes and in the extracellular space of the dying cells, adjacent to the exine wall (Fig. 5d). Following exine wall rupture, the small cells detached from the large cell domain (Fig. 5e). The process of cell detachment occurred in an

asynchronous way, since it was possible to identify small cells at different stages of cell dismantling in one ELS (data not shown). During cell detachment, the cell walls surrounding the large cells were not removed, but only the ones surrounding the dying cells (Fig. 5e, indicated by arrows). In advanced stages of cell dismantling, the cytoplasm appeared less electron-dense, mitochondria were collapsed and small vesicles were visible. Cytoplasmic material was contained by vesicles and large vacuoles (Fig. 5f-h). Despite the high degree of cytoplasm collapse, the condensed chromatin in the nucleus persisted until later stages of cell dismantling (Fig. 5f). After cell dismantling was completed, cell debris resulting from the disassembly of the small cells remained in contact with the cell wall of the large cell domain in 9 days-old ELSs (Fig. 5i).

The changes in the external morphology of the dividing structures around the time of exine wall rupture were studied by SEM. SEM observations revealed the subsequent stages in exine wall rupture during the transition of MCSs into ELSs (Fig. 6). The first stage was frequently observed after 7 days of culture and represented the rupture of the exine wall at the site of the small cell domain. This rupture generated a crack, exposing the dead small cells to the exine exterior (Fig. 6a). The small cell domain possessed a very compact structure and the cells showed a flattened shape with a smooth surface (Fig. 6a). The second stage in exine wall rupture was often observed in 7-9 days-old cultures. In the second stage, cell dismantling and cell detachment took place in the small cell domain (Fig. 6b-d). This produced a gap within the small-celled domain, which exposed the large cell domain to the exine exterior. The large cell domain possessed loose structure and the cells showed a round shape with a rough surface (Fig. 6b). While the debris of the small cells remained attached to the edges of the opening exine, the crack in the exine further expanded as the large cells divided (Fig. 6b-d). In the third stage, the exine detached from the large, embryogenic cells. During exine detachment, the continuous and smooth pattern of the outer surface of the exine changed, as it became fragmented by its adhesion to the contours of the large cells (Fig. 6e). After the exine wall was detached from the outer surface of the large-celled domain, 11 days-old ELSs resembled zygotic globular embryos (Fig. 6f).

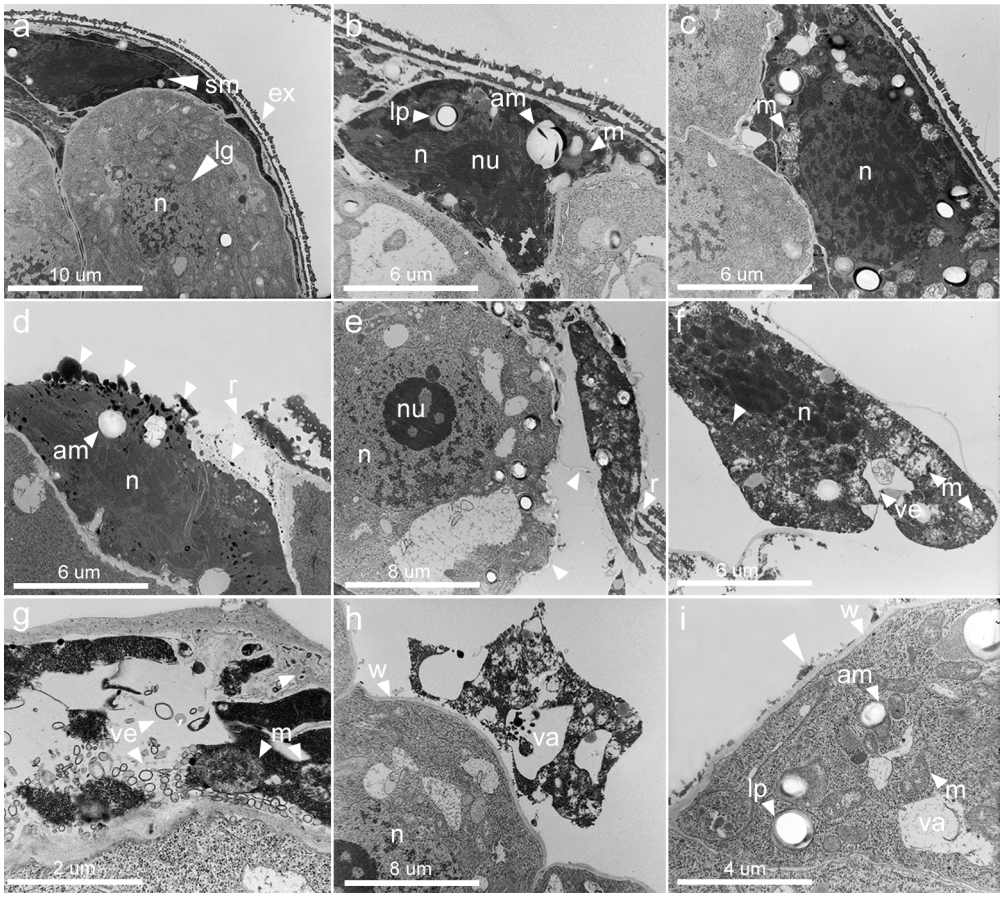

Figure 5. TEM analysis of PCD in MCSs and ELSs. (a-c) 5 days-old MCSs. (a) The cytoplasm of the small cell domain is highly electron-dense compared to the cytoplasm of the large cell domain. (b) A close-up of a small cell illustrates that the cytoplasm of the small cells contains amyloplasts, lipid bodies and mitochondria, while the nucleus shows a high degree of chromatin condensation. (c) The first ultrastructural changes associated with PCD are visualized by the formation of disorganized patches of chromatin in the nucleus and by a decrease in mitochondria electron-density. (d-h) 7 days-old MCSs showing the ultrastructure of the progressive stages of cell dismantling. Arrows in (d) indicate osmiophilic bodies while in (e) indicate cell wall detachment. (i) Region of 9 days-old ELS showing large cell domain after elimination of the small cells. *am* amyloplasts, *ex* exine wall, *lg* large cell domain, *lp* lipid bodies, *m* mitochondrion, *n* nucleus, *nu* nucleolus, *r* exine wall rupture, *sm* small cell domain, *ve* vesicles *va*, vacuole, *w* cell wall.

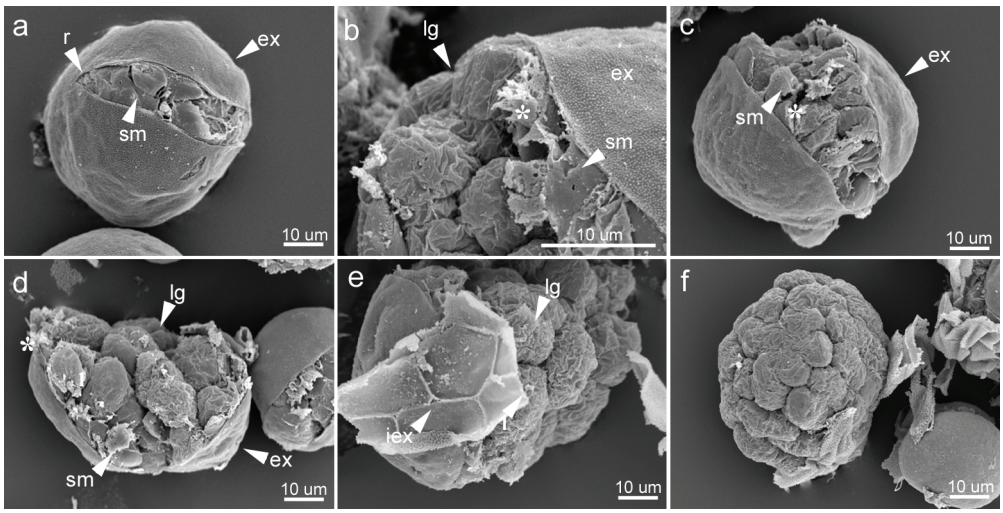

Figure 6. SEM analysis of MCSs and ELSs illustrating the 3 stages of exine wall rupture during the transition from MCSs to globular embryos. (a) Stage one, 7 days-old MCSs: rupture of the exine at the site of the small cell domain, exposing the small cells to the exine exterior. (b-d) Stage two, 7-9 days-old MCSs: cell dismantling and cell detachment of the small cell domain. Cell debris attached to the edges of the opening exine are marked by (*). (e) Stage three, 9 days-old ELS: exine wall detachment from the large cell domain. (f) 11 days-old ELS after exine wall detachment at the stage of globular embryo. *ex* exine wall, *iex* inner side of the exine wall, *lg* large cell domain, *r* exine wall rupture, *sm* small cell domain.

Discussion

Origin and fate of the two different cellular domains in embryogenic MCSs of barley

Cytological observations during the early stages of barley androgenesis revealed that both symmetric and asymmetric divisions result in the formation of MCSs. Symmetric divisions are characterized by the presence of two vegetative-like nuclei and give rise to homogeneous MCSs. On the other hand, asymmetric divisions lead to the formation of heterogeneous MCSs, characterized by a small cell domain with condensed chromatin structure of nuclei and a large cell domain showing normal chromatin structure of nuclei. The morphology of these nuclei resembles that of generative and vegetative nuclei of developing pollen grains (McCormick, 1993). These results indicate that both the B-pathway (Sunderland et al., 1976; Kasha et al., 2001) and the modified version of the A-pathway (Sunderland et al., 1979) contribute to MCS formation during barley androgenesis induced by an anther mannitol treatment. The progression of the embryogenic pathway during the transition of MCSs into ELSs in barley has been reported to occur only from MCSs that display cell death at the site of exine wall rupture (Maraschin et al., 2004). We further demonstrate that cell death takes

place in the small cell domain of heterogeneous MCSs, indicating that they represent the embryogenic MCSs previously described (Maraschin et al., 2004). This is the first report to show that heterogeneous MCSs developed via the modified A-pathway are the real embryogenic MCSs that result in the formation of ELSs in barley androgenesis.

The characterization of the events that resulted in the formation of heterogeneous MCSs indicates that the generative cell divides to give rise to a small cellular domain localized at the opposite side of the pollen germ pore. Cell tracking experiments have shown that the first divisions in embryogenic MCSs of barley take place at the opposite side of the pollen germ pore (Bolik and Koop, 1991; Kumlehn and Lörz, 1999; Maraschin et al., 2004). These findings suggest that the early stages of microspore embryogenesis in barley are marked by the divisions of the generative cell rather than the vegetative cell, which was shown to divide later. In barley, such division patterns have been reported to give rise to heterogeneous MCSs that have been termed 'partitioned units', to denote MCSs composed of different cellular types (Sunderland et al., 1979). Due to the compact cellular organization of the generative domain and the initial free nuclear divisions of the vegetative domain, these domains have been compared to the embryo and endosperm initials in zygotic embryogenesis (Sunderland and Huang, 1985). More recently, embryogenic and endosperm domains have been also described among wheat and maize MCSs (Bonet and Olmedilla, 2000; Magnard et al., 2000). Despite the similarities shared between the small and large cell domains described in the present work and the embryogenic and endosperm initials described previously (Sunderland et al., 1979; Sunderland and Huang, 1985), we show that the small cell domain is eliminated during the process of exine wall rupture and does not contribute to embryo formation, whereas the large cell domain gives rise to ELSs. By SEM, the morphology of ELSs released out of the exine wall resembles that of globular embryos, which showed no apparent signs of pattern formation. Our previous results have shown that pattern formation arises later in culture, when globular embryos released out of the exine wall acquire bilateral symmetry (Maraschin et al., 2003). The expression of the 14-3-3C isoform, a member of the conserved family of 14-3-3 regulatory proteins, has been reported to mark scutellum development during this process (Maraschin et al., 2003). These results indicate that pattern formation is probably not due to the different cellular domains present in MCSs contained within the exine as previously proposed (Sunderland et al., 1979; Sunderland and Huang, 1985). It appears more likely that pattern formation arises after exine wall rupture in globular embryos, a process that might involve new developmental cues.

PCD during the transition from MCSs to globular embryos

During development, uses of PCD include the formation of the plant body plans and specific organ shapes and the removal of unwanted or damaged cells. Three main cytological variants of PCD have been identified in plants (Fukuda, 2000). In apoptotic-like cell death, a process that is analogous to apoptosis in animal PCD, chromatin condensation, nuclear shrinkage and fragmentation, and DNA laddering are known to precede cytoplasm degradation (Pennel and Lamb, 1997). Though this appears to be the classical type of PCD during hypersensitive response and anther tapetum degeneration (Fukuda, 2000; Wang et al., 1999), during the differentiation of tracheary elements it is the vacuolar collapse that precedes nuclear DNA fragmentation (Obara et al., 2001). A third type of cell death morphology has been described within pro-embryos and suspensor cells during somatic embryogenesis of Norway spruce (*Picea abies* L. Karst). In this case, PCD showed apoptotic features concomitantly to autophagy, which was marked by the engulfment of cytoplasmic contents (Filonova et al., 2000).

The morphology of the small cells eliminated by PCD during exine wall rupture presents unique characteristics. Prior to exine wall rupture, the cytoplasm of the small cells is very dense, whereas the nucleus shows condensed chromatin structure. Condensation of nuclear chromatin and an electron-dense cytoplasm have been pointed as morphological markers of plant PCD (Pennel and Lamb, 1997; Domínguez et al., 2001; Aleksandrushkina et al., 2004). However, in the small cell domain of barley MCSs, these characteristics appear to be inherent to their generative cell origin rather than induced by PCD, since they were observed prior to any PCD event had started. The first morphological changes associated with PCD in the nucleus are DNA degradation and the aggregation of chromatin into disorganized patches, however condensed chromatin did not appear marginalized in the nuclear envelope like during pyknosis in most plant PCD events (Pennel and Lamb, 1997). In the cytoplasm, mitochondria became less electron-dense, an indication of mitochondria collapse (Ku et al., 2003). At the exine wall rupture site, osmiophilic bodies were present near the cell membranes and in the extracellular space of the small cells, a morphology that preceded cell detachment and subsequent cytoplasm dismantling. During the PCD events leading to leaf shape remodeling and nucellus degeneration, osmiophilic bodies have been reported near the cell membrane and tonoplast, and in the extracellular space prior to cytoplasm disassembly (Domínguez et al., 2001; Gunawardena et al., 2004). Though the identity of the vesicles heavily stained by osmium has not been identified yet, evidence points out that their presence marks the initiation of the events leading to cytoplasm dismantling during plant PCD.

A remarkable feature of the small dying cells is their detachment from the large cell domain after exine wall rupture. Cell detachment is a characteristic of PCD in the root cap of a wide range of plant species and it is also present during cell death in somatic embryogenic cultures of carrot (*Daucus carota* L.) (Pennel and Lamb, 1997; Willats et al., 2004). After detachment of the small cells from the large cell domain, cell dismantling is characterized by the presence of vesicles and large vacuoles that contain cytoplasmic material. The sequence of events during cytoplasm dismantling in the small cell domain appears to have similarities to the apoptotic-autophagic morphology described during somatic embryogenesis of Norway spruce (Filonova et al., 2000). Apoptotic-autophagic plant PCD is analogous to the cytoplasmic degenerative morphotype of animal PCD where cell death takes place *en masse*, as in the elimination of undesired tissues or complete organs, suggesting overlapping mechanisms of PCD across animal and plant kingdoms (Jones, 2000)

During apoptosis, the most studied case of animal PCD, the first irreversible step in the initiation of the cell death program is the activation of a proteolytic cascade involving caspase proteases. Despite the absence of canonical caspases in plants, dying cells have been reported to have increased proteolytic activities for caspase-1, -3 and -6 (Lam and del Pozo, 2000; Bozhkov et al., 2004). The apparent diversity in the different caspase-like proteases required for PCD in plants is in agreement with their role in animal PCD, since the death of specific cell types and diverse stimuli have been reported to involve different sets of caspases (Raff, 1998). Nevertheless, the most prevalent executioner caspase in animal cells has been pointed to be caspase-3 (Thornberry and Lazebnik, 1998). To date, no plant protease displaying caspase-3-like activity has been so far purified. Recent efforts to purify and characterize the proteases responsible for the caspase-like activites in plant cells has indicated that serine proteases and a vacuolar processing enzyme, which is a cysteine protease, might potentially account for the caspase-like activities upon plant PCD (Coffeen and Wolpert, 2004; Hatsugai et al., 2004). These results suggest that different plant proteases with similar substrate and inhibitor properties of the mammalian caspase-3 might be active during PCD in barley MCSs.

Following activation of the caspase cascade in animal cells, the DNA in the nucleus is cleaved into 180 bp fragments by a caspase-activated DNase (Enari et al., 1998; Sakahira et al., 1998). Upon plant PCD, caspase-like activity has been reported to precede DNA laddering (Lam, 2004), and several DNases have been implicated in this process (Mitler and Lam, 1997; Stein and Hansen, 1999). Though no caspase-activated DNases have been so far identified in plants, the DNA degradation observed during PCD followed the peak of caspase-3-like activity in barley MCSs. This sequence of events points to a possible role of caspase-3-dependent PCD in executing exine wall rupture. Additional roles for the elimination

of the small generative cells by PCD might be associated with sculpting of the microspore embryos, as caspase-6-dependent PCD has been recently demonstrated to be essential for correct embryo pattern formation during *in vitro* somatic embryogenesis in Norway spruce (Bozhkov et al., 2004). The characterization of the molecular events leading to PCD in barley androgenesis will help establishing a causal relation between PCD and exine wall rupture and will shed light on the mechanisms involved in plant PCD regulation. In this regard, biotechnological applications of PCD may be envisaged, since regulation of the PCD processes that take place during microspore and somatic embryogenesis may provide new tools for the manipulation of quality and yield of *in vitro*-developed plant embryos.

Acknowledgements

We are grateful to Dr. Wessel de Priester (Institute of Biology Leiden, Leiden University, The Netherlands) for valuable discussion and critical reading of the manuscript and to Peter Hock for the lay-out of figures.

References

Aleksandrushkina NI, Zamyatnina VA, Bakeeva LE, Seredina AV, Smirnova EG, Yaguzhinsky LS, Vanyushin BF (2004) Apoptosis in wheat seedlings grown under normal daylight. Biochemistry (Moscow) 69: 285-294

Bolik M, Koop HU (1991) Identification of embryogenic microspores of barley (*Hordeum vulgare* L.) by individual selection and culture and their potential for transformation by microinjection. Protoplasma 162: 61-68

Bonet FJ, Olmedilla A (2000) Structural changes during early embryogenesis in wheat pollen. Protoplasma 211: 94-102

Bozhkov PV, Filonova LH, Suarez MF, Helmersson A, Smertenko AP, Zhivotovsky, von Arnold S (2004) VEIDase is a principal caspase-like activity involved in plant programmed cell death and essential for embryonic pattern formation. Cell Death Differ 11: 175-182

del Pozo O, Lam E (1998) Caspases and programmed cell death in the hypersensitive response of plants to pathogens. Curr Biol 8: 1129-1132

Coffeen WC, Wolpert TJ (2004) Purification and characterization of serine proteases that exhibit caspase-like activity and are associated with programmed cell death in *Avena sativa*. Plant Cell 16: 857-873

Domínguez F, Moreno J, Cejudo FJ (2001) The nucellus degenerates by a process of programmed cell death during the early stages of wheat grain development. Planta 213: 352-360

Enari M, Sakahira H, Yokoyama H, Okawa K, Iwamatsu A, Nagata S (1998) A caspase-activated DNase that degrades DNA during apoptosis, and its inhibitor ICAD. Nature 391: 43-50

Filonova LH, Bozhkov PV, Brukhin VB, Daniel G, Zhivotovsky B, von Arnold S (2000) Two waves of programmed cell death occur during formation and development of somatic embryos in the

gymnosperm, Norway spruce. J Cell Sci 113: 4399-4411

Fukuda H (2000) Programmed cell death of tracheary elements as a paradigm in plants. Plant Mol Biol 44: 245-253

Hatsugai N, Kuroyanagi M, Yamada K, Meshi T, Tsuda S, Kondo M, Nishimura M, Hara-Nishimura (2004) A plant vacuolar protease, VPE, mediates virus-induced hypersensitive cell death. Science 305: 855-858

Hoekstra S, van Zijderveld MH, Louwerse JD, Heidekamp F, van der Mark F (1992) Anther and Microspore culture of *Hordeum vulgare* L. cv. Igri. Plant Sci 86: 89-96

Hoekstra S, van Zijderveld MH, Heidekamp F, van der Mark F (1993) Microspore culture of *Hordeum vulgare* L.: the influence of density and osmolarity. Plant Cell Rep 12: 661-665

Huang B (1986) Ultrastructural aspects of pollen embryogenesis in *Hordeum, Triticum* and *Paeonia*. In: Hu H, Hongyuan Y (eds) Haploids of higher plants *in vitro*. Springer-Verlag, Berlin Heidelberg, pp 91-117

Gunawardena AHLAN, Greenwood JS, Dengler NG (2004) Programmed cell death remodels lace plant shape during development. Plant Cell 16: 60-73

Indrianto A, Barinova I, Touraev A, Heberle-Bors E (2001) Tracking individual wheat microspores *in vitro*: identification of embryogenic microspores and body axis formation in the embryo. Planta 212: 163-174

Jones A (2000) Does the plant mitochondrion integrate cellular stress and regulate programmed cell death? Trends Plant Sci 5: 225-229

Kasha KJ, Hu TC, Oro R, Simion E, Shim YS (2001) Nuclear fusion leads to chromosome doubling during mannitol pretreatment of barley (*Hordeum vulgare* L.) microspores. J Exp Bot 52: 1227-1238

Kim M, Kim J, Yoon M, Choi DI, Lee KM (2004) Origin of multicellular pollen and pollen embryos in cultured anthers of pepper (*Capsicum annum*). Plant Cell Tiss Org 77: 63-72

Korthout HAAJ, Berecki G, Bruin W, van Duijn B, Wang M (2000) The presence and subcellular localization of caspase 3-like proteinases in plant cells. FEBS Lett 475: 139-144

Ku S, Yoon H, Suh HS, Chung YY (2003) Male-sterility of thermosensitive genic male- sterile rice is associated with premature programmed cell death of the tapetum. Planta 217: 559-565

Kumlehn J, Lörz H **(**1999) Monitoring sporophytic development of individual microspores of barley (*Hordeum vulgare* L.). In: Clement C, Pacini E, Audran JC (eds) Anther and pollen: from biology to biotechnology. Springer-Verlag, Berlin Heidelberg, pp 183-189

Lam E (2004) Controlled cell death, plant survival and development. Nat Rev Mol Cell Biol 5: 305-315

Lam E, del Pozo O (2000) Caspase-like protease involvement in the control of plant cell death. Plant Mol Biol 44: 417-428

Magnard JL, Le Deunff E, Domenech J, Rogowsky PM, Testillano PS, Rougier M, Risueño MC, Vergne P, Dumas C (2000) Genes normally expressed in the endosperm are expressed at early stages of microspore embryogenesis in maize. Plant Mol Biol 44: 559-574

Maraschin SF, Lamers GEM, de Pater BS, Spaink HP, Wang M (2003) 14-3-3 isoforms and pattern formation during barley microspore embryogenesis. J Exp Bot 51: 1033-1043

Maraschin SF, Vennik M, Lamers GEM, Spaink HP, Wang M (2004) Time-lapse tracking of barley androgenesis reveals position-determined cell death within pro-embryos. Planta, *in press*

McCormick S (1993) Male gametophyte development. Plant Cell 5: 1265-1275

Mitler R, Lam E (1997) Characterization of nuclease activities and DNA fragmentation induced upon hypersensitive response cell death and mechanical stress. Plant Mol Biol 34: 209-221

Mordhorst AP, Toonen MAJ, de Vries SC (1997) Plant Embryogenesis. Crit Rev Plant Sci 16: 535-576

Obara K, Kuriyama H, Fukuda H (2001) Direct evidence of active and rapid nuclear degradation triggered by vacuole rupture during programmed cell death in Zinnia. Plant Physiol 125: 615-626

Pennel RI, Lamb C (1997) Programmed cell death in plants. Plant Cell 9: 1157-1168

Pretova A, de Ruijter NCA, van Lammeren AAM, Schel JHN (1993) Structural observations during androgenic microspore culture of the 4c1 genotype of *Zea mays* L. Euphytica 65: 61-69

Raff M (1998) Cell suicide for beginners. Nature 396: 119-122

Raghavan V (1986) Pollen embryogenesis. In: Barlow PW, Green PB, Wylie CC (eds) Embryogenesis in angiosperms. Cambridge University Press, Cambridge, pp 153-189

Říhová L, Tupý J (1999) Manipulation of division symmetry and developmental fate in cultures of potato microspores. Plant Cell Tiss Org 59: 135-145

Sakahira H, Enari M, Nagata S (1998) Cleavage of CAD inhibitor in CAD activation and DNA degradation during apoptosis. Nature 391: 96-99

Stein JC, Hansen G (1999) Mannose induces an endonuclease responsible for DNA laddering in plant cells. Plant Physiol 121: 71-79

Sunderland N (1974) Anther culture as a means of haploid induction. In: Kasha KJ (ed) Haploids in higher plants: advances and potential. University of Guelph, Canada, pp 91-122

Sunderland N, Roberts M, Evans LJ, Wildon DC (1979) Multicellular pollen formation in cultured barley anthers. I. Independent division of the generative and vegetative cells. J Exp Bot 30: 1133-1144

Sunderland N, Evans LJ (1980) Multicellular pollen formation in cultured barley anthers. II. The A, B and C pathways. J Exp Bot 31: 501-514

Sunderland N, Huang B (1985) Barley anther culture – The switch of programme and albinism. Hereditas 3: 27-40

Thornberry NA, Lazebnik Y (1998) Caspases: enemies within. Science 281: 1312-1316

Touraev A, Pfosser M, Vicente O, Heberle-Bors E (1996) Stress as the major signal controlling the developmental fate of tobacco microspores: towards a unified model of induction of microspore/ pollen embryogenesis. Planta 200: 144-152

Touraev A, Vicente O, Heberle-Bors E (1997) Initiation of microspore embryogenesis by stress. Trends Plant Sci 2: 297-302

Vergne P, Delvallée I, Dumas C (1987) Rapid assessment of microspore and pollen development stage in wheat and maize using DAPI and membrane permeabilization. Stain Technol 62: 299-304

Wang M, van Bergen S, van Duijn B (2000) Insights into a key developmental switch and its importance for efficient plant breeding. Plant Physiol 124: 523-530

Wang M, Hoekstra S, van Bergen S, Lamers GEM, Oppedijk BJ, van der Heijden MW, de Priester W, Schilperoort RA (1999) Apoptosis in developing anthers and the role of ABA in this process during androgenesis in *Hordeum vulgare* L. Plant Mol Biol 39: 489-501

Willats WGT, McCartney L, Steele-King CG, Marcus SE, Mort A, Huisman M, van Alebeek GJ, Schols HA, Voragen AGJ, Le Goff A, Bonnin E, Thibault JF, Knox JP (2004) A xylogalacturonan epitope is specifically associated with plant cell detachment. Planta 218: 673-681

Zaki MAM, Dickinson HG (1991) Microspore-derived embryos in *Brassica*: the significance of division symmetry in pollen mitosis I to embryogenic development. Sex Plant Reprod 4: 48-55

Chapter 4

Heat-shock induced cell death is associated with an increase of caspase-3 and caspase-6 like activities in rice suspension cells

Gwénaël MDJ-M Gaussand, Gerda EM Lamers, Paul JJ Hooykaas, Mei Wang and Henrie AAJ Korthout.

Abstract

Programmed cell death (PCD) is an important process instrumental in animal cell death. The process controls cell proliferation, generation of developmental patterns and the defense against pathogens and environmental conditions. When a cell is committed to suicide, a proteolytic cascade activates caspase proteases. Although plant cells may die by PCD, genes coding for the caspases were not found in the plant genome. Caspase-like activities were measured in plant cells, though. Because plant cells may die by a PCD process involving caspase-like activities, further research was done to identify those proteases.

Heat-shock treatment was used to induce cell death in rice suspension cells. Heat-shock effects were analyzed by means of cytological staining and observation of DNA degradation. Heat-shock was established at 50ºC during 30 minutes. The experiments were continued with this heat-shock treatment and with the same procedure of analysis.

Rice suspension cells were given the above mentioned heat-shock. Eight hours after the treatment, cell death and DNA degradation were detected. Twenty hours after the initial heat-shock, increases were detected of cell death and DNA degradation. Faint fragments could be seen within the DNA degradation smear.

At each time point of the analysis, some rice suspension cells were taken and proteins were extracted from them. Using these extracts, biochemical assays to measure caspase-3 and -6 like activities were performed. Twenty hours after the initial heat-shock, a significant increase of caspase-like activities was measured. The increase of the caspase-like activities correlates with the increase of cell death and DNA degradation (with the appearance of faint DNA fragments in the DNA smear).

The link was studied between caspase-like activities, cell death and DNA degradation. The study employed caspase-3 and caspase-6 inhibitors. These inhibitors were added to the rice suspension cells immediately after heat-shock. The addition of the inhibitors inhibited caspase-3 and caspase-6 like activities. The inhibitors did not prevent DNA degradation or cell death. Only with the caspase-6 inhibitor, a slight attenuation of DNA fragmentation could be observed.

The results indicated that heat-shock treatment leads to cell death in rice suspension cells. The activation of caspase-like proteases as a response of the rice suspension cells occurred twenty hours after heat-shock. This long period might be necessary for optimal activation of the caspase-like proteases. It might also be necessary for optimal activation of the enzymes involved in DNA fragmentation.

Introduction

In animals, cells may die either by a process called necrosis or by programmed cell death (PCD). PCD is an important process to control cell proliferation, generation of developmental patterns and the defense against pathogens and environmental conditions. The process removes superfluous, damaged or infected cells in an organized manner (Steller et al. 1995; Lawen 2003). The first step in the initiation of the cell death program is the activation of caspase proteolytic cascades (Abraham et al. 2004). Caspases are the key executioners of apoptosis. They belong to a family of cysteine proteases, conserved through evolution (Kroemer & Martin 2005). Caspases are synthesized as proenzymes. The proenzymes are activated through cleavage at internal aspartate residues by other caspases or by autoactivation. Activated caspases cleave a variety of proteins after specific aspartate residues, ultimately leading to cell death. The cleaved proteins are cytoskeletal proteins - such as lamins, α-fodrin and actin - proteins involved in DNA repair and cell-cycle regulation - such as poly(ADP-ribose) polymerase (PARP) and retinoblastoma protein - (Launay et al. 2005; Ruchaud et al. 2002; Zhivotovsky 2003). Caspase-3 is activated during most apoptotic processes. It is generally believed to be the main executioner caspase. Caspase-6 has been shown to cleave lamin and several nuclear proteins such as transcription factor activator protein-2α and SATB1 (special AT-rich sequence binding protein 1) leading to the collapse of the nucleus (Nyormoi et al. 2001; Gotzmann et al. 2000). Caspase activation is strictly regulated by Bcl-2 family members. The Bcl-2 family controls the release of pro-apoptotic caspase activating factors - such as cytochrome c, APAF-1 and AIF - from the mitochondria into the cytosol (Broker et al. 2005). PCD is characterized by specific features such as cell shrinkage, blebbing of the plasma membrane, condensation and fragmentation of the nucleus, and internucleosomal cleavage of DNA (Nagata 2005; Zhivotovsky 2003).

In plants, a process seems to occur that is equivalent to PCD. This process is associated with senescence (Schmid et al. 2001), stress (Katsuhara 1997; Solomon et al. 1999), development (Runeberg-Roos et al. 1998; Groover et al. 1999; Schmid et al. 1999) and the hypersensitive response to pathogens (Dangl et al. 1996; Mittler et al. 1997; Pontier et al. 1998; Mackey et al. 2002; Abramovitch et al. 2003). Morphological similarities between animal and plant cells undergoing PCD were found. Similarities are condensation and shrinkage of the cytoplasm and the nucleus, and fragmentation of the DNA and the nucleus (Krishnamurthy et al. 2000). When fluorogenic caspase-1, -3 and -6 substrates were used, dying plant cells were found to have caspase-like activities (del Pozo et al. 1998; Lam et al. 2000; Sun et al. 1999; Bozhkov et al. 2004). Caspases are conserved through evolution in species ranging from *C. elegans* to human (Jiang et al. 2004). Caspases are not conserved

in plants. After the elucidation of the complete genomes of *A. thaliana* and rice, it has become clear that no genes for caspases and proteins of the Bcl-2 family are present in plants. Based on domain structure and sequence similarities, a family of distantly related caspase-like proteases named metacaspases were later discovered in plants, fungi and Plasmodium (Uren et al. 2000). The plant metacaspases can be divided into two classes based on sequence similarities within their caspase-like regions and their predicted domain structure. Whether these metacaspases possess caspase-like proteolytic activity and are involved in plant PCD remains largely unknown. The protein mcII-Pa (plant metacaspase type II) was found to be expressed during PCD in somatic embryogenesis in Norway spruce. In situ hybridization analysis showed accumulation of the mRNA in the part of embryogenic tissues and structures committed to die (Suarez et al. 2004).

Studying mechanisms of PCD in whole plants can be difficult as it may occur only in a small group of inaccessible cells buried in a mass of surrounding healthy cells. Plant suspension cells have been used to study a wide range of physiologically important cell processes including PCD. Suspension cells have the advantage to be easy material for biochemical work and they can be used to determine synchronized events after PCD induction. Furthermore, plant suspension cells can be generated easily and rapidly, and relatively homogeneous cells can be obtained in large quantities. Addition of compounds to cell cultures - such as viable stains and inhibitors of cell death - can be achieved and they can be studied easily by microscopy. In this study, cell death was triggered in rice suspension cells by heat-shock. This abiotic treatment was described previously as inducing PCD in plant cells. DNA laddering was described in cucumber (Balk et al. 1999), nuclear condensation and cytoplasm shrinkage were described in carrot (Mc Cabe et al. 1997), and caspase-like activity was detected in tobacco (Tian et al. 2000) and in oat (Coffeen et al. 2000) after heat-shock induction. In this work, rice suspension cells were used. First, the most effective conditions to induce cell death were established. These cells were then studied by both biochemical and cytological methods.

Material and methods

Rice suspension cells and heat-shock treatment

Rice suspension cells were obtained from primary callus grown on scutellum of mature seeds (*Oryza sativa* variety IR52). The cells were subcultured weekly by pipetting 6 ml of cell suspension in a 250 ml flask containing 50 ml of culture medium (4.4 g/l Linsmaier and Skoog medium including vitamins (Duchefa, L 0230), 4 mg/l 2, 4-D hormone and 30 g/l sucrose,

pH5.8 ± 0.1). The rice suspension cells were maintained in a dark climate chamber at 28°C with 50% relative humidity on a horizontal rotary shaker (120 rpm).

For heat-shock treatment, the flasks (5 days old, exponential growth) were submerged in different water baths and incubated for 30 minutes without shaking. The baths were at the temperatures of 45, 50 and 53°C, respectively. For the control samples (without heat-shock treatment), the flasks were just kept at room temperature on the laboratory bench for 30 minutes without shaking. As a next step, all the flasks were placed on a shaker in the dark climate chamber and re-incubated at 28°C for different periods of time. The re-incubation periods are referred to in the text.

Cells were harvested by filtration and the dry cell mass was frozen in liquid nitrogen for DNA extraction or used directly for soluble protein extraction.

Viability analysis

Cell death and cell viability in rice suspension cells were visualized by staining with Sytox orange (Molecular Probes) combined with fluorescein-diacetate (FDA, Sigma), respectively. Each sample (500 µl cells) taken at a given time point was stained with a combination of 4.10^{-2} µg.ml^{-1} FDA and 1 µM Sytox orange for 10 minutes at room temperature. Cells were studied with a Leica DM IRBE confocal microscope. An Argon (488 nm) and a Krypton (568 nm) laser were used for visualization of the FDA (Ex 488 nm, Em 502-540) and the Sytox orange (Ex 568, Em 570-610) signals, respectively.

DNA isolation and electrophoresis

Genomic DNA was isolated from cells that were frozen in liquid nitrogen immediately after sampling. Samples were ground with a mortar and pestle to a fine powder and DNA was isolated as described by Wang et al. (1999). For each sample, 10 µg of genomic DNA was separated on a 2% (w/v) agarose gel containing 0.02% (w/v) ethidium bromide in 0.2 M tris-acetate, 0.05 M EDTA pH 8.3 at 50 V for four hours, along with a Smart DNA ladder (Eurogentec).

Protein isolation and caspase assays

For measuring *in vitro* caspase-3 and -6 like activities, the samples were prepared as follows: about 4 g of rice suspension cells (fresh weight after filtration over one layer of Whatman paper no.1) were ground in 500 µl ice-cold extraction buffer containing 100 mM HEPES (pH 7.2), 10% (w/v) sucrose, 0.1% (w/v) CHAPS, 5 mM DTT and 10^{-6} % (v/v) NP40 using a glass mortar and pestle. Subsequently, the homogenate was incubated on ice for 15 minutes, filtered through three layers of cheesecloth and centrifuged first at 2000 g for 5 minutes. The

supernatant was then centrifuged for 10 minutes at 10000 g at 4°C to pellet cell debris. The lipid layer was removed with a needle and a syringe by sucking at the surface. The soluble protein extract was filtrated over a 0.22 µm Millex syringe driven filter unit (Millipore Corporation, Bradford, USA). Protein concentrations were determined using the Bradford method (Bio-Rad) with BSA as the standard (Bradford 1977).

75 µl of soluble protein extract containing 5 µg of proteins were mixed in a 96-well plate with 25 µl of the synthetic fluorogenic caspase-3 or caspase-6 substrates (Ac-DEVD-AMC or Ac-VEID-AMC, respectively, 75 µM final concentration in assay). The specificity of caspase activity assays was measured with the addition of caspase-3 or caspase-6 inhibitor (Ac-DEVD-CHO or Ac-VEID-CHO respectively, 250 µM final concentration in assay). During two hours, the proteolytic activity was measured in triplicates per sample every 10 minutes at room temperature. Substrate cleavage was detected in a Perkin Elmer fluorescence spectrometer LS50B (Perkin Elmer, Norwall, CT, USA) at an excitation wavelength of 380 nm and an emission wavelength of 460 nm. The standard setting used an excitation and an emission slit value of 5.0. Kinetics of substrate hydrolysis was tested to be linear throughout two hours of reaction. The activity was calculated in fluorescence units per µg protein per hour. The data presented were representative of three independent experiments (n = 3) with use of three different extracts for each experiment. The data were represented as mean ± SD. Comparison between mean values of the specific caspase-3 and caspase-6 like activities was tested with a Student's *t*-test (*, $P<0.01$ versus control (28°C)). The activity was also measured in control cells at different time points. The activity measured in control cells was identical at all time points. The mean ± SD of the activity is therefore referred to by one value, named control (c).

For the inhibition experiment, the cell permeable caspase inhibitors (Ac-DEVD-CHO or Ac-VEID-CHO respectively, 250 µM final concentration in assay) were added to the rice suspension cells immediately after heat-shock treatment. The cells were re-incubated for a given time. As an intermediate step, the rice suspension cells were washed in order to remove the excess of inhibitor. The rice suspension cells were then used for total soluble protein extraction and for DNA extractions, which were performed as previously described.

Results

Cell death and DNA degradation in rice suspension cells after heat-shock

Flasks of rice suspension cells grown at 28ºC were incubated for 30 minutes at different temperatures in order to induce cell death; flasks at 45ºC, at 50ºC and at 53ºC. The viability

of the cell population was analyzed with fluorescein diacetate (FDA) and Sytox orange after a twenty hours re-incubation at the normal growth temperature of 28ºC. Viable cells become fluorescent green in the presence of FDA as cytoplasmic esterases liberate the fluorescent molecule. Non viable cells are stained red with Sytox orange: the dye can only enter into cells with compromised membranes and then stains nucleic acids.

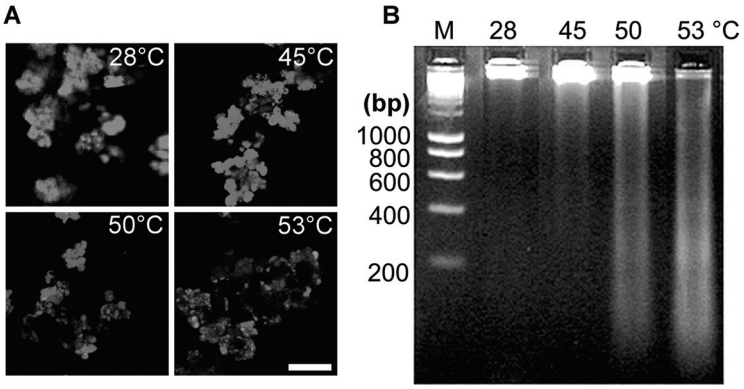

Figure 1: Induction of cell death and DNA degradation in rice suspension cells after heat-shock treatment. (A): cell viability of rice suspension cells visualized with FDA and Sytox orange stainings. Merged image top left: control sample. Merged image top right: rice suspension cells heat-shocked for 30 minutes at 45ºC. Merged image bottom left: rice suspension cells heat-shocked for 30 minutes at 50ºC. Merged image bottom right: rice suspension cells heat-shocked for 30 minutes at 53ºC. All observed twenty hours after treatment. Bar represents 400 µm. (B): 2% agarose gel electrophoresis of DNA samples obtained from the same samples described in (A). M, marker DNA.

The cells heat-shocked at 45ºC remained viable (figure 1A). Their viability was comparable with that of the non-treated cells (control sample growing at 28ºC). If more severe conditions were applied, e.g. heat-shock at 50º or 53°C, a dramatic decrease of cell viability was observed. Flasks heat-shocked at 50ºC showed about 50% viable cells after a twenty hours re-incubation; flasks heat-shocked at 53ºC retained less than 10% viable cells.

To test whether the decrease of cell viability was caused by programmed cell death (PCD) or by necrosis, the DNA from rice suspension cells subjected to heat-shock was extracted and analyzed on an agarose gel. In the case of PCD, DNA is fragmented at internucleosomal linker sites. The DNA fragmentation is seen as discrete bands of multiples of 180–200 bp, visible as a specific DNA ladder after gel electrophoresis of DNA samples. In contrast, after random degradation of DNA during necrosis, a smear of many different DNA fragments will be visible on a gel. As shown in figure 1B, control cells (28ºC) did not show any genomic DNA degradation. Some DNA degradation was seen after incubation at 45ºC, more at 50ºC and still more at 53ºC (figure 1B) which correlates with the amount of cell death observed by viability staining (figure 1A). To conclude, there is no obvious “laddering” of DNA degradation of the genomic DNA into internucleosomal fragments of multiples of 180 bp.

Thus cell death may have occurred by necrosis. For the rest of the study, the rice suspension cells were treated with heat-shock at 50ºC.

Time course of cell death

After cell death was induced by heat-shock at 50°C, the rice suspension cells were stained with FDA and Sytox orange. Observations were made at different time points (0, 4, 8, 16, 20 and 24 hours). As shown in figures 2 A and B, the heat-shocked rice suspension cells lost viability over time. Dead cells can already be seen four hours after the heat-shock treatment and the number of dead cells increases over time.

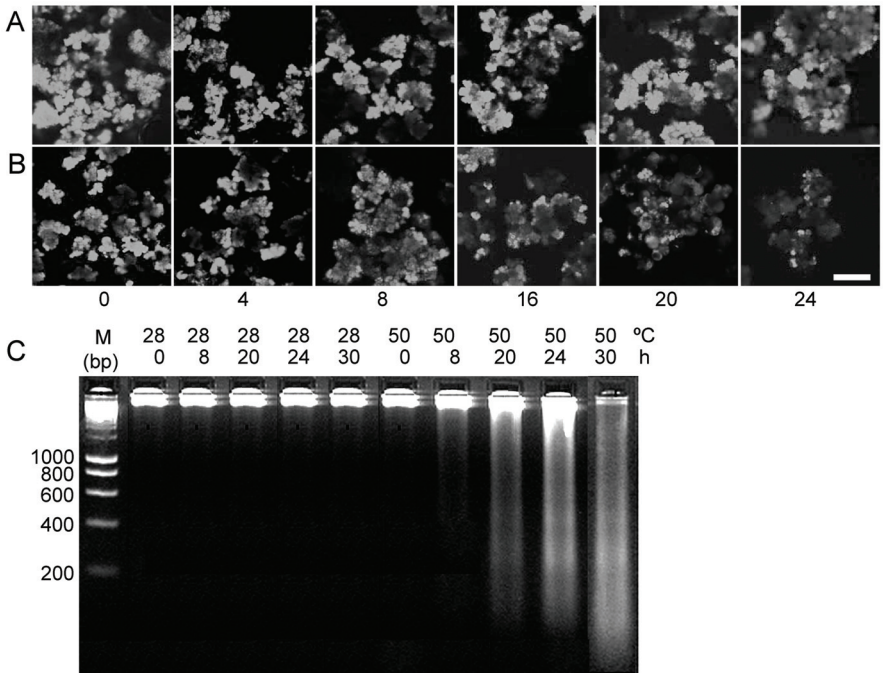

Figure 2: Increase of cell death and DNA degradation in rice suspension cells over time after heat-shock at 50°C. Cell viability is visualized with FDA and Sytox orange staining with CLSM. (A) Merged pictures of control rice suspension cells observed after 0, 4, 8, 16, 20 and 24 hours. (B) Merged images of rice suspension cells heat-shocked at 50ºC for 30 minutes and observed at different time points after re-incubation (at 0, 4, 8, 16, 20 and 24 hours). Bar represents 400 µm. (C): Conventional DNA gel electrophoresis with DNA extracted from samples described in (A) and (B) and analyzed after different re-incubation times (0, 8, 20, 24 and 30 hours). M, marker DNA.

To find out when the DNA starts to degrade, genomic DNA was extracted from heat-shocked cells after 0, 8, 20, 24 and 30 hours of re-incubation. The extracted genomic DNA was separated by conventional agarose gel electrophoresis. As shown in figure 2 C, DNA degradation starts eight hours after heat-shock. Much of the DNA seems to have degraded

after twenty hours, as is evident from an extensive DNA smearing with a faint DNA ladder (figure 2 C). After thirty hours, genomic DNA was completely degraded. No DNA degradation was apparent in DNA samples isolated from (non heat-shocked) control cells. Rice suspension cells apparently cannot survive a short (30 minutes) incubation at a temperature above 50°C. The rice suspension cells mostly die by necrosis as indicated by the DNA degradation smear on the gel. However, in the gels, faint DNA bands overlaying the DNA degradation smear can be seen. These bands indicate that some of the cells may have died by programmed cell death (PCD).

Caspase-like activities

In animals, caspase-like proteases are activated prior to DNA fragmentation. In order to find out whether this is also the case with plants, caspase-3 and -6 like activity assays were performed. The cleavage of the synthetic caspase-3 substrate Ac-DEVD-AMC and the synthetic caspase-6 substrate Ac-VEID-AMC was measured in rice suspension cell extracts. The cleavage of the respective substrates was inhibited by the respective caspase inhibitors as shown in figure 3. After a twenty hours re-incubation, the cleavage of both substrates took place in the soluble protein extract from heat-shocked samples. Figure 3 shows the increase of the caspase-3 and caspase-6 like proteolytic activities over time.

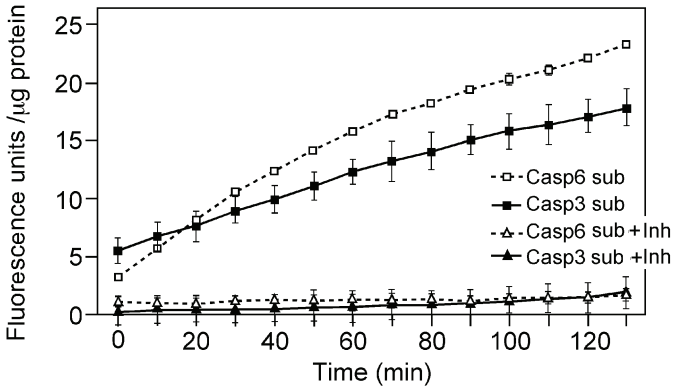

Figure 3: Kinetics of caspase-3 and caspase-6 like activities. Rice suspension cells were heat-shocked at 50°C for 30 minutes. Total soluble proteins were extracted from the treated cells after a twenty hours re-incubation of those cells. Caspase-3 and caspase-6 like activities were measured in the extracts, using caspase-3 and caspase-6 substrate with and without inhibitor. During two hours, these activities were measured every 10 minutes.

Caspase-3 and -6 like activities were measured in the soluble protein fraction extracted from heat-shocked rice suspension cells. The measurements were done after different periods of re-incubation at 28°C. As shown in figure 4, the heat-shocked cells show caspase-3 and -6

like activities. The activities began at background level (as in the control cells), and significantly increased twenty hours or more after heat-shock. At their peak twenty to twenty-three hours after heat-shock, caspase-6 like activity was found to be 2 to 3.5-fold higher than caspase-3 like activity. After their peak both activities significantly decreased. Each activity was inhibited by adding the respective inhibitor together with the substrate, as shown in figure 4.

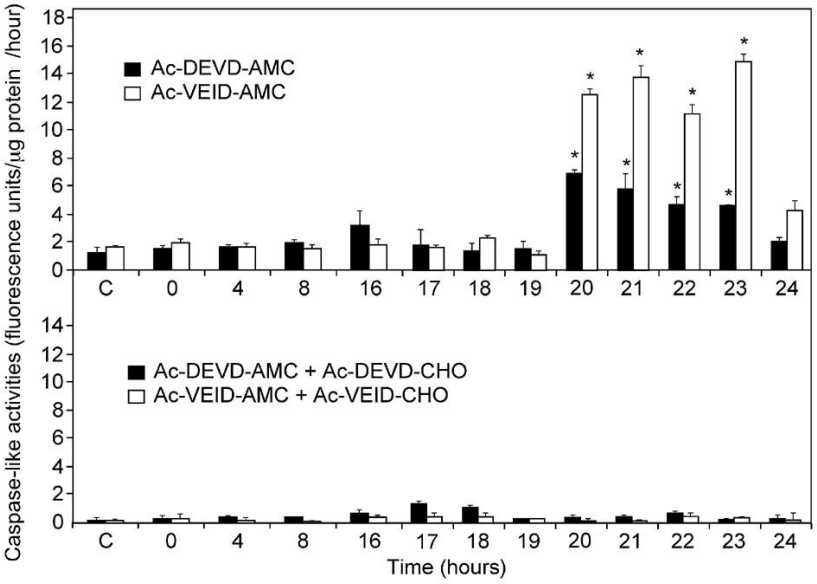

Figure 4: Rice suspension cells were heat-shocked at 50°C for 30 minutes. Total soluble proteins were extracted from the treated cells at various times after re-incubation of those cells (see time points in figure). Caspase-3 and caspase-6 like activities were measured in the extracts at 460 nm with the fluorogenic substrates Ac-DEVD-AMC (black) and Ac-VEID-AMC (white), respectively. Caspase-3 like activity was effectively inhibited by the caspase-3 inhibitor (Ac-DEVD-CHO, black). Caspase-6 activity was effectively inhibited by the caspase-6 inhibitor (Ac-VEID-CHO, white). (*n=3*)

The increase in caspase-like activities measured twenty hours after heat-shock correlates with the appearance of a faint DNA ladder in the smear of DNA fragmentation (in DNA samples from the same cells). Although they correlate, the caspase-like activities do not seem to preceed the DNA fragmentation.

Inhibition of caspase-like activities, DNA degradation and cell death

The question now is whether caspase-like activity is necessary for DNA fragmentation. In order to answer this question, cell permeable caspase inhibitors were added to the culture immediately after heat-shock treatment. The inhibitors' potential ability to block the pathway

leading to DNA fragmentation was analyzed. After heat-shock treatment, caspase-3 or caspase-6 inhibitor was added to the rice suspension cells. Twenty and twenty-two hours after heat-shock, the cells were collected so that caspase-3 or caspase-6 like activities could be measured, and so that DNA fragmentation could be detected. As shown in figure 5, a low level of caspase activity could be found in the cells. The inhibitors added immediately after heat-shock were apparently still active. Only some caspase-6 like activity was found, but this was 6 to 8-fold less than in control samples (not treated with the inhibitor). With control cells not incubated with any inhibitor clear DNA degradation smear was observed from twenty to twenty-six hours (figure 6). Twenty-four and twenty-six hours after heat-shock not only the DNA degradation smear could both be seen, but also a faint DNA ladder. The addition of caspase-3 inhibitor to the heat-shocked cells did not affect the smear. The DNA ladder, however, was less strong after twenty-two hours of re-incubation. The addition of caspase-6 inhibitor gave the same result: the smear remains visible but the DNA ladder decreased, now after twenty-four and twenty-six hours of re-incubation.

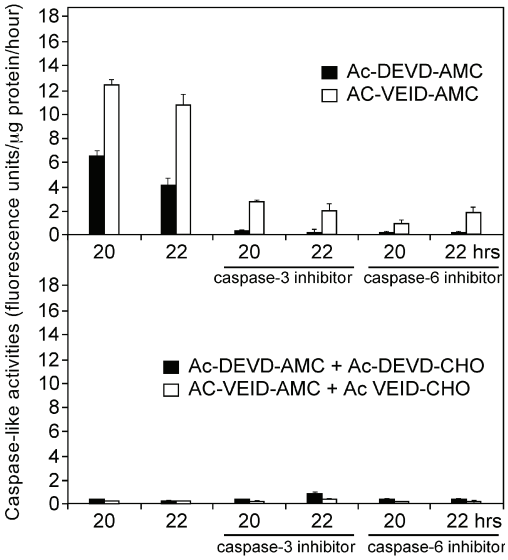

Figure 5: Inhibition of caspase-3 and caspase-6 like activities in total soluble protein extracts. Immediately after heat-shock at 50ºC for 30 minutes, caspase-3 inhibitor or caspase-6 inhibitor (Ac-DEVD-CHO and Ac-VEID-CHO, respectively; final concentration 250 µM) was added to the rice suspension cells. Total soluble proteins were extracted from the treated cells after a twenty hours re-incubation of those cells, and again two hours later. The activities were measured in the three different extracts (incubating without inhibitors, incubating with caspase-3 inhibitor, incubating with caspase-6 inhibitor), using caspase-3 substrate and inhibitor and caspase-6 substrate and inhibitor.

To conclude, the inhibitors for caspase-3 and caspase-6 decreased caspase-like activities and inhibited DNA laddering. Not only did the use of caspase-3 inhibitor block caspase-3 like activity, this sample did not show caspase-6 like activity either. And the use of caspase-6

inhibitor not only blocked caspase-6 like activity but also caspase-3 like activity. The experiment was performed in triplicate for caspase assay and DNA extraction after inhibitor incubation. The same result was obtained for each experiment. For these samples cell viability was analyzed. The addition of the inhibitors did not inhibit cell death (results not shown) since the effect of the heat-shock treatment on the rice suspension cells could not be made undone.

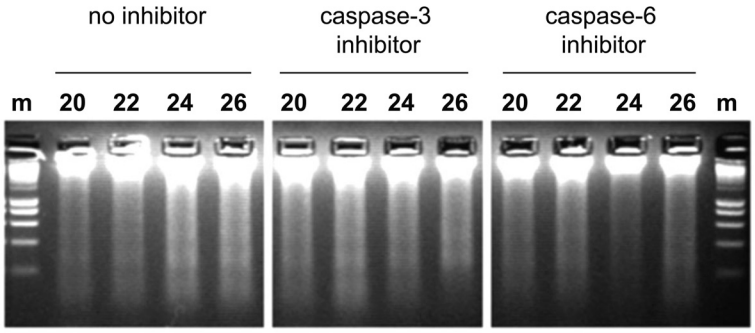

Figure 6: DNA extraction after inhibition of specific caspase-3 and caspase-6 like activities in rice suspension cells. The DNA was extracted from the same samples of rice suspension cells as described in figure 5 (which were treated with the caspase-3 or caspase-6 inhibitor) after a twenty hours re-incubation of those cells, and again two, four and six hours later (2% agarose gel. M, marker DNA).

Discussion

Cell death in rice suspension cells

There are two recognized cellular processes that result in the death of cells: necrosis and programmed cell death (PCD). Necrosis is usually triggered by extrinsic factors such as direct physical injury, acute changes in environmental conditions, pathogenic activity, and a collapse of cell integrity. The injury will often concurrently affect many cells within a tissue (Wyllie et al. 1980; Dunn et al. 2002). In contrast, PCD is triggered by intracellular signals activating genetically determined pathways that operate at a single-cell level. PCD has distinct morphological characteristics that differentiate this form of cell death from necrosis. PCD, well described as apoptosis in animal cells, is characterized by morphological changes including cell shrinkage, chromatin condensation and apoptotic cascades. These changes can be initiated through two major pathways: either activation of death receptor family members in response to ligand binding, or release of cytochrome c from the mitochondria. Initiation of an apoptotic pathway is followed by caspase activity and massive protein cleavage, resulting in cell demise and death. In contrast, necrosis is characterized by cellular swelling and disruption of the plasma membrane, leading to release of cellular components

and *in vivo*, an inflammatory tissue response.

In order to assess whether the model system (rice suspension cells and heat-shock treatment) is suitable to study PCD and necrosis, we have considered morphological and biochemical features. These features included DNA fragmentation, viability staining and caspase-like activity. Heat-shock was conducted at 50ºC for 30 minutes. In rice suspension cells, heat-shock induced both necrosis and PCD. After the treatment, necrosis was observed after eight hours. The observed symptoms were cell death increase and DNA smearing. After the treatment, PCD occurred after twenty hours. The observed symptoms were caspase-like activity and DNA fragmentation with faint bands known as “DNA ladder”.

Caspase-like activity in plant cells

The way to detect animal caspase activity is to measure the cleavage of synthetic substrates upon their incubation in lysates of apoptotic cells (Zhivotovsky 2003). A substrate contains a tetrapeptide sequence that mimicks the cleavage sites of the caspase targets. Fluorogenic substrates are commercially available to determine the activity of a specific caspase.

Protocols were established to extract soluble proteins and to measure caspase-like activities in plant cells. Two different tetrapeptide sequences coupled with coumarin were used to measure caspase-3 and caspase-6 like activities (Ac-DEVD-AMC and Ac-VEID-AMC, respectively). As observed, caspase-3 and caspase-6 like proteases were significantly active between twenty and twenty-three hours of re-incubation after heat-shock treatment. At the other time points following the treatment, and in the case of the untreated samples, measurement showed no increase of caspase activities.

In plant cells the main apoptotic executioner remains unknown (Lam & del Pozo 2000). Many reports have described different plant systems with specific activation of caspase-like proteases such as caspase-1, -3 and -6 (del Pozo et al. 1998; Sun et al. 1999; Korthout et al. 2000; Tian et al. 2000; Chen et al. 2000; Bozhkov et al. 2004; Maraschin et al. 2005). It is difficult, however, to interpret caspase-like activity in plants with the use of caspase substrates and inhibitors because those are originally designed for animal studies. The specificity of an animal substrate for a plant target is not certain and the plant targets are not known. According to the manufacturer (Calbiochem, Germany), caspase-3 substrate and inhibitor (Ac-DEVD-AMC and Ac-DEVD-CHO, respectively) can be used to study caspase-3, -6, -7, -8 and -10 in animal cells. Caspase-6 substrate and inhibitor (Ac-VEID-AMC and Ac-VEID-CHO, respectively) can only be used to study caspase-6. The plant research does not confirm the specificity: both inhibitors have an effect on both activities.

The results concerning caspase-like activities showed that after induction of PCD in rice suspension cells, proteases are activated at a certain time point. Their substrate

preference and inhibitor specificity proteases are shared with mammalian caspase-3 and caspase-6.

Sequential events in plant cells

Cell death and DNA degradation were observed after eight hours of re-incubation and more pronounced during the following hours. PCD with caspase-like activation and DNA fragmentation was observed after twenty hours of re-incubation. It is interesting to know why such a period is needed to get caspase-like poteases activated. Many reports have described that plant responses to PCD may vary according to the type of PCD, the type of PCD process, and the type of induction signal. Developmental PCD and pathogenic PCD are two types of PCD that can occur in a cell in response to different stimuli (van Doorn & Woltering 2005). The response seems to depend on how fast death is required. Pathogenic PCD, the hypersensitive response (HR), will generally occur when speed is required because the defense barrier has to be formed quickly. Developmental PCD is slower because degradation and the re-use of cell material need time.

Pathogenic PCD may unfold in either of two cell death responses in the affected plant. The first kind of cell death response is a hypersensitive response (HR). If a plant is resistant to a pathogen, a rapid cell death is triggered at the primary site of infection. This rapid cell death is accompanied by activation of local defense responses (Lam & del Pozo 2000). The second kind of cell death response is slower. If a plant is susceptible to a pathogen, disease develops locally or systemically.

It is unclear why the two kinds of PCD unfold at different speeds. It might be crucial that plant cells need time to mobilize enzymes necessary for PCD. A large central vacuole, which contains many enzymes, is a distinguishing feature of almost all plant cells. The collapse of this vacuole has been hypothesized to be common to all forms of plant PCD (Fukuda 2000; Jones 2001).

Cell death inhibition

The use of caspase-3 or caspase-6 inhibitors to stop caspase-like activity and DNA fragmentation was described in several reports. Belenghi et al. (2004) removed apical meristems from pea seedlings. The pea seedlings then developed two shoots. With the development of the primary shoot, the secondary shoot died. If PCD in the secondary shoot was inhibited with caspase-3 like inhibitor, both shoots continued to develop.

In animal cells, the proteolytic cleavage of lamins leading to the collapse of the nucleus is an important event in the apoptotic pathway. In menadione-treated tobacco cells,

Lamin-C proteins are degraded during PCD. Caspase-3 inhibitor (Ac-DEVD-CHO) was found to prevent DNA fragmentation in these tobacco cells (Sun et al. 1999).

Bozhkov et al. (2004), in their study of plant embryogenesis, looked at PCD during embryonic pattern formation. They found that caspase-6 like activity was the essential caspase activity in PCD. This caspase-6 like activity could be inhibited by a caspase-6 inhibitor. Without PCD, embryo development was disturbed because caspase-6 like activity is required for embryo-suspensor differentiation.

In the present study, caspase-3 and caspase-6 like activities were inhibited if immediately after treatment caspase inhibitors were added to the rice suspension cells (figure 5). The inhibitors did not decrease the DNA degradation smear that indicates necrosis (figure 6). What the inhibitors did do, the caspase-6 inhibitor in particular, was to decrease the DNA ladder that indicates PCD. The effect of the inhibitors upon DNA ladder was much less strong than in the cases described by Belenghi, Sun and Bozhkov. An attenuation but not inhibition of DNA ladder was also described in human studies. Chen et al. (2002), for instance, used a caspase-3 like protease inhibitor (Ac-DEVD-CHO) with human promyeloleukemic HL-60 cells. They showed that the inhibitor attenuated emodine-induced apoptotic responses. At concentrations of 200 and 400 μm, both the amount of smearing and the DNA ladder decreased. In an example featuring UV-induced apoptosis in human leukemia cells, apoptotic nuclear changes and DNA fragmentation were attenuated to about 50% by a caspase-3 inhibitor (Ac-DEVD-CHO) (Kimura et al. 1998).

Necrosis was found to start after eight hours of re-incubation while PCD was found after twenty hours of re-incubation. Both were then overlaying after twenty hours of re-incubation. The caspase inhibitors inhibited plant caspase-like proteases. They did not affect the necrotic pathway, overlaying the PCD pathway. For this reason, in the present study, DNA fragmentation was attenuated and cell death still occurred.

Caspase-3 and caspase-6 like activities are inhibited in plants. It could be that another plant caspase-like protease was still active and was not inhibited by the inhibitors used. It remains a question to what degree caspase substrates and inhibitors for animal caspase can be used to study plant caspase-like proteases.

The putative proteases responsible for caspase-like activity remain to be identified, but it is tempting to speculate that they may be caspase-like or related proteins activated through a caspase-like pathway. That would extend the importance of these enzymes from the animal kingdom to the plant kingdom. A biochemical approach is needed to purify the proteases responsible for the caspase-like activity in rice suspension cells.

Acknowledgments

We are grateful to Dr. Sylvia de Pater (Institute of Biology Leiden, Leiden University, The Netherlands) and Dr. Wouter-Jan Oosten (Sociotext Foundation) for valuable discussion and critical reading of the manuscript and to Mr. Peter Hock for the lay-out of the figures. The work was financially supported by Stichting BVS (Binair Vector Systeem).

References

Abraham MC and Shaham S. (2004) Death without caspases, caspases without death. Trends Cell Biol.14(4): 184-193.

Abramovitch RB, Kim YJ, Chen S, Dickman MB and Martin GB. (2003) Pseudomonas type III effector AvrPtoB induces plant disease susceptibility by inhibition of host programmed cell death. EMBO J. 22(1): 60-69.

Balk J, Leaver CJ and McCabe PF. (1999) Translocation of cytochrome c from the mitochondria to the cytosol occurs during heat-induced programmed cell death in cucumber plants. FEBS Lett. 463: 151-154.

Belenghi B, Salomon M and Levine A. (2004) Caspase-like activity in the seedlings of *Pisum sativum* eliminates weaker shoots during early vegetative development by induction of cell death. J Exp Bot. 55(398): 889-897.

Bozhkov PV, Filonova LH, Suarez MF, Helmersson A, Smertenko AP, Zhivotovsky B and von Arnold S. (2004) VEIDase is a principal caspase-like activity involved in plant programmed cell death and essential for embryonic pattern formation. Cell Death Differ 11(2): 175-182.

Bradford MM. (1977) A rapid and sensitive method for the quantitation of microgram quantities of protein utilizing the principle of protein-dye binding. Anal Biochem. 72: 248-254.

Broker LE, Kruyt FA and Giaccone G. (2005) Cell death independent of caspases: a review. Clin Cancer Res. 11(9): 3155-3162.

Chen HM, Zhou J and Dai YR. (2000) Cleavage of lamin-like proteins *in vivo* and *in vitro* apoptosis of tobacco protoplasts induced by heat shock. FEBS Lett. 480(2-3): 165-168.

Chen YC, Schen SC, Lee WR, Hsu FL, Lin HY, Ko CH and Tseng SW. (2002) Emodin induces apoptosis in human promyeloleukemic HL-60 cells accompanied by activation of caspase-3 cascade but independent of reactive oxygen species production. Biochem Pharmacol. 64(12): 1713-1724.

Coffeen WC and Wolpert TJ. (2004) Purification and characterization of serine proteases that exhibit caspase-like activity and are associated with programmed cell death in *Avena sativa*. Plant Cell. 16(4): 857-873.

Cohen GM. (1997) Caspases: the executioners of apoptosis. Biochem J. 326: 1-16.

Dangl JL, Dietrich RA and Richberg MH. (1996) Death don't have no mercy: cell death programs in plant-microbe interactions. Plant Cell. 8(10): 1793-1807.

Del Pozo O and Lam E. (1998) Caspases and programmed cell death in the hypersensitive response of plants to pathogens. Curr Biol. 8: 1129-1132.

Doorn van WG and Woltering EJ. (2005) Many ways to exit? Cell death categories in plants. Trends Plant Sci. 10(3): 117-122.

Dunn SR, John C. Bythell JC, Le Tissier MDA, Burnett WJ and Thomason JC. (2002) Programmed cell death and cell necrosis activity during hyperthermic stress-induced bleaching of the symbiotic sea anemone *Aiptasia sp*. J Exp Mar Biol Ecol. 272: 29-53.

Fukuda H. (2000) Programmed cell death of tracheary elements as a paradigm in plants. Plant Mol Biol. 44(3): 245-253.

Gotzmann J, Meissner M and Gerner C. (2000) The fate of the nuclear matrix-associated-region-binding protein SATB1 during apoptosis. Cell Death Differ. 7(5): 425-438.

Groover A and Jones AM. (1999) Tracheary element differentiation uses a novel mechanism coordinating programmed cell death and secondary cell wall synthesis. Plant Physiol. 119: 375-384.

Jiang X and Wang X. (2004) Cytochrome C-mediated apoptosis. Annu Rev Biochem. 73: 87-106.

Jones AM. (2001) Programmed cell death in development and defense. Plant Physiol. 125(1): 94-97.

Katsuhara M. (1997) Apoptosis-like cell death in barley roots under salt stress. Plant Cell Physiol. 38: 1087-1090.

Kimura C, Zhao QL, Kondo T, Amatsu M and Fujiwara Y. (1998) Mechanism of UV-induced apoptosis in human leukemia cells: roles of Ca2+/Mg(2+)-dependent endonuclease, caspase-3, and stress-activated protein kinases. Exp Cell Res. 239(2): 411-422.

Korthout HAAJ, Berecki G, Bruin W, van Duijn B and Wang M. (2000) The presence and subcellular localization of caspase 3-like proteinases in plant cells. FEBS Lett. 475: 139-144.

Krishnamurthy KV, Krishnaraj R, Chzhavendan R and Samuel Christopher F. (2000). The programme of cell death in plants and in animals- A comparison. Curr Sci India. 79(9): 1169-1181.

Kroemer G and Martin SJ. (2005) Caspase-independent cell death. Nat Med. 11(7): 725-730.

Lam E and del Pozo O. (2000) Caspase-like protease involvement in the control of plant cell death. Plant Mol Biol. 44: 417-428.

Launay S, Hermine O, Fontenay M, Kroemer G, Solary E and Garrido C. (2005) Vital functions for lethal caspases. Oncogene. 24(33): 5137-5148.

Lawen A. (2003) Apoptosis- an introduction. Bioessays. 25: 888-896.

Mackey D, Holt BF 3rd, Wiig A and Dangl JL. (2002) RIN4 interacts with *Pseudomonas syringae* type III effector molecules and is required for RPM1-mediated resistance in Arabidopsis. Cell. 108(6): 743-754.

McCabe PF, Levine A, Meijer PJ, Tapon NA and Pennell RI. (1997) A programmed cell death pathway activated in carrot cells cultured at low cell density. Plant J. 12(2): 267-280.

Maraschin S, Gaussand G, Pulido A, Olmedilla A, Lamers GE, Korthout H, Spaink HP, Wang M. (2005) Programmed cell death during the transition from multicellular structures to globular embryos in barley androgenesis. Planta. 221(4): 459-470.

Mittler R and Lam E. (1997) Characterization of nuclease activities and DNA fragmentation induced upon hypersensitive response cell death and mechanical stress. Plant Mol Biol 34: 209-221.

Nagata S. (2005) DNA degradation in development and programmed cell death. Annu. Rev. Immunol. 23: 853-875.

Nyormoi O, Wang Z, Doan D, Ruiz M, McConkey D and Bar-Eli M. (2001) Transcription factor AP-2alpha is preferentially cleaved by caspase 6 and degraded by proteasome during tumor necrosis factor alpha-induced apoptosis in breast cancer cells. Mol Cell Biol. 21(15): 4856-4867.

Pontier D, Balague C and Roby D. (1998) The hypersensitive response. A programmed cell death associated with plant resistance.C R Acad Sci III. 321(9): 721-734.

Porter AG and Janicke RU. (1999) Emerging role of caspase-3 in apoptosis. Cell Death Differ. 6: 99-104.

Ruchaud S, Korfali N, Villa P, Kottke TJ, Dingwall C, Kaufmann SH and Earnshaw WC. (2002) Caspase-6 gene disruption reveals a requirement for lamin A cleavage in apoptotic chromatin condensation.EMBO J. 21(8): 1967-1977.

Runeberg-Roos P and Saarma M. (1998) Phytepsin, a barley vacuolar aspartic proteinase, is highly expressed during autolysis of developing tracheary elements and sieve cells. Plant J. 15(1): 139-145.

Schmid M, Simpson DJ, Sarioglu H, Lottspeich F and Gietl C. (2001) The ricinosomes of senescing plant tissue bud from the endoplasmic reticulum. Proc Natl Acad Sci USA. 98(9): 5353-5358.

Schmid M, Simpson DJ and Gietl C. (1999) Programmed cell death in castor bean endosperm is associated with the accumulation and release of a cysteine endopeptidase from ricinosomes. Proc Natl Acad Sci USA. 96(24): 14159-14164.

Solomon M, Belenghi B, Delledonne M, Menachem E and Levine A (1999) The involvement of cysteine proteases and protease inhibitor genes in the regulation of programmed cell death in plants. Plant Cell. 11: 431-444.

Steller H (1995). Mechanisms and genes of cellular suicide. Science. 267: 1445-1449.

Suarez MF, Filonova LH, Smertenko A, Savenkov EI, Clapham DH, von Arnold S, Zhivotovsky B and Bozhkov PV. (2004) Metacaspase-dependent programmed cell death is essential for plant embryogenesis. Curr Biol. 14(9): R339-340.

Sun YL, Zhao Y, Hong X and Zhai ZH. (1999) Cytochrome c release and caspase activation during menadione-induced apoptosis in plants. FEBS Lett. 462(3): 317-321.

Tian R, Zhang GY, Yan CH and Dai YR. (2000) Involvement of poly (ADP-ribose) polymerase and activation of caspase-3-like protease in heat shock-induced apoptosis in tobacco suspension cells. FEBS Lett. 474(1): 11-15.

Uren AG, O'Rourke K, Aravind LA, Pisabarro MT, Seshagiri S, Koonin EV and Dixit VM. (2000) Identification of paracaspases and metacaspases: two ancient families of caspase-like proteins, one of which plays a key role in MALT lymphoma. Mol Cell. 6(4): 961-967.

Wang M, Hoekstra S, van Bergen S, Lamers GE, Oppedijk BJ, van der Heijden MW, de Priester W and Schilperoort RA. (1999) Apoptosis in developing anthers and the role of ABA in this process during androgenesis in Hordeum vulgare L. Plant Mol Biol. 39(3): 489-501.

Wyllie AH, Kerr JF and Currie AR. (1980) Cell death: the significance of apoptosis. Int Rev Cytol. 68: 251-306.

Zhivotovsky B. (2003) Caspases: the enzymes of death. Essays Biochem. 39: 25-40.

Chapter 5

Purification of caspase-3 like proteases in *Oryza sativa* with the fluorogenic Biotin-DEVD-CHO

Gwénaël M.D.J-M Gaussand, Marco Gaspari, Elwin R. Verheij, Mei Wang and Henrie A.A.J. Korthout.

Abstract

In animals and yeasts, the proteolytic activity associated with programmed cell death (PCD) is due to enzymes called caspases. Caspases have a unique strong preference for cleavage of the target proteins next to an aspartate residue. In plants, caspases have not been found. However, a similar specific peptide cleavage could be observed during plant PCD. In this work, we used a biotinylated human caspase-3 substrate to purify the plant protease responsible for this peptide cleavage by means of avidin-biotin chromatography. Although the recovery of the affinity chromatography step was rather low, some proteins could be specifically eluted. These proteins were subjected to LC-MS/MS analysis followed by database search. With this method, the copper chaperone homolog CCH could be identified. The purification of proteases responsible of caspase-3 like activity in rice extract and the possible role of the copper chaperone homolog CCH during PCD in plants are discussed.

Introduction

Since the beginning of the 1990s, research on PCD has grown spectacularly. The regulator of cell death in the nematode *Caenorhabditis elegans*, CED-3, was found to be related to the mammalian cysteine protease interleukin-lβ converting enzyme also named ICE or caspase-1 (Yuan et al. 1993). This finding suggested that the mechanism of cell death is largely conserved across species and that proteases are integral to the death program. Subsequently, caspases (cysteine-dependent aspartate-specific proteases) have been found in hydra, nematodes and other animals. Using the DNA sequence encoding the active site of caspase-1 and CED-3 to search an expressed sequence tag (est) database, a human sequence was identified. The human sequence was cloned and shown to encode a 32 KDa cysteine protease, called CPP32 (Fernandes Alnemri et al. 1994). Independently, other researchers identified a related caspase that was called caspase-3, one group naming it Yama (the Hindu god of death) and the other group apopain (Tewari et al. 1995; Nicholson et al. 1995). Caspase-3 turned out to be one of the key executioners of apoptosis, being responsible either totally or partially for the proteolytic cleavage of many key proteins. The key proteins all contain a common Asp-Xaa-Xaa-Asp (DXXD) motif, similar to the one in poly(ADP-ribose) polymerase PARP. Based on this cleavage site of PARP (DEVD↓G), a synthetic model substrate was developed: Ac-DEVD-AMC. Besides, Ac-DEVD-CHO and its biotinylated derivative (biotin-DEVD-CHO) were synthesized as specific inhibitors of PARP cleavage and as affinity ligands for purification of the protease.

In plants, synthetic caspase substrates and inhibitors were used to measure caspase-like activity in relation to PCD. This was demonstrated in different studies (Del Pozo et al. 1998; Sun et al. 1999; Tian et al. 2000; De Jong et al. 2000; Mlejnek et al. 2002; Danon et al. 2004; Belenghi et al. 2004, Maraschin et al. 2005). Those studies have pointed out that different systems exist which have different caspase-like proteases such as caspase-1, -3 and -6 (Chen et al. 2000; Bozhkov et al. 2004). Several proteases involved in PCD are already described. All these proteases seem to be present in the vacuole. However, it was shown in *Chara corallina* cells that caspase-3 like proteases were localized in the cytosol (Korthout et al. 2000). Besides, caspase-3 inhibitor was found to regulate PCD in different plant systems. In menadione-induced cell death tobacco protoplasts, Ac-DEVD-CHO was found to inhibit DNA laddering (Sun et al. 1999). In tobacco suspension cells in which PCD was induced with high concentrations of nicotinamide, PARP cleavage and DNA fragmentation could be inhibited with the caspase-3 inhibitor Ac-DEVD-CHO (Zhang et al. 2003). In pea seedlings, the injection of the caspase-3 like inhibitor into the remainder of the epicotyl strongly inhibited the death of the secondary shoot, resulting in a seedling with two equal shoots (Belenghi et al. 2004). Considering these results, one may propose functional similarity of animal caspases and plant caspase-like proteases in controlling and executing the PCD process.

Different approaches to purify and characterize the caspase-like activity have been described (Coffeen & Wolpert 2004; Belenghi et al. 2004). A purification protocol was developed to purify the proteases responsible for caspase-3 like activity. The protocol is based on avidin-biotin chromatography and modern proteomics technology.

In affinity chromatography, the avidin–biotin system is an important tool which contributes to the interaction between biotin chemically coupled to a binder molecule (e.g., a protein, DNA, hormone, etc) and its target molecule avidin (Wilchek et al. 1988). The binding between avidin/streptavidin and biotin has long been regarded as the strongest, non covalent, biological interaction known, having a dissociation constant, Kd, in the order of 10^{-14}M. The bond forms very rapidly and is stable in wide ranges of pH and temperature (Savage et al. 1992). In order to purify the animal caspase-3, the avidin-biotin affinity chromatography was already successfully applied by use of a biotinylated inhibitor biotin-DEVD-CHO (Nicholson et al. 1995).

Proteomics have rapidly evolved into a group of technologies used to identify and compare proteins. They are also used to determine post-translational modifications, sub-cellular locations and molecular interactions. Research benefits from modern technologies at different levels of proteomic studies (separation, identification, quantification and protein analysis). This involves sophisticated equipment, computer software and protein databases.

Both *Arabidopsis* and rice genomes were published in 2000 and 2002 respectively. Since then, much work has been done to assign a function to the genes so far found in the genome, many of which have no known function but a putative one.

In this work, the avidin-biotin affinity chromatography and modern proteomics technology were combined in order to purify the caspase-3 like proteases. The results and the advantages/disadvantages of this purification method are discussed.

Material and methods

Plant material and culture maintenance

Rice suspension cells obtained from primary callus grown on scutellum of mature seeds (*Oryza sativa* variety IR52) were subcultured weekly. The subculture involved pipetting 6 ml of cell suspension in a 250 ml Erlenmeyer flask, with aluminium caps, containing 50 ml of culture medium (4.4 g/l Linsmaier and Skoog medium including vitamins (Duchefa, L 0230), 4 mg/l 2,4-D hormone and 30 g/l sucrose, pH5.8 ± 0.1). The rice suspension cells were maintained in a dark climate chamber at 28°C with 50% relative humidity on a horizontal rotary shaker (120 rpm).

Crude protein extraction

All extraction steps were performed at 4ºC. To collect about 600 g of rice suspension cells, the rice suspension cells were filtrated over one layer of Whatman paper no.1. The collected rice suspension cells were then ground in 750 ml ice-cold extraction buffer (buffer A: 100 mM HEPES (pH 7.2), 10% (w/v) sucrose, 0.1% (w/v) CHAPS, 5 mM DTT and 10^{-6} % (v/v) NP40) with an Ultrathurrax (three pulses at 24,000 rpm of 30 seconds each, with intervals of 30 seconds, on ice). Subsequently, the homogenate was incubated on ice for 15 minutes, filtered through three layers of cheesecloth and then centrifuged first at 2,000 g for 5 minutes to pellet cell debris. Next, the supernatant was centrifuged for 10 minutes at 100,000 g to pellet cell debris and microsomal fraction. The lipid layer was removed from the surface of the supernatant with a needle and a syringe. The soluble protein extract, that is the supernatant without lipids, was filtrated over a 0.22 µm Millex syringe driven filter unit (Millipore Corporation, Bradford, USA). The soluble protein extract was frozen in liquid nitrogen and stored at -80ºC.

Assay for specific caspase-3 like activity

The soluble protein extract obtained from rice suspension cells was used to measure caspase-3 like activity. 75 µl of soluble protein extract containing 5 µg of proteins were mixed in a 96-well plate with 25 µl of the synthetic fluorogenic caspase-3 substrate *N*-acetyl-Asp-Glu-Val-Asp-7-amino-4-methylcoumarin (Calbiochem, UK; Ac-DEVD-AMC, 75 µM final concentration in assay). The specificity for caspase-3 like activity was measured by addition of caspase-3 inhibitor (Calbiochem, UK; Ac-DEVD-CHO, 250 µM final concentration in assay) to the assay. During two hours, the proteolytic activity was measured every 10 minutes at room temperature in triplicates per sample. Substrate cleavage was detected in a Perkin Elmer fluorescence spectrometer LS50B (Perkin Elmer, USA) at an excitation wavelength of 380 nm and an emission wavelength of 460 nm. The standard setting of excitation and emission slit values of 5.0 was used. The kinetic of substrate cleavage was tested to remain linear during at least two hours. The caspase-3 like activity was measured by subtracting the value obtained after one hour of assay and the value at the beginning of the assay. Specific caspase-3 like activity was expressed as units per hour per µg protein for each mean value ± standard deviation, *n=3*. Samples obtained during the purification were first desalted with PD10 desalting columns (Pharmacia biotech) in buffer A in order to measure their caspase-3 like activity.

Purification of caspase-3 like activity from crude protein extract

A two-step chromatographic procedure was employed to purify the caspase-3 like proteases from a crude protein extract. Caspase-3 substrate and inhibitor were used to monitor specific caspase-3 like activity. The experiments were performed at room temperature.

(i) ion-exchange chromatography on DEAE-sepharose

Approximately 45 ml of clear crude extract was loaded onto a DEAE-Sepharose Fast Flow anion-exchange column (GE Healthcare; 5 mL; 1 ml/min) that was previously equilibrated in buffer A. After loading, the column was first washed with 50 mL buffer A. The proteins were then eluted from the column using a linear gradient of buffer B (buffer A + 1 M NaCl). 15 Fractions (4 ml each) were collected, desalted in buffer A with PD10 desalting columns (GE Healthcare) according to the manufacturer's instructions. The fractions were then tested for caspase-3 like activity. The active fraction (AIEX 4) was used to measure caspase-3 like activity, or pooled with AIEX 4 fractions collected with the same method.

(ii) Biotin-avidin chromatography

DEVD affinity chromatography using biotinylated–DEVD and monomeric avidin was performed as described by Nicholson et al. (1995). The pooled AIEX 4 fractions obtained after anion-exchange chromatography were desalted and subsequently divided in four equal

aliquots (2 ml each) and then pre-incubated with biotin-DEVD-CHO (Calbiochem, UK), Ac-DEVD-CHO or D-Biotin (250 µM final concentration in assay) at room temperature. After one hour of incubation, each sample was tested for specific activity by adding the caspase-3 substrate Ac-DEVD-AMC. After two hours of incubation, the samples were desalted with PD10 column and the caspase-3 like activity was measured as described previously. The samples were then loaded onto a 1 mL monomeric avidin column (Pierce, USA) that was previously equilibrated in buffer A. The flow-through was collected and the avidin column was washed with ten column volumes of buffer A. The caspase-3 like proteases/biotinylated-DEVD complex retained by the monomeric avidin was selectively eluted with 2 mM D-biotin in buffer A at a flow rate of 1 mL/min. Flow-through and fractions of 0.5 mL were collected, desalted in buffer A for the caspase assay, or in MilliQ water to be lyophilized and analyzed by SDS-PAGE.

Analytical methods

Protein concentration was determined by using Bradford's method (Bradford 1976); with BioRad assay reagent (BioRad, USA) and bovine serum albumin (BSA) as the standard. Molecular masses were determined by running standard protein markers (BioRad, USA). The lyophilized samples were mixed with SDS-sample buffer (60 mM Tris pH 6.8, 10% glycerol, 5% β-mercaptoethanol, 0.025% bromophenol blue and 2% SDS) and boiled for 10 min at 95-100 °C. Based on the Laemmli method (1970), sodium dodecyl sulfate (SDS)-polyacrylamide gel electrophoresis (PAGE) was carried out on 4.5% stacking gels and on 10, 15 and 17.5% polyacrylamide separating gels with 0.3% cross-linking in the presence of β-mercaptoethanol with vertical slab gel apparatus. The gels were stained with 0.1% Coomassie brilliant blue R-250 (Sigma) in 40% (v/v) methanol and 10% (v/v) acetic acid, followed by incubation in 20% (v/v) methanol and 10% (v/v) acetic acid.

In-gel digestion

Gel slices (1 mm thickness) were washed three times at 37° C in a 1:1 (V/V) mixture of water (Milli-Q grade, Millipore) and acetonitrile (Biosolve BV, NL). Then, after a triplicate quick wash in water, they were dried in a vacuum centrifuge. The dried gel slices were re-hydrated in digestion buffer composed of: 12.5 ng/µL of sequencing grade modified trypsin (Promega, USA), 2 mM dithiothreitol (Sigma-Aldrich), 1 mM calcium chloride (Sigma-Aldrich) and 100 mM ammonium bicarbonate (BDH laboratory Supplies, England). After overnight incubation, peptide digests were extracted using 15 minutes sequential washes of acetonitrile, water/formic acid (Merck) 95:5 (V/V) and acetonitrile again, all at 37° C. Pooled extracts were dried in a vacuum centrifuge and stored at -20° C prior to mass spectrometric analysis.

Nanoliquid chromatography/mass spectrometry

Dried extracts were reconstituted in 20 µL of 1 mM dithio-threitol, 4 M urea, 10 mM tris/HCl (Sigma) at pH 7.5. Half of the resulting solution was injected in a nanoliquid chromatographic system composed by a trap column, 0.3 X 5 mm, and an analytical column, 0.075 X 150 mm, both packed with C_{18} stationary phase pepmap (LC Packings, The Netherlands). Gradient elution from 0 to 80% B in 40 minutes was performed using an Ultimate gradient pump (LC Packings). The mobile phase A was water/acetonitrile/formic acid 97.9/2/0.1 (V/V/V) and the mobile phase B was water/acetonitrile/formic acid 19.9/80/0.1 (V/V/V).

The effluent of the nanoseparation was coupled on-line to an LCQ classic (Thermo Electron, USA) using a nanoelectrospray interface (Proxeon, Denmark). The mass spectrometer was operated in data dependent mode, achieving both a higher resolution zoom scan and a MS/MS spectrum for the top three highest intensity peaks detected in each survey full scan.

MS/MS data were converted in data files and searched in the NCBI database using the search engine Mascot (www.matrixscience.com) and the following search parameters: taxonomy: viridiplantae; enzyme: trypsin; fixed modifications: none; variable modifications: deamidation, methionine oxidation, pyro-glu, pyro-gln, pyro-cmC; mass accuracy (parent and fragment): 1.5 Da. Gene product identification was considered to be significant when based on at least a single peptide achieving a score higher than the significance threshold. Nevertheless, when gene product identification came from just a single peptide, manual inspection of MS/MS data to confirm reliability of results was always performed.

Results

Purification of caspase-3 like proteases from rice suspension cells

Caspase-3 like activity was optimal only when the rice suspension cells were heat-shocked. However, this activity was rather unstable and therefore not suitable for large scale purification. Non heat-shocked cells had some activity at a lower level, and this activity proved to be more stable during different chromatographical purification steps at room temperature. Non heat-shocked cells were therefore used to purify the caspase-3 like proteases. The purification protocol (as depicted in figure 1) comprises four steps: extraction of soluble proteins from rice suspension cells, anion exchange chromatography, biotin-avidin affinity chromatography, and identification of the purified proteins by LC-MS/MS after in-gel digestion. An overview of caspase-3 like activity during the different steps of purification is shown in table 1.

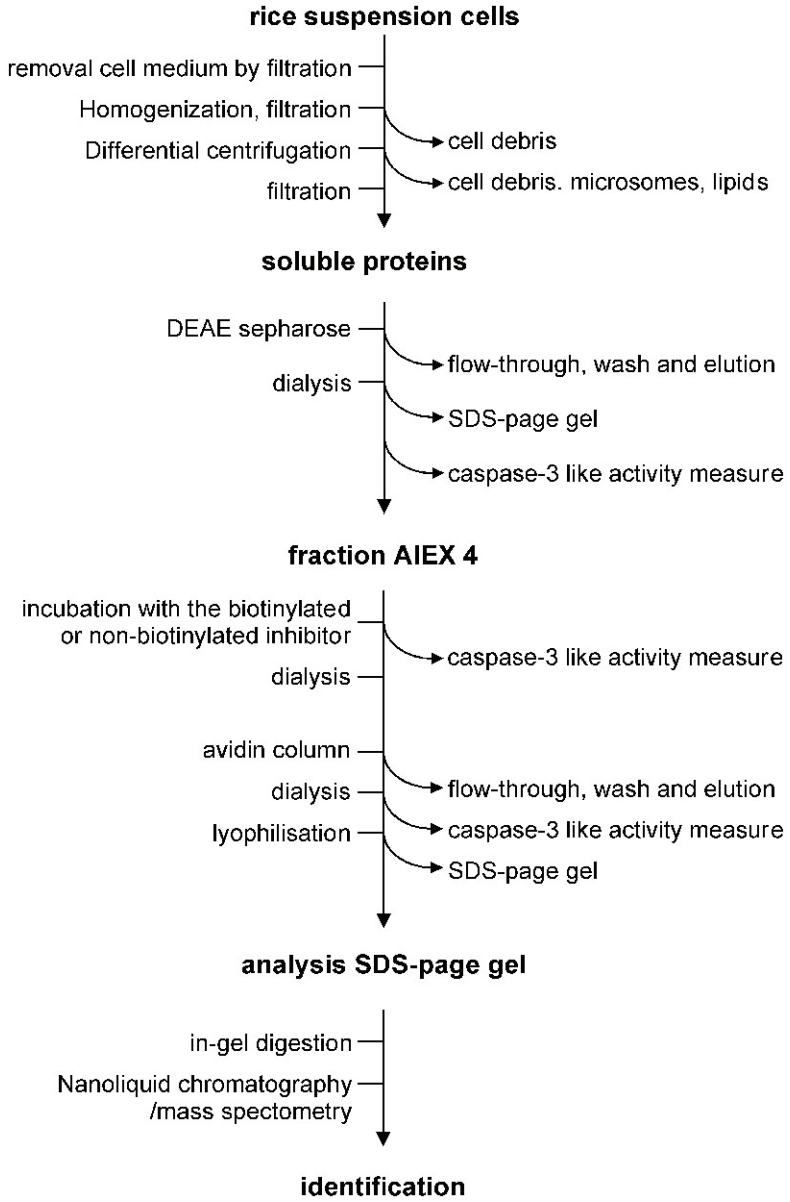

Figure 1: flow chart of the different steps to purify the caspase-3 like proteases from rice suspension cells. The protocol involves four steps: differential centrifugation and filtration, anion exchange chromatography, affinity chromatography, and SDS-PAGE analysis.

Table 1: overview of the different steps of purification.

Step			total activity (unit)	protein (mg)	specific activity (units/µg)	yield (%)	purification fold
1	extraction	crude extract	5332667	18667	0,29	100	1
2	DEAE	AIEX 4	4479115	2688	1,67	84	5,8
3	Avidin	ft A	4021956	2198	1,83	90	1,09
4	Avidin	elution A	27234	197	0,14	0,61	0,08

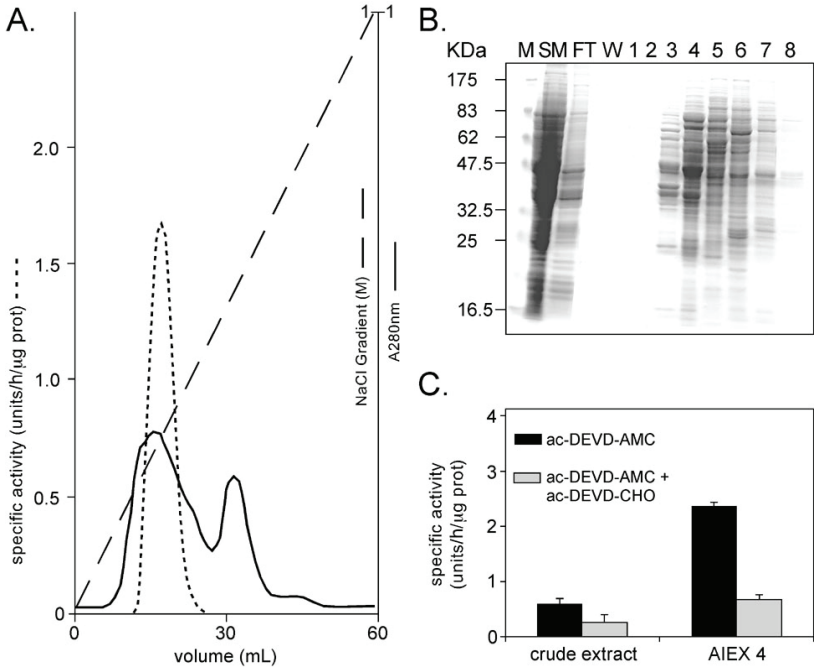

Figure 2: anion exchange and specific caspase-3 like activity
A: elution profile of DEAE-sepharose Fast Flow anion exchange chromatography. The soluble protein extract was loaded onto a DEAE-sepharose Fast Flow column pre-equilibrated with buffer A. After the column was washed with 10 column volumes of buffer A, the proteins were eluted with an increasing gradient of NaCl from 0 to 1 M. Each fraction was collected, dialyzed against buffer A and used to measure specific activity. The peak of activity was found in fraction AIEX 4.
B: 10% SDS-PAGE of protein samples before and after anion exchange chromatography. M: marker; SM: crude extract of soluble proteins; FT: flow-through of the DEAE-sepharose Fast Flow column; W: wash; 1 to 8: fractions AIEX 1 to 8 eluted from the column with the NaCl gradient.
C: specific activity measured after dialysis in crude extract and in fraction AIEX 4 with caspase-3 substrate Ac-DEVD-AMC and caspase-3 inhibitor Ac-DEVD-CHO.

Soluble protein extraction and anion exchange chromatography

To obtain soluble proteins for the purification (step 1, table 1), rice suspension cells were first homogenized by sonication. The extract thus obtained underwent differential centrifugation in

order to remove cell debris and membranes. The specific caspase-3 like activity of the soluble protein extract was about 0.29 units/h/µg protein (Table 1 and figure 2C).

The soluble protein extract was loaded onto an anion exchange column (step 2, table 1). After loading the column (containing DEAE sepharose, 5 mL) with the extract, the flow-through of unbound proteins was collected. After a wash with 10 column volumes of buffer A, the bound proteins were eluted from the column with a gradient of 0 to 1 M NaCl (buffer B). The elution profile showed that the majority of the proteins were eluted between 0.13 and 0.53 M NaCl (fraction AIEX 2 to AIEX 8, figure 2A). Eluted proteins were visualized by SDS-PAGE analysis (figure 2B). The flow-through and all eluted fractions were subjected to desalting with PD10 columns and subsequently tested for specific caspase-3 like activity. The activity was found mainly in fraction 4 (AIEX 4) eluted from the column between 200 and 267 mM NaCl. The specific activity of the fraction AIEX 4 was about 1.67 units/h/µg proteins (table 1 and figure 2C). As a result of this step, the enriched caspase-3 like activity was 5.8. About 84% of caspase-3 like activity measured in the crude extract was present in the fraction AIEX 4 (Table 1).

Avidin chromatography

Two fractions AIEX 4, eluted in different experiments but under the same conditions, were pooled and desalted (step 3, table 1). The mix was divided in four equal aliquots. As shown in table 2, the caspase-3 inhibitors (Ac-DEVD-CHO and/or Biotin-DEVD-CHO) or D-biotin were added to each aliquot and left to incubate. After incubation at room temperature, the aliquots were tested for specific caspase-3 like activity. The aliquots were desalted in order to remove an excess of biotinylated inhibitor. The excess of biotinylated inhibitor might bind to the avidin column, while the biotinylated caspase-3 like protease should bind to that column. To know the effects of inhibition and desalting, caspase-3 like activity was measured after desalting the aliquots. As shown in figure 3, the inhibitors inhibited the reaction whereas addition of D-biotin had no significant effect. The inhibition effect was the same after desalting. Biotin-DEVD-CHO inhibited more strongly than its unbiotinylated counterpart Ac-DEVD-CHO.

Table 2: incubation of the desalted AIEX 4, divided in four parts, with the different caspase-3 inhibitors or D-biotin at room temperature for two hours.

experiment	Fraction AIEX 4	Biotin-DEVD-CHO (1)	Ac-DEVD-CHO (2)	(1) and (2)	D-biotin
A	x	x			
B	x		x		
C	x			x	
D	x				x

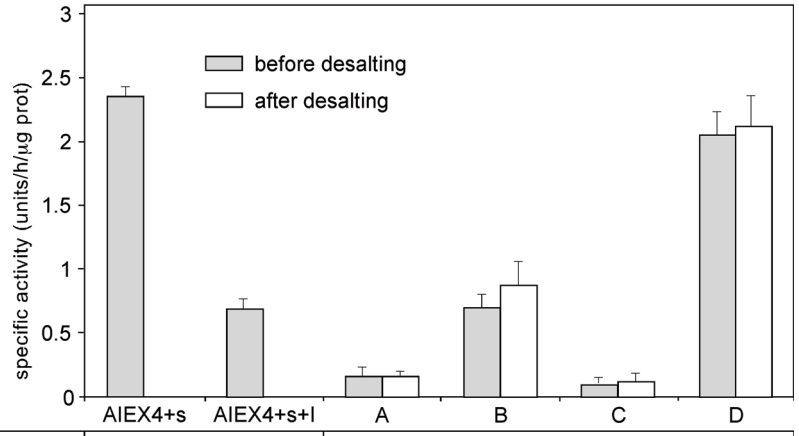

	AIEX4+s	AIEX4+s+I	A	B	C	D
AIEX4	+	+	+	+	+	+
Ac-DEVD-AMC	+	+	+	+	+	+
biotin-DEVD-CHO			+		+	
Ac-DEVD-CHO		+		+	+	
D-biotin						+

Figure 3: specific caspase-3 like activity in fraction AIEX 4.
Specific activity measured in the original fraction AIEX 4 (S: ac-DEVD-CHO and I: ac-DEVD-CHO) and in presence of the addition of the different caspase-3 inhibitors or D-biotin as described in table 2 (A-D) before and after desalting with PD10 columns.

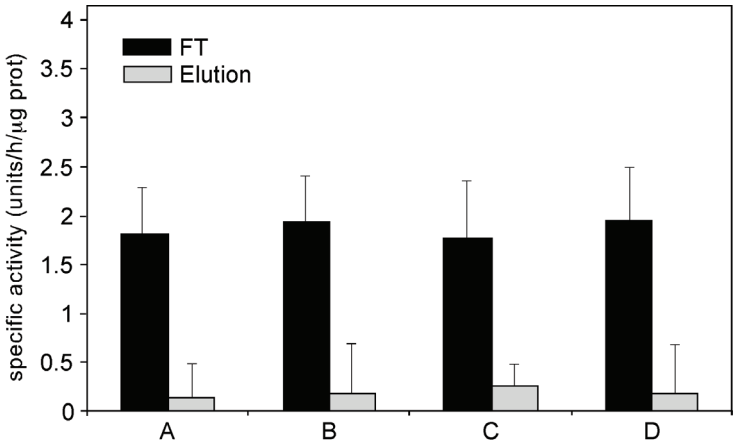

	A	B	C	D
AIEX4	+	+	+	+
Ac-DEVD-AMC	+	+	+	+
biotin-DEVD-CHO	+		+	
Ac-DEVD-CHO		+	+	
D-biotin				+

Figure 4: avidin chromatography and specific caspase-3 like activity. After two hours of incubation, A, B, C and D described in table 2 were dialysed. Each was then loaded into an avidin column. Flow-through and elution for each sample were collected and used to measure specific activity.

The samples described in table 2, after desalting, were loaded on an avidin column. The flow-through was collected and the column was washed with 10 column volumes of buffer A. The bound proteins retained by the monomeric avidin were selectively eluted with 2 mM D-biotin in buffer A. Flow-throughs and eluted fractions of each experiment described in table 2 were collected, desalted in buffer A and then tested for the caspase-3 like activity. As shown in figure 4, high caspase-3 like activity was found in the flow-through fractions, even in parts A and C. This is very surprising since the activity was blocked by the inhibitors before loading on the column (figure 3). The binding of the biotin-moiety to avidin probably causes steric hindrance which results in releasing the inhibitor from the caspase-3 like protease (figure 5). Still, the proteins of parts A, B, C and D that were eluted from the avidin column were analyzed by SDS-PAGE.

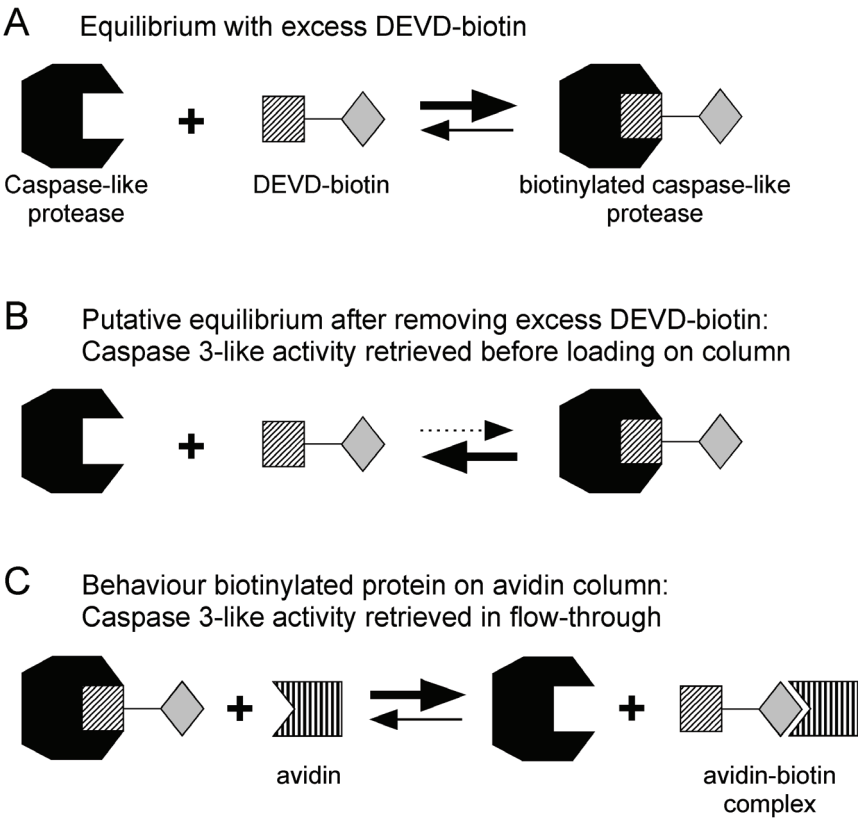

Figure 5: schematic models explaining the putative binding between Ac-DEVD-biotin and the caspase-like protease before desalting (A), after desalting (B) and during avidin chromatography (C).

As shown in figure 6B, many proteins could be eluted, even in the fraction lacking the biotinylated compound, indicating that non specific binding occurs. However, the profile of the eluted proteins of parts A and C differ slightly from parts B and D. In the parts A and C, three visible protein bands of 35.2, 28.1 and 20.5 KDa (figure 6B, arrows) were present. These are the samples with the biotinylated compound. The bands indicate that some proteins were still bound to biotin-DEVD-CHO and could be captured by avidin affinity chromatography.

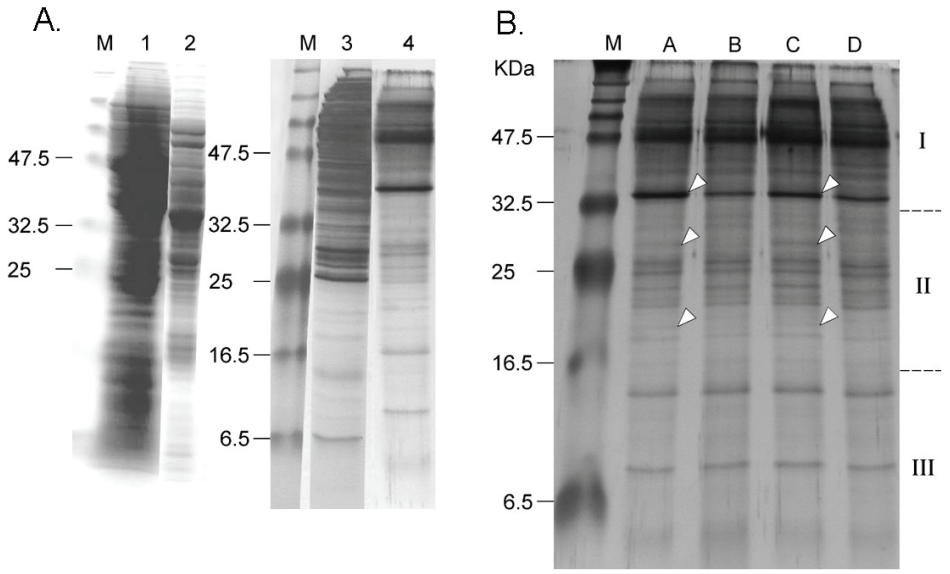

Figure 6: SDS-PAGE analysis.
A: overview of the caspase-3 like protein fractions collected during various stages of the purification: crude extract (lane 1, 10% SDS-PAGE), AIEX 4 (lane 2, 10% SDS-PAGE), avidin flow-through FTA (lane 3, 15% SDS-PAGE) and elution A (lane 4, 15% SDS-PAGE).
B: detailed information on 17.5% SDS-PAGE of proteins eluted from the avidin column for the different experiments A, B, C and D (table 2). The gel was cut in three parts (I, II and III) and each lane (A, B, C and D) was treated with trypsin prior to mass spectrometric analysis. Arrowheads show protein bands that are only found with the samples incubated with biotin-DEVD-CHO (A and C, table 2).
Lanes M: molecular mass markers.

MS/MS analysis and Mascot search

To optimize the identification of the proteins on gel, the coomassie stained gels were cut into three portions, separating the proteins in 3 molecular weight categories (proteins above 32 KDa, proteins between 32 and 16 KDa and proteins below 16 KDa). The gel slices were washed, dried and then re-hydrated in trypsin digestion buffer. Dried extracted peptide digests were injected in a nanoliquid chromatographic system. The effluent of the nanoseparation was coupled on-line to an LCQ classic, using a nanoelectrospray interface. MS/MS data were converted in data files and searched in the NCBI database, using the search engine Mascot.

The digested peptide identification obtained from the MS/MS analysis and Mascot search is shown in the Tables 3 A, B C and D. Table 3 lists only the gene products identified from slice III. Gene products identified in slices I and II were identical across the four lanes. Only one protein, the copper chaperone homolog CCH (GenBank accession number gi|11290108), was present in slice III in both samples that contained the biotinylated inhibitor (Tables 3 A and C). This protein was not present in the other samples. The copper chaperone homolog CCH is a protein of about 13 KDa which was not visible on coomassie stained SDS-PAGE (figure 6). The method did not identify the other bands seen on gel (35.2, 28.1 and 20.5 KDa, figure 6, slices I and II, arrows).

To confirm the reliability of digested peptide identification from a single peptide such as the copper chaperone homolog CCH, manual inspection of MS/MS data was always performed. The data were reprocessed by the computer software to provide the ion chromatogram for selected masses. This procedure provides a selected ion chromatogram (SIC) for each mass detected in the spectrum. To be sure that the protein of 13 KDa was really purified by avidin chromatography, the selected ion chromatograms of each experiment (A, B, C and D described previously) were analyzed as shown in figure 7. Two peaks are indeed seen in the graphs A and C at m/z 916.6 at retention times 20 and 30 min. The first one is the one identified as belonging to the copper chaperone homolog CCH at retention time 20 min. This peak is not present in graphs B and D.

The copper chaperone homolog CCH was the only protein identified with this method. More proteins were detected on SDS-PAGE but those could not be identified.

Discussion

This study described different sequential steps to purifiy the proteases that trigger plant caspase-3 like activity. Many bands were visible in the SDS-page gel. This suggests a high non-specific binding to the avidin column or specific binding to endogenous biotinylated plant proteins. The proteins of interest were faint bands, which suggests a low specific binding or low abundance. After in-gel digestion, the copper chaperone homolog CCH (GenBank accession number gi|11290108) was found to be the only identified protein after LC-MS/MS analysis and a Mascot search.

Tables 3 (A, B, C, D): gene product identification from slice III obtained from the MS/MS analysis and database search. The gene product shown in bold was present only when biotin-DEVD-CHO was used during the incubation.
Table 3A: (Biotin-DEVD-CHO) elution from the avidin column of sample AIEX 4 desalted and incubated with biotin-DEVD-CHO.

Accession number	Protein description	Theoretical MW (Da)	Total score	Number peptide matches	Ions score	Peptide sequence
gi|37535658	putative N-acetyl-gamma-glutamyl-phosphate reductase [Oryza sativa (japonica cultivar-group)]	45446	162	2	92	APELQQEAVYGLTEVL
					85	EANLYTEIAEGIHAYGIK
gi|50882147	putative translation elongation factor eEF-1 beta' chain [Oryza sativa (japonica cultivar-group)]	23398	101	1	101	AVGVNLPGGGAASSAAA AAPAAK
gi|32352154	nascent polypeptide associated complex alpha chain [Oryza sativa (japonica cultivar-group)]	22264	82	1	86	IEDLSSQLQTQAAEQFK
gi|16604368	At2g19940/F6F22.3 [Arabidopsis thaliana]	44136	63	1	63	IGLLGASGYTGAEIVR
gi|38345562	OSJNBa0032F06.19 [Oryza sativa (japonica cultivar-group)]	176067	53	2	34	MAPQDEHK + Deamidation(NQ); Oxidation (M)
					33	KGLENGAADALSR + Deamidation (NQ)
gi|42407753	putative phosphoribosyl glycinamide formyltransferase, chloroplast precursor [Oryza sativa (japonica cultivar-group)]	31132	52	1	52	VVPVLANDTPEQLAAR
gi|11290108	**copper chaperone homolog CCH [imported] – rice**	**13085**	**49**	**1**	**53**	**MEGVETFDIDMEQQK + 2 Oxidation (M)**

Table 3B: (ac-DEVD-CHO) elution from the avidin column of sample AIEX 4 desalted and incubated with ac-DEVD-CHO.

Accession number	Protein description	Theoretical MW (Da)	Total score	Number peptide matches	Ions score	Peptide sequence
gi|37535658	putative N-acetyl-gamma-glutamyl-phosphate reductase [Oryza sativa (japonica cultivar-group)]	45446	208	3	24	IVDLSADFR
					100	APELQQEAVYGLTEVLR
					91	EANLYTEIAEGIHAYGIK
gi|4586602	pyruvate kinase [Cicer arietinum]	15424	95	1	99	AEATDVANAVLDGSDAILLGAETLR
gi|16604368	At2g19940/F6F22.3 [Arabidopsis thaliana]	44136	84	2	24	IVDLSADFR
					59	IGLLGASGYTGAEIVR
gi|34907258	putative nascent polypeptide associated complex alpha chain [Oryza sativa (japonica cultivar-group)]	22079	69	1	73	SPNSDTYVIFGEAK
gi|15219360	protein kinase family protein [Arabidopsis thaliana]	84580	52	2	56	GTRNGSVAIAIDK
gi|41052604	hypothetical protein [Oryza sativa (japonica cultivar-group)]	80695	50	1	55	GSMLICNPATR + Deamidation (NQ); Oxidation (M)
gi|32352154	nascent polypeptide associated complex alpha chain [Oryza sativa (japonica cultivar-group)]	22264	90	1	90	IEDLSSQLQTQAAEQFK

Table 3C: (ac-DEVD-CHO and Biotin-DEVD-CHO) elution from the avidin column of sample AIEX 4 desalted and incubated with ac-DEVD-CHO and biotin-DEVD-CHO.

Accession number	Protein description	Theoretical MW (Da)	Total score	Number peptide matches	Ions score	Peptide sequence
gi|42407753	Putative phosphoribosyl glycinamide formyltransferase, chloroplast precursor [Oryza sativa (japonica cultivar-group)]	31132	107	2	55	VVPVLANDTPEQLAAR
					51	YSGPTVHFVDEHYDTGR
gi|37535658	Putative N-acetyl-gamma-glutamyl-phosphate reductase [Oryza sativa (japonica cultivar-group)]	45446	90	1	97	APELQQEAVYGLTEVLR
gi|11290108	**copper chaperone homolog CCH [imported] – rice**	**13085**	52	1	57	**MEGVETFDIDMEQQK + Oxidation (M)**

Table 3D: (D-biotin) elution from the avidin column of sample AIEX 4 desalted and incubated with D-Biotin

Accession number	Protein description	Theoretical MW (Da)	Total score	Number peptide matches	Ions score	Peptide sequence
gi|34907258	putative nascent polypeptide associated complex alpha chain [Oryza sativa (japonica cultivar-group)]	22079	140	2	58	SPNSDTYVIFGEAK
					87	IEDLSSQLQTQAAEQFK
gi|37535658	putative N-acetyl-gamma-glutamyl-phosphate reductase [Oryza sativa (japonica cultivar-group)]	45446	104	1	104	APELQQEAVYGLTEVLR
gi|50882147	putative translation elongation factor eEF-1 beta' chain [Oryza sativa (japonica cultivar-group)]	23398	88	1	93	AVGVNLPGGGAASSAAA AAPAAK
gi|13899101	alpha NAC-like protein [Arabidopsis thaliana]	23670	84	1	89	IEDLSSQLQTQAAQQFK
gi|34393337	putative 5-formyltetrahydrofolate cycloligase [Oryza sativa (japonica cultivar-group)]	30071	74	1	81	NSMNILEPSPLDASGNAR + Oxidation (M)
gi|34394937	putative beta-1,3-glucanase [Oryza sativa (japonica cultivar-group)]	59325	68	1	68	DADNLMDPQSVVSLLR + Oxidation (M)
gi|32352154	nascent polypeptide associated complex alpha chain [Oryza sativa (japonica cultivar-group)]	22264	75	1	75	IEDLSSQLQTQAAEQFK
gi|13899101	alpha NAC-like protein [Arabidopsis thaliana]	23670	71	1	75	IEDLSSQLQTQAAQQFK + Deamidation (NQ)
gi|18396922	expressed protein [Arabidopsis thaliana]	45851	50	1	50	EALITCLEIAAR

Three bands that were visible on SDS-PAGE were not identified. These results were confirmed by manual inspection of selected ion chromatograms (SIC). The liquid chromatography/tandem mass spectrometry (LC-MS/MS) is the bioanalytical method of choice because of its speed, selectivity and sensitivity. Using this nanoelectrospray technology, it is possible to obtain MS/MS spectra for 1 fmol of peptide or less. Because of its sensitivity, the LC-MS/MS is most suitable to identify proteins in gel. Nonetheless the three major visible bands on gel were not identified. This could be explained by putative post-translational modifications or an insufficient number of tryptic peptides.

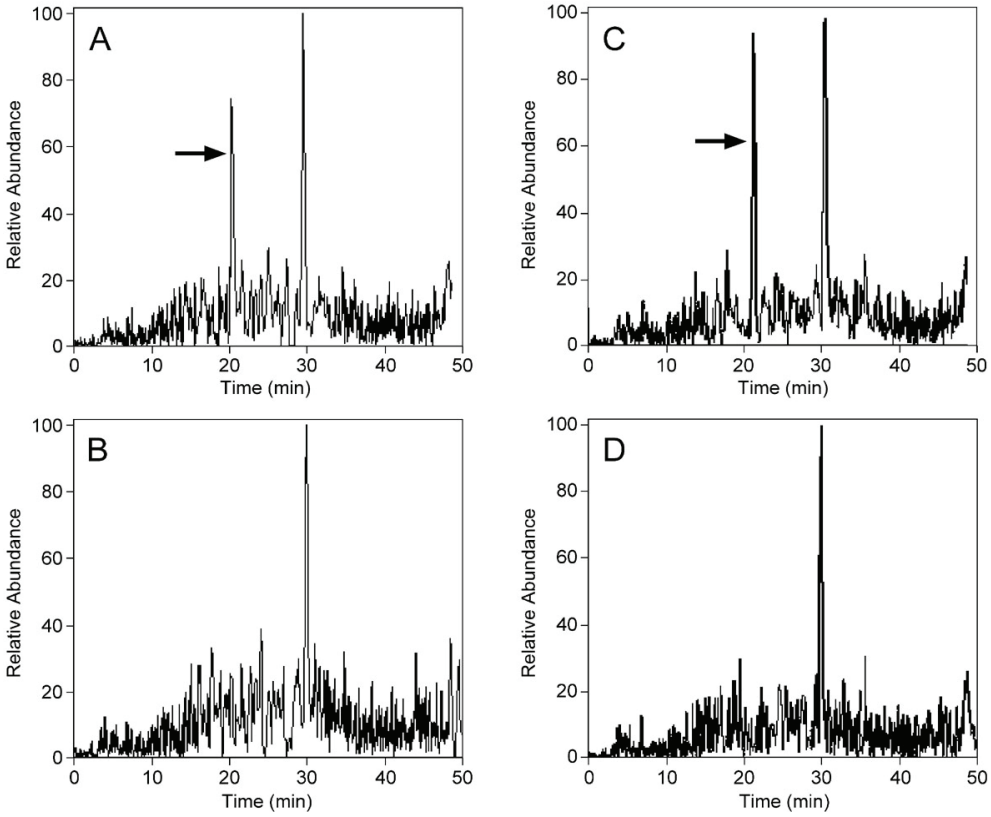

Figure 7: selected ion chromatograms (SIC) at m/z 916.6 of experiments A, B, C and D described previously. Two peaks are present in the graphs A and C at retention time 20 and 30 min. The first one is the one identified as belonging to the chaperone protein at retention time 20 min. This peak is not present in graphs B and D at m/z 916.6 and retention time 20 min.

A third possible explanation is that a high abundance of protein spots might have interfered with protein spots that were less abundant and in a quantity too low for these protein spots to be identified by MALDI peptide mapping. The facts that at least three visible bands could not

be identified by this method and that the copper chaperone homolog CCH could be identified without being visible suggest that more proteins could be retained specifically by the avidin column. If that is true, the copper chaperone homolog CCH might be part of a complex or bound to another protein that exhibits caspase-3 like activity. Nothing is known about a putative proteolytic activity of the copper chaperone homolog CCH. However, several studies have shown that this protein is involved in PCD.

Copper chaperones have been conserved during evolution and exist in diverse eukaryotic organisms from yeast to human (Wintz et al. 2002). CCH plays a role in the homeostatic regulation of copper within plant cells, but little is known about the function that this protein might have in the physiology and development of plants. CCH mRNA has been shown to be up-regulated during natural and ozone-accelerated leaf senescence in Arabidopsis (Himelblau et al. 1998; Miller et al. 1999) but the role of the copper chaperone during these processes is unclear. The expression of LeCCH (*Lycopersicon esculentum* copper chaperone) in tomato after fungal infection with the phytopathogen *Botrytis cinerea* suggests a relationship between copper homeostasis and plant defense responses (Company & Gonzalez-Bosch 2003). In spite of the possible involvement of the copper chaperone homolog CCH in plant PCD, there is no indication that this protein exerts caspase-like activity itself. Moreover, there are no indications that the copper chaperone homolog CCH is able to bind specifically to avidin, neither direct nor indirect via biotin. This opens the possibility that the copper chaperone homolog CCH is eluted from the column as a part of a complex. The fact that at least three unidentified polypeptides were co-eluted with molecular weights that are different from the molecular weight of the copper chaperone homolog CCH supports this hypothesis. Hence, the copper chaperone homolog CCH might be associated with a second protein with caspase-like proteolytic activity by direct interaction, or it might be part of or associated with a much bigger protein complex.

In case of direct interaction with one other protein, the copper chaperone CCH could have the function to modulate the activity of the plant caspase by associating the protease and copper ions. Cysteine proteases represent a broad class of proteolytic enzymes widely distributed among living organisms such as cathepsin B, papain and caspases. They contain a Cys-His pair in their peptidolytic site which is simultaneously a peptidolytic site, a metal-binding site, a redox-reactive site and a proton-interactive site (Lockwood 2004). The human cathepsin B is a cysteine protease containing a Cys-His pair in the peptidolytic site (Salahuddin & Kaur 1996). The inactivation of cathepsin B activity has been demonstrated with metal ions such as Ca^{2+} and Cu^{2+} (Salahuddin & Kaur 1996). In the case of Papain, both Cu^{2+} and ascorbic acid bind to the enzyme to form an inhibited complex (Kanazawa et al. 1993). Other researchers have suggested that Zn^{2+} is a natural inhibitor of caspases

(Stennicke & Salvesen 1997) and that some inactive caspases might exist in preventive Zn^{2+} associations (Truong-Tran et al. 2001). In that sense, the copper chaperone CCH, in order to activate or inactivate the plant proteases, could be the adaptor to release the divalent ion Cu^{2+} from the plant protease responsible for caspase-like activity during PCD, or to bind the divalent ion Cu^{2+} to that plant protease.

In the other case, the copper chaperone homolog CCH might be associated with a complex. That complex might very well be the 26S proteasome. The majority of proteins are degraded by the 26S proteasome. The comparison of the subunit compositions of the spinach 26S proteasome with those of the rat enzyme suggested that these heterogeneous subunit structures are common to plants and other organisms ranging from Drosophila to man (Fujinami et al. 1994). The 26S proteasome complex consists of the 20S proteasome and one or two 19S regulatory complexes. The 20S particle is a hollow cylinder composed of four stacked rings. Two inner β-rings are identical in subunit composition and each β-ring contains three different proteolytic sites (Groll et al. 1997). The chymotrypsin-like site cleaves peptide bonds after hydrophobic residues, the trypsin-like site cuts after basic residues, and the third site, generally termed postglutamyl peptide hydrolase (PGPH) 1, cuts after acidic residues. Because this last site was found to cleave after aspartates in fluorogenic substrates of caspases, the name “caspase-like” was suggested (Kisselev et al. 2003). Heat shock is well known to cause misfolding of cellular proteins, thus increasing the accumulation of substrates for the ubiquitin-proteasome pathway (Alberts et al. 1994; Peng et al. 2001). Furthermore, heat-shock was shown to be a convenient inducer of caspase-3 like activity in rice suspension cells in the previous chapter. CCH could be implicated with the opening of the proteasome lid, the 19S regulatory complexes, during heat-shock. Moreover, organic copper complexes can potently and selectively inhibit the chymotrypsin-like activity of the proteasome (Daniel et al. 2004).

In plants, a putative role for the proteasome in PCD was already suggested. During barley androgenesis, PCD takes place during induction by stress and during the transition from multicellular structures into globular embryos. A cDNA array analysis was performed to study up-regulated stress-induced genes. The induction of androgenesis by stress was marked by the up-regulation of some subunits of the proteasome (Maraschin 2005).

It has been shown that the disruption of the proteasome function by gene silencing of the proteasome subunits activates PCD in plants (Kim et al. 2003). The proteasome-mediated PCD exhibited characteristic features of apoptotic cell death, such as nuclear condensation, DNA fragmentation, involvement of reactive oxygen species (ROS), cytochrome c release from mitochondria, activation of caspase-like protease activities and transcriptional induction of defence-related genes.

In order to test the hypotheses as described above, more information is required concerning the identity of the purified components. The affinity chromatography step should be improved. Endogenous biotinylated plant proteins should be removed by running the extracts over the avidin column before the incubation with the different caspase-3 inhibitors or D-biotin. The poor recovery after the avidin column might be caused by steric hindrance after binding of the biotin moiety and avidin. A longer spacer between biotin and the specific caspase-3 substrate would be an option. Moreover, the proteomics tools should be adjusted or improved. The fact that at least three visible polypeptides could not be identified might be caused by trypsin insensitivity or post-translational modifications. Interestingly, the molecular weights of these polypeptides correspond with those of some subunits of the proteasome. However, it is known of the human proteasome that its polypeptides can be easily digested in gel by trypsin and subsequently sequenced (Fuji et al. 2005).

Acknowledgments

We are grateful to Prof. Dr. Paul Hooykaas (Institute of Biology Leiden, Leiden University, The Netherlands) and to Dr. Wouter-Jan Oosten (Sociotext Foundation) for valuable discussion and critical reading of the manuscript and to Mr. Peter Hock for the lay-out of the figures. This work was financed by the BVS Foundation (Binair Vector Systeem).

References

Belenghi B, Salomon M and Levine A. (2004) Caspase-like activity in the seedlings of *Pisum sativum* eliminates weaker shoots during early vegetative development by induction of cell death. J Exp Bot. 55(398): 889-897.

Bozhkov PV, Filonova LH, Suarez MF, Helmersson A, Smertenko AP, Zhivotovsky B and von Arnold S. (2004) VEIDase is a principal caspase-like activity involved in plant programmed cell death and essential for embryonic pattern formation. Cell Death Differ 11(2): 175-182.

Bradford MM. (1976) A rapid and sensitive method for the quantitation of microgram quantities of protein utilizing the principle of protein-dye binding. Anal Biochem. 72: 248-254.

Chen HM, Zhou J and Dai YR. (2000) Cleavage of lamin-like proteins in *in vivo* and *in vitro* apoptosis of tobacco protoplasts induced by heat shock. FEBS Lett. 480(2-3): 165-168.

Coffeen WC and Wolpert TJ. (2004) Purification and characterization of serine proteases that exhibit caspase-like activity and are associated with programmed cell death in *Avena sativa*. Plant Cell. 16(4): 857-873.

Company P and Gonzalez-Bosch C. (2003) Identification of a copper chaperone from tomato fruits infected with *Botrytis cinerea* by differential display. Biochem Biophys Res Commun. 304(4): 825-830.

Daniel KG, Gupta P, Harbach RH, Guida WC and Dou QP. (2004) Organic copper complexes as a new class of proteasome inhibitors and apoptosis inducers in human cancer cells. Biochem Pharmacol. 67(6): 1139-1151.

Danon A, Rotari VI, Gordon A, Mailhac N and Gallois P. (2004) Ultraviolet-C overexposure induces programmed cell death in Arabidopsis, which is mediated by caspase-like activities and which can be suppressed by caspase inhibitors, p35 and Defender against Apoptotic Death. J Biol Chem. 279(1): 779-787.

De Jong AJ, Hoeberichts FA, Yakimova ET, Maximova E and Woltering EJ. (2000) Chemical-induced apoptotic cell death in tomato cells: involvement of caspase-like proteases. Planta 211: 656-662.

Del Pozo O and Lam E. (1998) Caspases and programmed cell death in the hypersensitive response of plants to pathogens. Curr Biol. 8: 1129-1132.

Fernandes-Alnemri T, Litwack G and Alnemri ES. (1994) CPP32, a novel human apoptotic protein with homology to Caenorhabditis elegans cell death protein Ced-3 and mammalian interleukin-1 beta-converting enzyme. J Biol Chem. 269(49): 30761-30764.

Fujinami K, Tanahashi N, Tanaka K, Ichihara A, Cejka Z, Eaumeisterg W, Miyawaki M, Sato T and kagawan H. (1994) Purification and Characterization of the 26S Proteasome from Spinach Leaves. J Biol Chem. 269 (41): 29905-25910

Groll M, Ditzel L, Lowe J, Stock D, Bochtler M, Bartunik HD, and Huber R. (1997) Structure of 20S proteasome from yeast at 2.4 A resolution. Nature. 386(6624): 463-471.

Himelblau E, Mira H, Lin SJ, Culotta VC, Penarrubia L and Amasino RM. (1998) Identification of a functional homolog of the yeast copper homeostasis gene ATX1 from Arabidopsis. Plant Physiol. 117(4): 1227-1234.

Kim M, Ahn JW, Jin UH, Choi D, Paek KH and Pai HS. (2003) Activation of the Programmed Cell Death Pathway by Inhibition of Proteasome Function in Plants. J Biol Chem. 278(21): 19406-19415.

Kisselev AF, Garcia-Calvo M, Overkleeft HS, Peterson E, Pennington MW, Ploegh HL, Thornberry NA and Goldberg AL. (2003) The caspase-like sites of proteasomes, their substrate specificity, new inhibitors and substrates, and allosteric interactions with the trypsin-like sites. J Biol Chem 278(38): 35869-35877.

Korthout HAAJ, Berecki G, Bruin W, van Duijn B and Wang M. (2000) The presence and subcellular localization of caspase 3-like proteinases in plant cells. FEBS Lett 475: 139-144.

Laemmli UK. (1970) cleavage of structural proteins during the assembly of the head of bacteriophage T4. Nature 277: 680-685.

Lockwood TD. (2004) Cys-His proteases are among the wired proteins of the cell. Arch Biochem Biophys. 432(1): 12-24.

Maraschin S.F. (2005) Androgenic switch in barley microspores. PhD thesis, Leiden University.

Maraschin SF, Gaussand G, Pulido A, Olmedilla A, Lamers GEM, Korthout H, Spaink HP and Wang M. (2005) Programmed cell death during the transition from multicellular structures to globular embryos in barley androgenesis. Planta 221(4): 459-470.

Miller JD, Arteca RN and Pell EJ. (1999) Senescence associated gene expression during ozone-induced leaf senescence in Arabidopsis. Plant Physiol. 120: 1015-1024.

Mlejnek P and Prochazka S. (2002) Activation of caspase-like proteases and induction of apoptosis by isopentenyladenosine in tobacco BY-2 cells. Planta 215: 158-166.

Nicholson DW and Miller DK. (1995) Identification and inhibition of the ICE/CED-3 protease necessary for mammalian apoptosis. Nature 376: 37-43.

Salahuddin A and Kaur H. (1996) Studies on Activation and Inhibition of Cathepsin B from Buffalo Liver. J Prot Chem. 15(1): 87-93.

Savage D, Mattson G, Desai S, Nielander G, Morgensen S and Conklin E. eds. (1992) Avidin-Biotin Chemistry: A Handbook, Pierce Chemical Company, Rockford, IL.

Stennicke HR and Salvesen GS. (1997) Biochemical characteristics of caspases-3, -6, -7, and -8. J. Biol. Chem. 272(41): 25719-25723.

Sun YL, Zhao Y, Hong X and Zhai ZH. (1999) Cytochrome c release and caspase activation during menadione-induced apoptosis in plants. FEBS Lett. 462(3): 317-321.

Tewari M and Dixit VM (1995) Fas- and tumor necrosis factor-induced apoptosis is inhibited by the poxvirus crmA gene product. J. Biol. Chem. 270: 3255-3260.

Tian R, Zhang GY, Yan CH and Dai YR. (2000) Involvement of poly (ADP-ribose) polymerase and activation of caspase-3-like protease in heat shock-induced apoptosis in tobacco suspension cells. FEBS Lett. 474(1): 11-15.

Truong-Tran AQ, Carter J, Ruffin RE and Zalewski PD. (2001) The role of zinc in caspase activation and apoptotic cell death. Biometals. 14(3-4): 315-330.

Wilchek M and Bayer EA. (1988) The avidin-biotin complex in bioanalytical applications. Anal. Biochem. 171: 1-32.

Yuan JY, Shaham S, Ledoux S, Ellis HM and Horvitz HR. (1993) The *C. elegans* cell death gene ced 3 encodes a protein similar to mammalian interleukin 1 beta converting enzyme. Cell 75: 641-652.

Zhang GY, Zhu RY, Tian RH and Dai YR. (2003) Cleavage of poly(ADP-ribose) polymerase during apoptosis induced by nicotinamide at high concentrations in tobacco suspension cells. Plant Growth Regulation 41: 93–98.

Chapter 6

Summary and general discussion

The development of multicellular organisms involves an important balance between cell growth, cell division and cell death. In animals, programmed cell death (PCD) plays a key role by forming and deleting structures, controlling cell numbers and eliminating abnormal damaged cells (Baehrecke 2002). Apoptosis is a genetically and morphologically encoded form of PCD, defined by condensation of the nucleus and cytoplasm, association of chromatin with the nuclear periphery, DNA fragmentation, membrane blebbing, and engulfment and lysosomal degradation of the dying cell by a phagocyte (Kerr et al. 1972). Caspases were found to be the executioners of the apoptotic pathway and certain proteins of the mitochondria - such as IAP and Bcl-2 family proteins - were found to be the regulators.

In plants, PCD plays an important role in development and in the responses to pathogens and abiotic stresses (Pennell & Lamb 1997; Dangl & Jones 2001; Kuriyama & Fukuda 2002; Danon et al. 2004). Some common features of apoptosis were found to be conserved in both plants and animals (Danon & Gallois 1998; Yao et al. 2004). These include cytoplasm shrinkage, cytochrome c leakage out of mitochondria, chromatin condensation, altered nuclear morphology, DNA fragmentation in large fragments and DNA laddering. After the elucidation of the complete sequences of plant genomes such as those of Arabidopsis and rice, it has become clear that no genes for the caspases or for the apoptotic regulators of the IAP and Bcl-2 families are present in plants. However, animal Bcl-2 members have been found to modify cell death processes in plants (Lam et al. 1999; Baek et al. 2004). This indicates that a similar apoptotic machinery may still be present in plants.

The studies described in this thesis are focussed on the determination of the existence of caspase-like activities in plants during PCD. In **chapter 2** of this thesis, the Arabidopsis spontaneous necrotic spots (*sns*) mutant, developing necrotic spots during development is described. Both the T-DNA and the binary vector are inserted in the 3'UTR of the gene At1g13020 which encodes a putative eukaryotic translation initiation factor, eIF4B5. The insertion provoked a chromosomal rearrangement and caused changes in expression of several genes surrounding the location of the insertion. Necrotic spots become visible on the leaves after two or three weeks of growth, resembling the lesions that accompany the hypersensitive response after a pathogen attack. The phenotype of the *sns* mutant plants was analyzed in detail. By use of TUNEL analysis DNA fragmentation was found in the nuclei of cells in the necrotic spots. In addition a significant increase of caspase-3 and -6 like activities was found in *sns* leaf extracts. This indicated that the mutation causes local cell death by PCD.

Since the position-determined cell death process appeared to be an important step in the commitment of microspores to the embryogenic route, this process was characterized in detail in **chapter 3**. Morphological analysis showed that these pro-embryos were

composed of two different cellular domains: a large vegetative domain, and a small generative domain positioned at the opposite side of the pollen germ pore. During the transition from multicellular structures into globular embryos, the generative cell domain died by a process of PCD. Hallmarks of programmed cell death such as chromatin condensation, DNA degradation and an increase in the activity of caspase-3-like proteases preceded massive cell death of the generative cell domain. After elimination of the small generative domain by PCD, further embryogenesis came about exclusively by the large vegetative domain. These results show that programmed cell death is an important feature of the embryogenic pathway of barley microspores.

C**hapter 4** described a rice suspension cells system. Heat-shock treatment was used to study the development of necrosis and programmed cell death (PCD) in this system. Caspase-like activity was measured twenty hours after the initial heat-shock, followed by DNA degradation. The increase of the caspase-like activities was in correlation with the increase of cell death. The added caspase-3 and caspase-6 inhibitors inhibited caspase-3 and caspase-6 like activities. These inhibitors did not prevent DNA degradation or cell death. These rice suspension cells constitute an excellent system. They can be cultured at large scale for purification purposes.

During the research of this thesis, other researchers have found that caspase-like activity was associated with PCD (Lam & del Pozo 2000; Tian et al. 2000; Korthout et al. 2000; de Jong et al. 2000; Mlejnek & Prochazka 2002; Danon et al. 2004; Belenghi et al. 2004; Maraschin et al. 2005). If caspase-like activities can be measured in plant extracts during PCD, this strongly suggests that caspase-like proteases are involved in plant PCD. Caspase-like activities in plant extracts are due to enzymatic reactions of unknown plant proteases with a fluorogenic caspase substrate from animal origin that mimics the caspase substrate recognition sites. During the reaction, the fluorescent moiety of the fluorescent substrate is cleaved after the aspartate residue (for example, -AMC of the caspase-3 substrate Ac-DEVD-AMC). To test if the cleavage is done by regular cysteine protease activity or by specific caspase-like proteins, a specific caspase inhibitor from animal origin can be used. In order to purify the human caspase-3, the avidin-biotin affinity chromatography was effectively applied by use of a biotinylated inhibitor biotin-DEVD-CHO (Nicholson et al. 1995). This inhibitor was designed on the basis of the natural caspase-3 substrate, the poly (ADP-ribose) polymerase (PARP). Using the same technology, caspase-3 like activity might be possibly purified from plant extracts. In **chapter 5**, the development and implementation of the protocol to purify plant caspase-3 like activity is described. The rice suspension cells were cultured at large scale. The same biotinylated human caspase-3 inhibitor, biotin-DEVD-CHO, was used to purify the plant protease responsible for this peptide

cleavage by means of avidin-biotin chromatography. The only protein which was identified was the copper chaperone homolog CCH. In this chapter, the possible roles of the copper chaperone homolog CCH during PCD in plants are discussed. However the more important point is that the protein of interest, the caspase-like protease was not identified. Although the recovery of the affinity chromatography step was rather low, some proteins could be specifically eluted. These proteins were subjected to LC-MS/MS analysis followed by database search. With this method, several proteins could not be identified. This result suggested either (i) that the method was not optimal, (ii) or that the plant protease could be part of a protein complex, or (iii) that the affinity of the plant protease for the biotinylated inhibitor was not so strong.

Another point to discuss here is to explain why CCH was purified with this method. One possibility is of course that it is part of a complex involved in PCD. Another possibility is that the chaperone binds the biotin-DEVD-CHO by artefact. The CCH belongs to a family of 31 genes coding for proteins that possess a heavy-metal-associated (HMA) domain similar to the ATX1 HMA domain of yeast (Wintz & Vulpe 2002). These proteins have a conserved HMA domain of approximately 30 amino acid residues. The HMA domain contains two cysteine residues that are important in binding and transfer of metal ions, such as copper, cadmium, cobalt and zinc. In the case of copper, stoichiometry of binding is one Cu^{+} ion per binding domain. CCH contains the metal-binding sequence MXCXGC present in this type of copper chaperones from plants, yeast, and animals. It is possible that the biotin-DEVD-CHO bound to this sequence. Indeed, catalysis of caspase substrates is mediated by a mechanism involving a catalytic dyad, composed of Cys163 and His121, on the large subunit of the caspases. The substrate-binding gap recognizes a short 4 amino-acid stretch within protein substrates, directly N-terminal to the cleavage site (Rotonda et al. 1996). This tetrapeptide motif, which is sufficient to bind specifically to the active caspase, is the basis for the design of the synthetic inhibitors, such as Ac-DEVD-CHO or biotin-DEVD-CHO.

Recent efforts to purify and characterize the proteases responsible for the caspase-like activities in plant cells have indicated that serine proteases and vacuolar processing enzymes, which are cysteine proteases, might potentially account for the caspase-like activities associated with plant PCD (Coffeen & Wolpert 2004; Hatsugai et al. 2004). In those studies similar problems with the biotinylated compound were mentioned. For example, Coffeen and Wolpert (2004) were unsuccessful to visualize on a biotin blot an activity B protease obtained after separation on a HIC column with the biotinylated caspase inhibitor biotin-VAD-FMK (Coffeen & Wolpert 2004). They found that biotin-VAD-FMK prevented Z-VAD-AFC hydrolysis but did not covalently label the protein. Even after successful purification of a protein by using caspase inhibitor tags, it still needs to be proven that the activity is

involved in PCD because the inhibitors are not specific to plants and they could inhibit several proteases in the cell. Affinity labelling with biotinylated irreversible caspase inhibitors has been shown to be useful to detect caspases in cell extracts by means of western blotting using streptavidin linked to horse radish peroxidase. In extracts from *N. tabacum* cell suspensions, cytosolic proteins interacting with Biotin-VAD-fmk, ranging from 20 to 150 kDa, were identified (Elbaz et al. 2002). This indicates that more than one protease may be involved. This is also the case in chapter 5, there were many bands of different molecular weight which were not identified. In *Pisum sativum* seedlings, the PCD of secondary shoots could be blocked by both caspase inhibitors and cysteine-protease inhibitors. Using anion exchange chromatography of a partially purified fraction, a 55 kDa protein band was detected by an in-gel protease assay with the fluorogenic substrate Ac-YVAD-AMC (Belenghi et al. 2004). In extracts from oat leaves undergoing victorin-induced PCD, biotin-YVAD-cmk labelled numerous proteins in a partially purified VAD/AADase activity peak. One of the proteins, with molecular weight of 84 kDa, seemed to bind specifically to this inhibitor because the labelling could be competitively inhibited by Ac-VAD-cmk but not by Ac-DEVD-cmk (Coffeen & Wolpert 2004).

Although caspase-like activities seem to be involved in plant PCD, it is clear that orthologs of the animal genes for caspases are not present in plants. In the search for the proteases that are involved in plant PCD, other proteins have been found and described as playing a role in plant PCD. Uren et al. (2000) found a family of distantly related caspase-like proteases - named metacaspases - in plants, fungi and Plasmodium. Many investigations indicate that metacaspases can have a role in PCD. Hoeberichts et al. (2003) have shown that mRNA levels of LeMCA1 - a tomato (*Lycopersicon esculentum*) type II metacaspase - increased upon infection of leaves with the fungal pathogen *Botrytis cinerea*. This increase correlates with the formation of primary necrotic lesions. The protein mcII-Pa (plant metacaspase type II) was expressed during PCD in somatic embryogenesis in Norway spruce. *In situ* hybridization analysis showed mRNA accumulation in the part of embryogenic tissues and structures committed to die (Suarez et al. 2004). The activation of proteases cleaving the caspase-6 substrate (VEIDase activity) is essential for PCD and embryogenesis in Norway spruce (*Picea abies*) (Bozhkov et al. 2004). Silencing of *P. abies* metacaspase gene *mcII-Pa* inhibited VEIDase activity, suppressed PCD in the embryos and blocked suspensor differentiation (Suarez et al. 2004). Immunolocalization analyses and functional assays showed that mcII-Pa accumulates in the nuclei of the suspensor cells and that it is directly involved in the execution of nuclear disassembly (Bozhkov et al. 2005). Watanabe and Lam (2005) found that two type I metacaspases (At5g64240 and At1g02170) were up-regulated in Arabidopsis plants after infiltration by a bacterial pathogen, whereas type II

metacaspases were not significantly affected. The vacuolar processing enzymes (VPEs) promote the maturation and the activation of various vacuolar proteins in plants (Yamada et al. 1999; Shimada et al. 2003; Rojo et al. 2003; Gruis et al. 2004). Recent data suggested that VPEs might be key factors in vacuolar collapse-triggered cell death. Arabidopsis VPE genes are up-regulated in dying cells during development and senescence of tissues (Kinoshita et al. 1999). There is no sequence similarity between VPEs and caspases. However, VPEs have a proteolytic activity toward a caspase-1 substrate, and VPE activity is inhibited by a caspase-1 inhibitor. Tobacco VPE exhibits the caspase-1 like activity that is required for the completion of cell death during TMV-induced HR in tobacco (Hatsugai et al. 2004). The saspase-A and -B, belonging to the substilisin-like serine protease family, have been found to be involved in victorin-induced PCD in oat (*Avena sativa*) (Coffeen & Wolpert 2004). They were found to cleave caspase specific substrates and they were found to be inhibited by caspase-specific inhibitors. The two oat saspases show hydrolytic activities for caspase-6, -8 and -9 substrates (VKMD, IETD, and LEHD, respectively) but not for DEVD and VEID.

In recent years, there has been a considerable increase in the amount of information concerning the cellular and molecular aspects involved in PCD in both animals and plants. A certain question “Do plant caspases exist?” was asked by Woltering et al. (2002). Already a good question at that time, it remains a good one today. Following the same point of view as described by Woltering et al. (2002), if there is plant caspase-like protease, it might be like in animals, which means a cysteine protease that cleaves adjacent aspartate residue. Nowadays there is an accumulation of evidence that plant caspase-like proteases exist since caspase-like proteolytic activity is present in plants and this activity does play a pivotal role in plant PCD. But the main plant executioner in plants during PCD is still unknown.

The research described in this thesis has provided a substantial contribution towards understanding the role of caspase-like proteases during plant PCD. The optimizations of a protocol to measure caspase-like activity, of the extraction buffer, and of the purification protocol have been crucial in this research. In addition, the different plant systems analysed in this thesis represent useful tools for further analysis of PCD. The identification of such proteases is essential to reveal the molecular mechanism that operates in plant PCD, and to provide some insights into differences between plant and animal PCD.

It would still be exciting to discover those proteases. The much desired caspase-like protease might one day be caught.

References

Baehrecke EH. (2002) How death shapes life during development. Nat Rev Mol Cell Biol. 3 (10): 779-787

Baek D, Nam J, Koo YD, Kim DH, Lee J, Jeong JC, Kwak SS, Chung WS, Lim CO, Bahk JD, Hong JC, Lee SY, Kawai-Yamada M, Uchimiya H and Yun DJ. (2004) Bax-induced cell death of Arabidopsis is meditated through reactive oxygen-dependent and -independent processes. Plant Mol Biol. 56 (1): 15-27.

Belenghi B, Salomon M and Levine A. (2004) Caspase-like activity in the seedlings of *Pisum sativum* eliminates weaker shoots during early vegetative development by induction of cell death. J Exp Bot. 55 (398): 889-897.

Bozhkov PV, Filonova LH, Suarez MF, Helmersson A, Smertenko AP, Zhivotovsky B and von Arnold S. (2004) VEIDase is a principal caspase-like activity involved in plant programmed cell death and essential for embryonic pattern formation. Cell Death Differ. 11 (2): 175-182.

Bozhkov PV, Suarez MF, Filonova LH, Daniel G, Zamyatnin AA Jr, Rodriguez-Nieto S, Zhivotovsky B, Smertenko A. (2005) Cysteine protease mcII-Pa executes programmed cell death during plant embryogenesis. Proc Natl Acad Sci USA. 102 (40): 14463-14468.

Coffeen WC and Wolpert TJ. (2004) Purification and characterization of serine proteases that exhibit caspase-like activity and are associated with programmed cell death in *Avena sativa*. Plant Cell. 6 (4): 857-873.

Dangl JL and Jones JD. (2001) Plant pathogens and integrated defence responses to infection. Nature. 411 (6839): 826-833.

Danon A, Rotari VI, Gordon A, Mailhac N and Gallois P. (2004) Ultraviolet-C overexposure induces programmed cell death in Arabidopsis, which is mediated by caspase-like activities and which can be suppressed by caspase inhibitors, p35 and Defender against Apoptotic Death. J Biol Chem. 279 (1): 779-787.

Danon A and Gallois P. (1998) UV-C radiation induces apoptotic-like changes in *Arabidopsis thaliana*. FEBS Lett. 437 (1-2): 131-136.

De Jong AJ, Hoeberichts FA, Yakimova ET, Maximova E, Woltering EJ. (2000) Chemical-induced apoptotic cell death in tomato cells: involvement of caspase-like proteases. Planta.211 (5): 656-662.

Elbaz M, Avni A and Weil M. (2002) Constitutive caspase-like machinery executes programmed cell death in plant cells. Cell Death Differ. 9 (7): 726-733.

Gruis D, Schulze J and Jung R. (2004) Storage protein accumulation in the absence of the vacuolar processing enzyme family of cysteine proteases. Plant Cell. 16 (1): 270-290

Hatsugai N, Kuroyanagi M, Yamada K, Meshi T, Tsuda S, Kondo M, Nishimura M and Hara-Nishimura I. (2004) A plant vacuolar protease, VPE, mediates virus-induced hypersensitive cell death. Science. 305 (5685): 855-858.

Hoeberichts FA, ten Have A and Woltering EJ. (2003b) A tomato metacaspase gene is upregulated during programmed cell death in Botrytis cinerea-infected leaves. Planta. 217 (3): 517-522.

Kerr JF, Wyllie AH and Currie AR. (1972) Apoptosis: a basic biological phenomenon with wide-ranging implications in tissue kinetics. Br J Cancer. 26(4): 239-257

Kinoshita T, Yamada K, Hiraiwa N, Kondo M, Nishimura M and Hara-Nishimura I. (1999) Vacuolar processing enzyme is up-regulated in the lytic vacuoles of vegetative tissues during senescence and under various stressed conditions. Plant J. 19 (1): 43-53.

Korthout HA, Berecki G, Bruin W, Van Duijn B and Wang M. (2000) The presence and subcellular localization of caspase 3-like proteinases in plant cells. FEBS Lett. 475 (2): 139-144.

Kuriyama H and Fukuda H. (2002) Developmental programmed cell death in plants. Curr Opin Plant Biol. 5 (6): 568-573.

Lam E and del Pozo O. (2000) Caspase-like protease involvement in the control of plant cell death. Plant Mol Biol. 44: 417-428.

Lam E, del Pozo O and Pontier D. (1999) BAXing in the hypersensitive response. Trends Plant Sci. 4(11): 419-421.

Maraschin SF, Gaussand G, Pulido A, Olmedilla A, Lamers GEM, Korthout H, Spaink HP and Wang M. (2005) Programmed cell death during the transition from multicellular structures to globular embryos in barley androgenesis. Planta. 221 (4): 459-470.

Mlejnek P and Prochazka S. (2002) Activation of caspase-like proteases and induction of apoptosis by isopentenyladenosine in tobacco BY-2 cells. Planta. 215 (1): 158-166.

Nicholson DW, Ali A, Thornberry NA, Vaillancourt JP, Ding CK, Gallant M, Gareau Y, Griffin PR, Labelle M, Lazebnik YA, Munday NA, Raju SM, Smulson ME, Yamin TT, Yu VL and Miller DK. (1995) Identification and inhibition of the ICE/CED-3 protease necessary for mammalian apoptosis. Nature. 376 (6535): 37-43.

Pennell RI and Lamb C. (1997) Programmed cell death in plants. Plant Cell 9 (7): 1157-1168.

Rojo E, Zouhar J, Carter C, Kovaleva V and Raikhel NV. (2003) A unique mechanism for protein processing and degradation in Arabidopsis thaliana. Proc. Natl. Acad. Sci. USA 100 (12): 7389-7394.

Rotonda J, Nicholson DW, Fazil KM, Gallant M, Gareau Y, Labelle M, Peterson EP, Rasper DM, Ruel R, Vaillancourt JP, Thornberry NA and Becker JW. (1996) The three-dimensional structure of apopain/CPP32, a key mediator of apoptosis. Nat Struct Biol. 3 (7): 619-625.

Shimada T, Yamada K, Kataoka M, Nakaune S, Koumoto Y, Kuroyanagi M, Tabata S, Kato T, Shinozaki K, Seki M, Kobayashi M, Kondo M, Nishimura M, Hara-Nishimura I. (2003) Vacuolar processing enzymes are essential for proper processing of seed storage proteins in *Arabidopsis thaliana*. J Biol Chem. 278 (34): 32292-32299.

Suarez MF, Filonova LH, Smertenko A, Savenkov EI, Clapham DH, von Arnold S, Zhivotovsky B and Bozhkov PV. (2004) Metacaspase-dependent programmed cell death is essential for plant embryogenesis. Curr biol. 14 (9): R339–R340.

Tian R, Zhang G, Yan C and Dai Y. (2000) Involvement of poly (ADP-ribose) polymerase and activation of caspase-3- like protease in heat shock-induced apoptosis in tobacco suspension cells. FEBS Lett. 474 (1): 11-15.

Uren AG, O'Rourke K, Aravind LA, Pisabarro MT, Seshagiri S, Koonin EV, Dixit VM. (2000) Identification of paracaspases and metacaspases: two ancient families of caspase-like proteins, one of which plays a key role in MALT lymphoma. Mol Cell. 6 (4): 961-967.

Wintz H and Vulpe C. (2002) Plant copper chaperones. Biochem Soc Trans. 30 (4): 732-735.

Woltering EJ, van der Bent A and Hoeberichts FA. (2002) Do plant caspases exist? Plant Physiol. 130 (4): 1764-1769.

Yamada K, Shimada T, Kondo M, Nishimura M, Hara-Nishimura I. (1999) Multiple functional proteins are produced by cleaving Asn-Gln bonds of a single precursor by vacuolar processing enzyme. J Biol Chem. 274 (4): 2563-2570.

Yao N, Eisfelder BJ, Marvin J and Greenberg JT. (2004) The mitochondrion - an organelle commonly involved in programmed cell death in *Arabidopsis thaliana*. Plant J. 40 (4): 596-610.

Samenvatting

Bij de ontwikkeling van multicellulaire organismen speelt de balans tussen celgroei, celdeling en celdood een belangrijke rol. Bij dieren speelt geprogrammeerde celdood (PCD) een centrale rol bij het vormen en het verwijderen van structuren, het beheersen van het aantal cellen en het elimineren van beschadigde cellen. Apoptose is een genetisch bepaalde en morfologisch herkenbare vorm van PCD, gedefinieerd door samentrekking van de celkern en het cytoplasma, door verbinding van het chromatine met de nucleaire periferie, DNA fragmentatie, door membraan “blebbing” en door het opnemen en lysosomale afbraak van de stervende cel door een fagocyt. Van caspases is ontdekt dat zij de apoptose uitvoeren, en van bepaalde eiwitten van de mitochondria, zoals van de IAP- en de Bcl-2-familie, is ontdekt dat zij de apoptose regelen.

Bij planten speelt PCD een belangrijke rol bij de ontwikkeling en bij de reacties op pathogenen en abiotische stress. Sommige gemeenschappelijke kenmerken van apoptose blijken te zijn bewaard in zowel planten als dieren. Enkele van die kenmerken zijn het krimpen van het cytoplasma, het lekken van cytochrome c uit mitochondria, chromatine condensatie, verandering van nucleaire morfologie, DNA-fragmentatie in grote fragmenten en “laddering” van DNA. Nadat de volledige sequenties van plantgenomen zoals die van Arabidopsis en rijst volledig in kaart gebracht waren, werd het duidelijk dat er voor de caspases of voor de apoptotische regulators van de IAP- en Bcl2-families geen genen aanwezig zijn in planten. Echter, van dierlijke Bcl2-leden is vast komen te staan dat zij celdoodprocessen in planten kunnen beinvloeden. Dit impliceert dat een vergelijkbare apoptotische regulatie nog steeds aanwezig kan zijn in planten.

De in dit proefschrift beschreven studies zijn gericht op de bepaling van het bestaan van caspase-achtige activiteiten in planten gedurende PCD. In **hoofdstuk 2** van dit proefschrift is de Arabidopsis spontane necrotische vlekkenmutant (*sns*), die bij ontwikkeling necrotische vlekken ontwikkelt, beschreven. Zowel het T-DNA als de binaire vector zijn ingebouwd in de 3’UTR van het gen Atlg13020. Dit gen codeert voor een vermoedelijke eukaryotische translatie initiatiefactor, eIF4B5. De integratie resulteerde in een chromosomale hergroepering en veroorzaakte daardoor veranderingen in de expressie van verscheidene genen rondom de plaats van het insert. Necrotische vlekken worden zichtbaar op de bladeren na twee of drie weken van groei, hetgeen lijkt op de kneuzingen die gepaard gaan met de overgevoeligheids reactie na een pathogene aanval. Het fenotype van de *sns*-mutantplanten is gedetailleerd geanalyseerd. Door het gebruik van een TUNEL-analyse is DNA-fragmentatie gevonden in de kernen van cellen in de necrotische vlekken. Verder is er een significante toename van caspase-3 en -6-achtige activiteiten gevonden in *sns*-bladextracten. Dit wijst erop dat de mutatie plaatselijke celdood door PCD veroorzaakt.

Aangezien het plaatsbepaalde celdoodproces een belangrijke stap leek te zijn in de toewijding van microsporen aan de embryogenetische route, is dit proces in detail gekarakteriseerd in **hoofdstuk 3**. Morfologische analyse heeft uitgewezen dat deze pro-embryo's zijn samengesteld uit twee verschillende cellulaire domeinen: een groot vegetatief domein en een klein generatief domein die zich bevinden aan de overzijde van het pollen kiemspoor. Gedurende de overgang van multicellulaire structuren naar globulaire embryo's stierf het generatieve celdomein door een proces van PCD. Hoofdkenmerken van geprogrammeerde celdood zoals chromatine samentrekking, uiteenvallen van DNA en activiteitstoename bij caspase-3-achtige proteases gingen vooraf aan grootschalig celsterven van het generatieve celdomein. Na eliminatie van het kleine generatieve domein door PCD ontstond verdere embryogenese uitsluitend door het grote vegetatieve domein. Deze resultaten tonen aan dat geprogrammeerde celdood een belangrijk aspect is van het embryogenetische traject van microsporen van gerst.

Hoofdstuk 4 beschrijft een rijst-cel-suspensie-systeem. Om de ontwikkeling van necrose en geprogrammeerde celdood (PCD) in dit systeem te bestuderen is een temperatuur-schok-behandeling gebruikt. Caspase-achtige activiteiten zijn twintig uur na de aanvankelijke temperatuurschok gemeten, gevolgd door degradatie van het DNA. De toename van de caspase-achtige activiteiten correleerde met de toename van celdood. De toevoeging van caspase-3- en caspase-6-remmers remde caspase-3 en caspase-6-activiteiten. Deze remmers gingen DNA-degradatie of celdood echter niet tegen. De rijst-suspensie-cellen kunnen op grote schaal gekweekt worden voor zuiveringsdoeleinden.

Gedurende het onderzoek van dit proefschrift hebben andere onderzoekers ook ontdekt dat caspase-achtige activiteit aan PCD gerelateerd was. Indien caspase-achtige activiteiten in plantenextracten tijdens PCD gemeten kunnen worden, is dat een sterke aanwijzing dat caspase-achtige proteasen betrokken zijn bij planten-PCD. Caspase-achtige activiteiten in plantenextracten kunnen worden ontdekt met behulp van een fluorogeen caspase-substraat van dierlijke origine dat de caspase-substraat herkenningsplaatsen imiteert. Tijdens de reactie wordt het fluorescerende deel van het fluorescerende substraat afgeknipt na het aspartaat residu (bijvoorbeeld -AMC van het caspase-3-substraat Ac-DEVD-AMC). Om na te gaan of het knippen geschiedt door een gewone cysteïne protease-activiteit of door specifieke caspase-achtige eiwitten kan een specifieke caspaseremmer van dierlijke origine worden gebruikt. Teneinde het humane caspase-3 te zuiveren, is avidine-biotine-affiniteitschromatografie gebruikt in combinatie met de gebiotinyleerde caspaseremmer biotin-DEVD-CHO. Deze remmer was ontworpen op basis van het natuurlijke caspase-3-substraat, poly(ADP-ribose)polymerase (PARP). Met gebruikmaking van dezelfde technologie zou caspase-3-achtige activiteit mogelijk uit plantenextracten gezuiverd kunnen

worden. In **hoofdstuk 5** is de ontwikkeling en implementatie beschreven van het protocol om plantencaspase-3-achtige activiteit te zuiveren. De rijst-suspensie-cellen zijn op grote schaal gecultiveerd. Dezelfde gebiotinyleerde humane caspase-3-blokkeerder, biotin-DEVD-CHO, is gebruikt om de plantenprotease te zuiveren. Het enige eiwit dat is geïdentificeerd, is de koper chaperone homoloog CCH. In dit hoofdstuk worden de mogelijke rollen van de koper chaperone homoloog CCH bij PCD in planten besproken. Het eiwit, de caspase-achtige protease, is echter niet geïdentificeerd. Hoewel de opbrengst van de affiniteitschromatografiestap tamelijk laag was, konden sommige eiwitten specifiek geëlueerd worden. Deze eiwitten werden geanalyseerd met LC-MS/MS-analyse, gevolgd door een database-zoekactie. Met deze methode konden verscheidene proteïnen niet geïdentificeerd worden. Dit resultaat doet veronderstellen ofwel (i) dat de methode niet optimaal was, (ii) of dat de plantenprotease onderdeel zou kunnen zijn van een eiwit-complex, of (iii) dat de affiniteit van de plantenprotease voor de gebiotinyleerde remmer niet zo sterk was.

Een ander punt om hier te bespreken is de verklaring van waarom CCH met deze methode gezuiverd is. Een mogelijkheid is natuurlijk dat het deel uitmaakt van een bij PCD betrokken complex. Een andere mogelijkheid is dat de binding van het chaperone aan biotin-DEVD-CHO een artefact is. De CCH behoort tot een familie van 31 eiwitten die een zware-metalen-geassocieerd (HMA) domein bezitten dat verwant is aan het ATX1 HMA-domein van gist. Deze eiwitten hebben een geconserveerd HMA-domein van ongeveer 30 aminozuur residuen. Het HMA-domein bevat two cysteïne residuen die belangrijk zijn voor het binden en transporteren van metaalionen, zoals koper, cadmium, kobalt en zink. In het geval van koper is er stoïchiometrisch één Cu^{+}-ion per bindend domein. CCH bevat de metaal bindende sequentie MXCXGC die aanwezig is in dit type koper chaperones van planten, gisten en dieren. Het is mogelijk dat biotin-DEVD-CHO bond aan deze sequentie. De katalytische activiteit van caspasen wordt inderdaad gemediëerd door een catalytische dyade, bestaande uit Cys163 en His121. De substraatbindende opening herkent een korte sequentie van 4 aminozuren in eiwitsubstraten, die direct N-terminal ligt voor de knipplaats. Dit tetrapeptide is voldoende om specifiek te binden aan de actieve caspase, en dit vormt de basis voor het ontwerp van de synthetische remmers, zoals Ac-DEVD-CHO of biotin-DEVD-CHO.

Recente experimenten die erop gericht waren om de proteases verantwoordelijk voor de caspase-achtige activiteiten in plantencellen te zuiveren en karakteriseren, hebben uitgewezen dat serine proteasen en vacuolaire cysteïne proteasen mogelijk de caspase-achtige activiteiten in planten-PCD veroorzaken. In de betreffende onderzoeken is men met vergelijkbare problemen met de gebiotinyleerde substraten en remmers geconfronteerd. Coffeen en Wolpert hadden bijvoorbeeld geen succes met het aantonen van een protease activiteit die verkregen was na scheiding op een HIC-kolom met de gebiotinyleerde remmer

biotin-VAD-FMK. Zij stelden vast dat biotin-VAD-FMK Z-VAD-AFC-hydrolyse remde, maar het eiwit niet covalent bond. Zelfs na succesvolle zuivering van een eiwit met behulp van caspase-remmer tags dient nog bewezen te worden dat de activiteit betrokken is bij PCD, omdat de remmers mogelijk niet specifiek zijn voor alleen het planten caspase achtige eiwit.

Hoewel caspase-achtige activiteiten betrokken lijken te zijn bij planten-PCD, was het duidelijk dat orthologen van de dierlijke genen voor caspases niet aanwezig zijn in planten. In de zoektocht naar de proteases die betrokken zijn bij planten-PCD zijn andere eiwitten ontdekt en beschreven als mogelijke actoren in planten-PCD. Er is een familie ontdekt van verre verwanten van caspase-achtige proteasen - metacaspases genoemd - in planten, schimmels en Plasmodium. Er wordt vermoedt dat metacaspases een rol spelen bij PCD. De mRNA concentraties van LeMCA1 - een tomaat (*Lycopersicon esculentum*) type II metacaspase – nemen toe na besmetting van bladeren met het schimmelpathogeen *Botrytis cinerea*. Deze toename correleert met de vorming van primaire necrotische aantastingen. Het eiwit mcII-Pa (plantenmetacaspase type II) komt gedurende PCD tot expressie tijdens de somatische embryogenese van Noorse spar. *In situ* hybridisatie-analyse toonde mRNA-opeenhoping in het deel van de embryogene weefsels en structuren welke zijn gedoemd om af te sterven. De activatie van proteasen die het caspase-6-substraat knippen (VEIDase-activiteit) is essentieel voor PCD en embryogenese in de Noorse spar (*Picea abies*). Het tot zwijgen brengen van het *P. abies* metacaspase gen *mcII-Pa* blokkeerde VEIDase-activiteit, onderdrukte PCD in de embyro's en belette suspensor differentiatie. Immunolokalisatie-analyses en functionele analyses toonden aan dat mcII-Pa zich ophoopt in de kernen van de suspensorcellen en dat het direct betrokken is bij de nucleaire deassemblage. Twee type I metacaspases komen in Arabidopsis-planten hoger tot expressie na infiltratie met een bacterieel pathogeen. De vacuolair verwerkende enzymen (VPE's) bevorderen de maturatie en de activering van verscheidene vacuolaire eiwitten in planten. Recente gegevens suggereren dat VPE's sleutelfactoren kunnen zijn in vacuolair -gestarte celdood. Er bestaat geen verwantschap in sequentie tussen VPE's en caspases. Toch hebben VPE's een proteolytische activiteit gericht op een caspase-1 substraat, en VPE-activiteit wordt geblokkeerd door een caspase-1-remmer. Tabaks-VPE vertoont de caspase-1-achtige activiteit die vereist is voor de celdood als gevolg van TMV geïnduceerde HR in tabak. De saspasen-A en -B, behorend tot de substilisin-achtige seriene protease-familie, zijn betrokken bij door victorine geïnduceerde PCD in haver (*Avena sativa*). Zij breken caspase-specifieke substraten af en worden geremd door caspase-specifieke remmers. De twee haver-saspases kunnen caspase-6, -8 en -9-substraten afbreken, maar niet DEVD en VEID.

De laatste jaren is de kennis met betrekking tot de cellulaire en moleculaire aspecten van PCD in zowel dieren als planten enorm toegenomen. De vraag "Bestaan er

plantencaspases?” is al lang geleden gesteld. Dat was toen al een goede vraag en het is vandaag de dag nog immer een goede vraag. Als er inderdaad een plantencaspase-achtige protease bestaat, zou dat het zoals in dieren een cysteïne protease kunnen zijn dat eiwitten knipt naast aspartate residuen. Tegenwoordig stapelt het bewijs zich op dat plantencaspase-achtige proteases bestaan, aangezien caspase-achtige proteolytische activiteit aanwezig is in planten en deze activiteit een centrale rol speelt in planten-PCD. Maar de voornaamste plantaardige uitvoerder van planten PCD is nog onbekend.

Het onderzoek beschreven in dit proefschrift heeft een aanzienlijke bijdrage geleverd aan het begrijpen van de rol van caspase-achtige proteases bij planten-PCD. Het optimaliseren van een protocol om caspase-achtige activiteit te meten, van de extractiebuffer en van het zuiveringsprotocol zijn cruciaal geweest in dit onderzoek. Verder vormen de verschillende plantensystemen die zijn geanalyseerd in dit proefschrift nuttige hulpmiddelen voor verdere analyse van PCD. De identificatie van voor PCD verantwoordlijke proteases is essentieel om het moleculaire mechanisme bloot te leggen dat ten grondslag ligt aan PCDin planten, en om inzicht te geven in de verschillen tussen planten- en dieren-PCD. Het zou opwindend zijn om die proteasen te ontdekken.

Curriculum vitae

Gwénael Gaussand was born on the 21st of January 1975 in Blois, France. He attended the Lycée Dessaignes in Blois. In September 1994, he started the study of medicine at the Faculté de Médecine of the Université Francois Rabelais in Tours. From September 1996 until September 2000, he was a student at the Faculté des Sciences et Techniques at the same university. In the meanwhile, from July 1999 until September 1999, he was a research trainee at Pau Euralis Génétique in Blois, where he worked on cross breeding and corn selection. Mr JP Sampoux supervised this traineeship. Then from February 2000 to September 2000, Gwénaël was an Erasmus Exchange research trainee with the Department of Applied Plant Sciences of TNO Quality of Life in Leiden, the Netherlands. This traineeship concerned the biosynthesis of starch in wheat, and it was supervised by Dr S de Pater. In September 2000, Gwénaël received his master degree in cellular biology and plant physiology, with a specialization in microbiology and plant biotechnology, from his university in Tours. From December 2000 to February 2005, he worked on a PhD research project at Leiden University. This project was supported by the Stichting Binair Vector Systeem. This work took place at (1) the Molecular and Developmental Biology Section of the Institute of Biology Leiden, under the supervision of Dr S de Pater and Prof Dr P Hooykaas, and (2) the Department of Applied Plant Sciences of TNO Quality of Life, under the supervision of Dr H Korthout and Dr M Wang. From September 2005 to April 2006, he worked as a post-doc in the Laboratory of Stress, Defenses and Plant Reproduction of the Université de Reims Champagne-Ardenne in Reims, France. Here, under the direction of Prof Dr C Clément, he participated in the EU Haplotech research project. In the meanwhile, he took up the voluntary position of program advisor ‘humanity, technology and earth’ with the Sociotext Foundation in The Hague, the Netherlands. Since September 2006, he works as a biochemist for Yacht Chemie and Life Sciences at Solanic, an Avebe group company.

Color Supplement

Figure 2, chapter 2

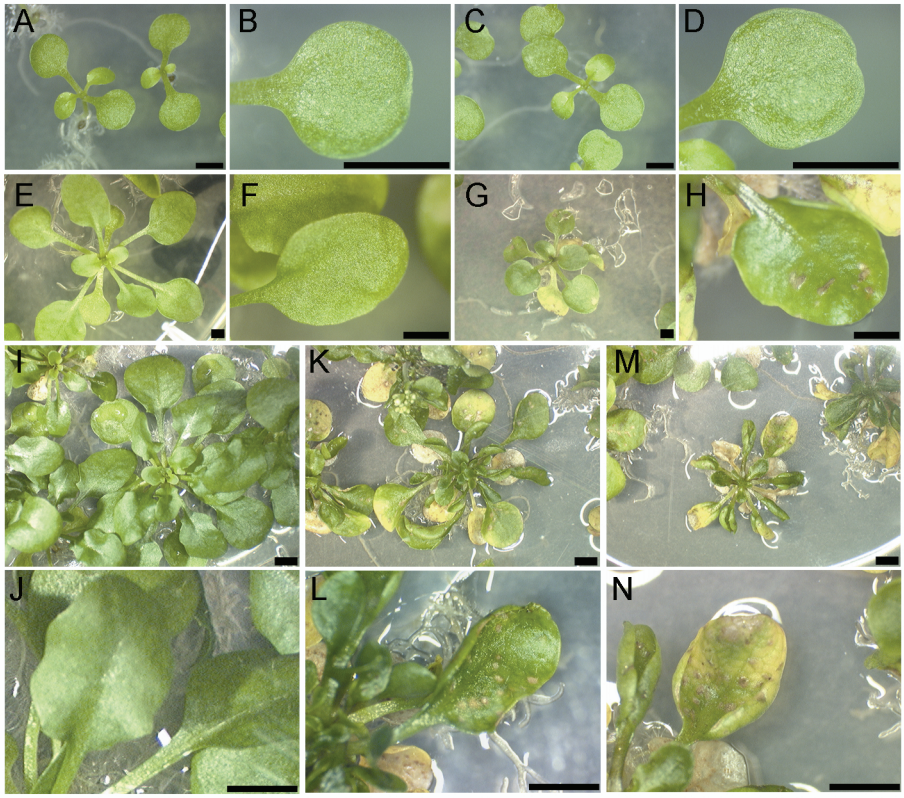

Figure 5, chapter 2

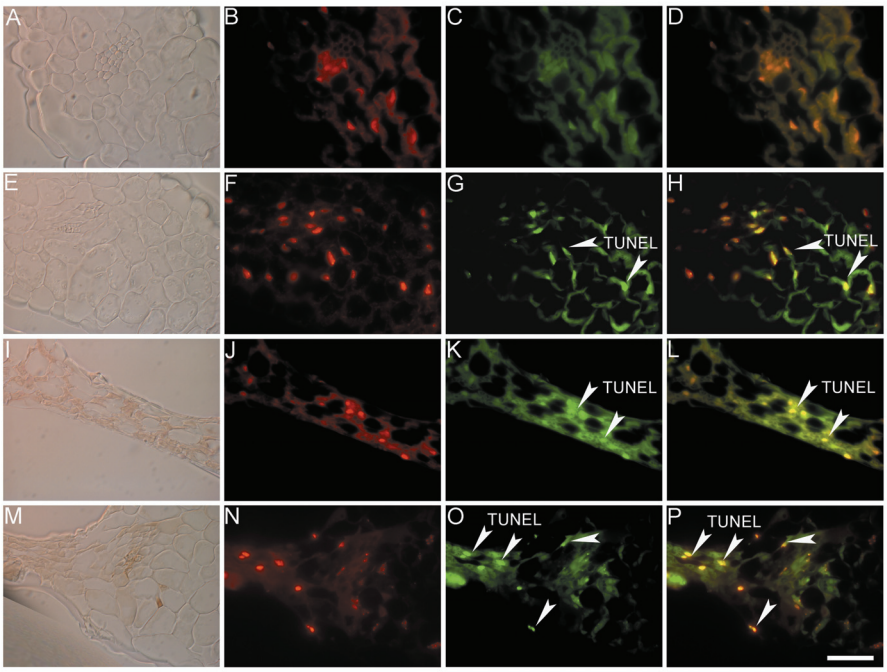

Figure 8, chapter 2

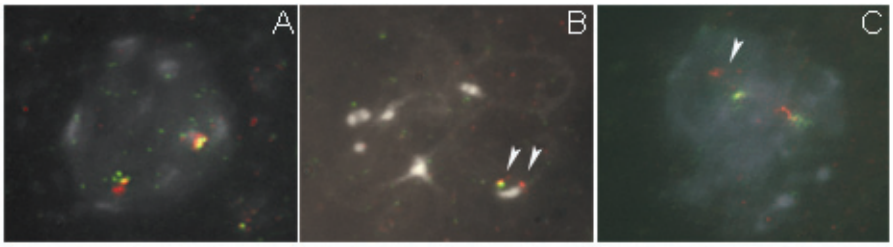

Figure 1, chapter 3

Fig. 1

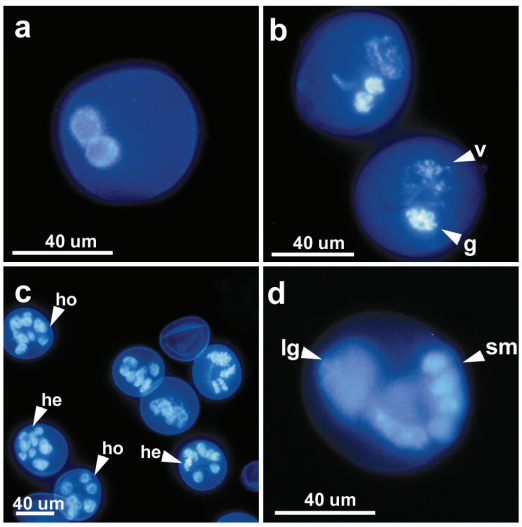

Figure 2, chapter 3

Fig. 2

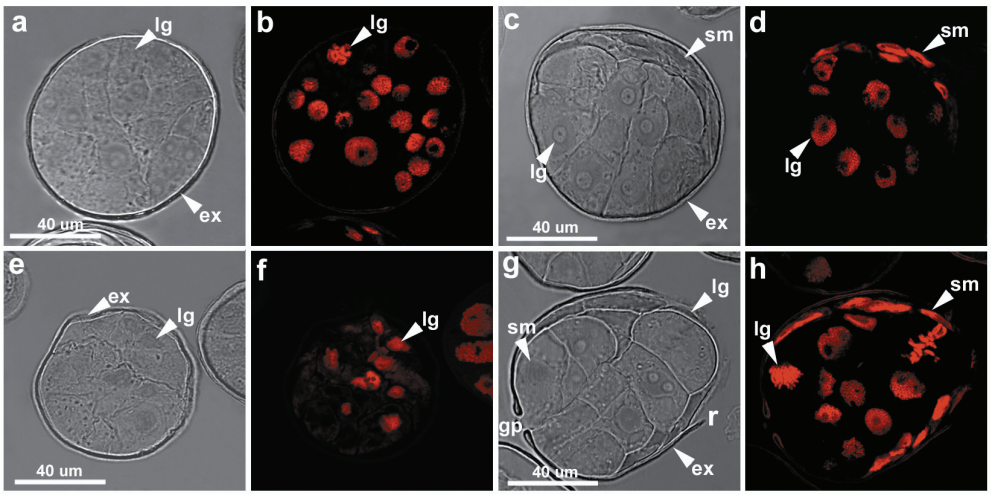

Figure 3, chapter 3

Fig. 3

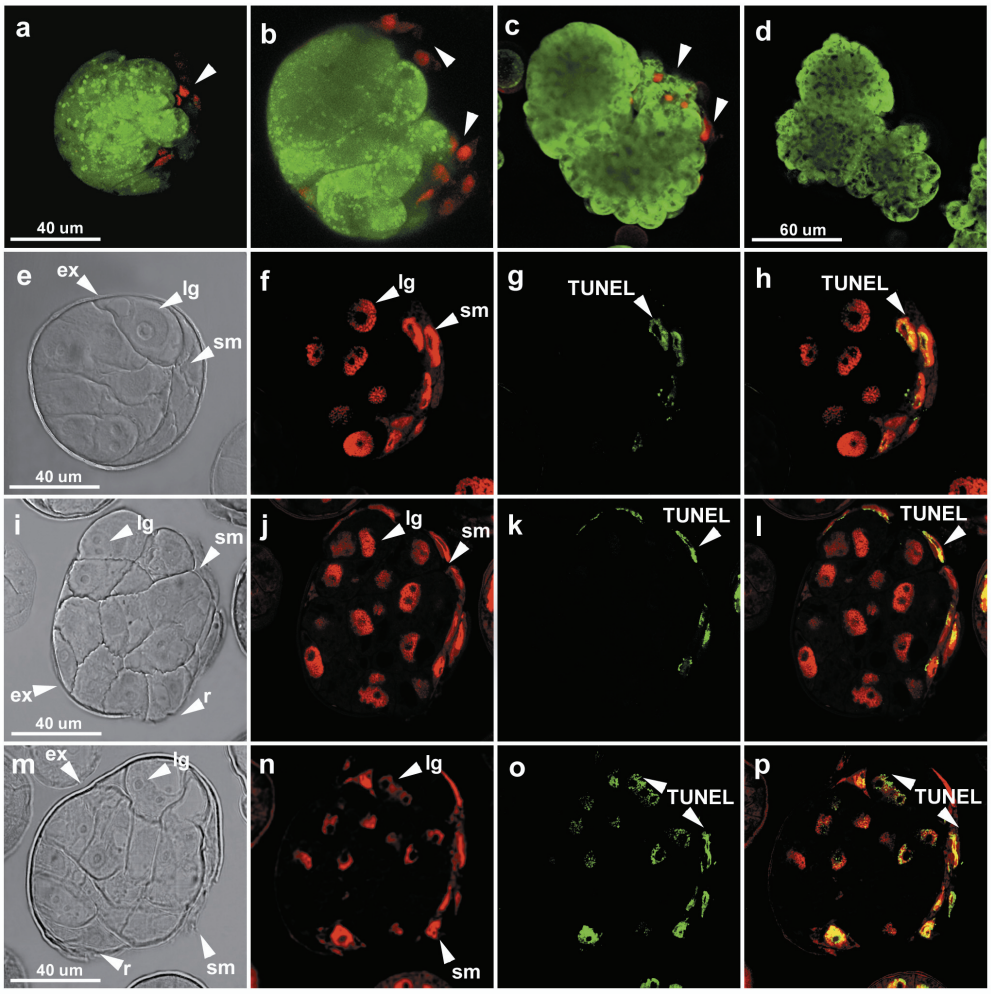

Figure 1, chapter 4

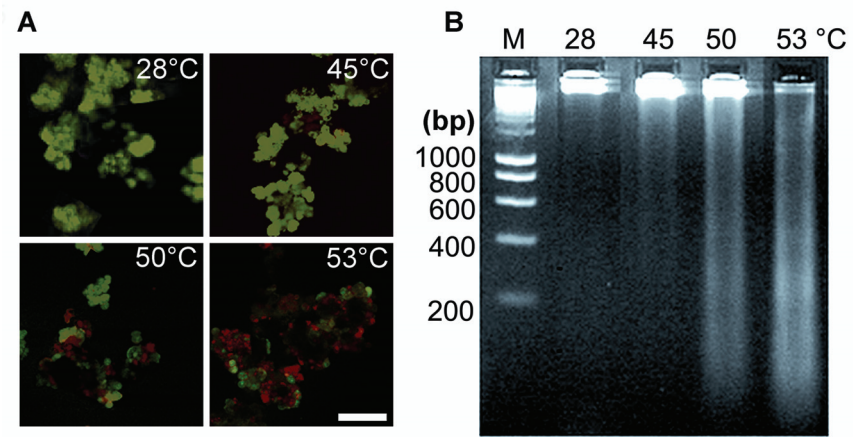

Figure 2, chapter 4